Supporting Information

Isolation, Biosynthesis and Chemical Modifications of Rubterolones A–F: Rare Tropolone Alkaloids from *Actinomadura* sp. 5-2

Huijuan Guo+,[a] René Benndorf+,[a] Daniel Leichnitz,[a] Jonathan L. Klassen,[b] John Vollmers,[c] Helmar Görls,[d] Matthias Steinacker,[a] Christiane Weigel,[a] Hans-Martin Dahse,[a] Anne-Kristin Kaster,[c] Z. Wilhelm de Beer,[e] Michael Poulsen,[f] and Christine Beemelmanns*[a]

Table of Content

1. General Experimental Procedures

NMR measurements were performed on a Bruker AVANCE III 500 MHz and 600 MHz spectrometer, equipped with a Bruker Cryoplatform. The chemical shifts are reported in parts per million (ppm) relative to the solvent residual peak of DMSO-d_6 (^{1}H: 2.50 ppm, quintet; ^{13}C: 39.52 ppm, heptet). ^{13}C-^{13}C 2D INADEQUATE NMR spectra were acquired with delay time D4 = 0.02 s/0.04 s/0.0065 s respectively. **LC-ESI-HRMS** measurements were carried out on an Accela UPLC system (Thermo Scientific) coupled with a Accucore C18 column (100 x 2.1 mm, particle size 2.6 µm) combined with a Q-Exactive mass spectrometer (Thermo Scientific) equipped with an elecrospray ion (ESI) source. **UHPLC-MS measurements** were performed on a Shimadzu LCMS-2020 system equipped with single quadrupole mass spectrometer using a Phenomenex Kinetex C18 column (50 x 2.1 mm, particle size 1.7 µm, pore diameter 100 Å). Column oven was set to 40 °C; scan range of MS was set to m/z 150 to 2,000 with a scan speed of 10,000 u/s and event time of 0.25 s under positive and negative mode. DL temperature was set to 250 °C with an interface temperature of 350 °C and a heat block of 400 °C. The nebulizing gas flow was set to 1.5 L/min and dry gas flow to 15 L/min. **Semi-preparative HPLC** was performed on a Shimadzu HPLC system using a Phenomenex Luna C18(2) 250 x 10 mm column (particle size 5 µm, pore diameter 100 Å). **IR spectra** were recorded on an FT/IR-4100 ATR spectrometer (JASCO). **Optical rotations** were recorded in DMSO on a P-1020 polarimeter (JASCO). **Solid phase extraction** was carried out using Chromabond C18ec cartridges filled with 2 g and 10 g of octadecyl-modified silica gel (Macherey-Nagel, Germany). **Open column chromatography** was performed on Sephadex LH20 (GE Healthcare, Sweden). **Chemicals**: Methanol (VWR, Germany); water for analytical and preparative HPLC (Millipore, Germany); formic acid (Carl Roth, Germany); acetonitrile (VWR as LC-MS grade); media ingredients (Carl Roth, Germany); [1-^{13}C] sodium acetate, [2-^{13}C] sodium acetate, [1,2-^{13}C$_2$] sodium acetate (Sigma-Aldrich, USA).

Media cultures:

ISP medium 2 agar (ISP2A): 4.0 g/L yeast extract, 10.0 g/L malt extract, 4.0 g/L glucose, 20.0 g/L agar

ISP medium 2 broth (ISP2): 4.0 g/L yeast extract, 10.0 g/L malt extract, 4.0 g/L glucose

chitin agar:[1] 4.0 g/L chitin, 0.7 g/L K$_2$HPO$_4$, 0.3 g/L KH$_2$PO$_4$, 0.57 g/L MgSO$_4$•7H$_2$O, 0.01 g/L FeSO$_4$•7H$_2$O, 0.0018 g/L ZnSO$_4$•7H$_2$O, 0.0016 g/L MnCl$_2$•4H$_2$O, 20 g/L agar

Basic Minimal media: 0.4 g/L sodium acetate, 2 g/L NH$_4$Cl, 0.7 g/L K$_2$HPO$_4$, 0.3 g/L KH$_2$PO$_4$, 0.57 g/L MgSO$_4$•7H$_2$O, 0.01 g/L FeSO$_4$•7H$_2$O, 0.0018 g/L ZnSO$_4$•7H$_2$O, 0.0016 g/L MnCl$_2$•4H$_2$O

Minimal medium A (2 L): 1-^{13}C CH$_3$CO$_2$Na (400 mg/L) instead of CH$_3$CO$_2$Na

Minimal medium B (500 mL): 2-^{13}C CH$_3$CO$_2$Na (400 mg/L) instead of CH$_3$CO$_2$Na

Minimal medium C (2 L): 1, 2-^{13}C$_2$ CH$_3$CO$_2$Na (200 mg/L) + CH$_3$CO$_2$Na (200 mg/L)

Minimal medium D (2 L): glycine (25 mM)

Minimal medium E (2 L): L-alanine (25 mM)

Minimal medium F (2 L): β-alanine (25 mM)

Minimal medium G (2 L): L-lysine (25 mM)

Minimal medium D (2 L): glycine (25 mM)

2. Strain Isolation and Genomic Characterization

Biological material and fermentation

Biological material (soldiers, workers) was collected from the nest of *Macrotermes natalensis* termite colony Mn154 (S25° 44.581'' E28° 15.659'') in January 2015 in South Africa, Pretoria. Whole insects were stored in 50% glycerol and kept on ice until stored at -80 °C within one day.

Isolation of gut bacteria

Major termites workers were surface sterilized with 70% EtOH and washed in sterile Ringer solution (7.5 g NaCl, 0.35 g KCl, 0.21 g $CaCl_2$ per litre). Five termites were dissected using sterile, fine tipped forceps. Intact guts were immediately removed and stored in 500 µL PBS on ice until further use. Dissected guts were crushed and a series of dilution (10^{-3} to 10^{-6} in PBS) was produced. Bacteria were isolated by platting 100 µL of dilution levels on two different selective low-nutrient media (chitin and microcrystalline medium supplemented with 0.05 mg/L cycloheximide).[2] Isolates with *Actinobacteria*-like morphology were chosen and transferred to a nutrient-richer medium ISP2 and sub-cultured until pure.

DNA extraction and sequencing

Actinobacteria were grown in nutrient-rich liquid media ISP2 for five to seven days at 30 °C. Cells were harvested, and genomic DNA was extracted using the GenJet Genomic DNA Purification Kit (Thermo Scientific, #K0721) following the manufacturer's instructions with the following modifications: a) lysozyme treatment was extended to 40 min, and b) proteinase K treatment was extended to 40 min. DNA was quantified photometrically using a Nanodrop Lite Spectrometer (Thermo Scientific) photometer. For phylogenetic studies, the 16 S rRNA gene was amplified using the primer set 1492R/27F.[3] Amplification reactions were prepared in a 25 µL final reaction volume containing 7.25 µL distilled water, 5 µL HF buffer, 5 µL of each primer (2.5 µM), 0.5 µL dNTPs (10 µM), and 0.25 µL Phusion High Fidelity DNA Polymerase (New England Biolabs) and 2 µL of extracted DNA (template). PCR was performed under the following conditions: 98 °C/38 s, 32 cycles of 98 °C/30 s, 52 °C/45 s, 72 °C/1 min 20 sec, and a final extension of 72 °C/8 min. PCR products were separated by agarose gel electrophoresis. PCR reactions were purified using the PCR Purification Kit (Thermo Scientific). DNA fragments were sequenced at GATC (Konstanz).

Phylogenetic analysis

Amplified 16S rRNA sequences were assessed for purity and mismatches using BioEdit.[4] Forward and reverse sequences of each sequence were assembled with BioEdit and tested for chimeras using DECIPHER.[5] Resulting sequences (GenBank accessions numbers KY312017-KY312022) were used for a BLASTn search in GenBank.[6] A phylogenetic analysis was performed with the 16S sequences obtained from the first hits from the BLASTn search (GenBank accessions numbers AB184063.2, AB862127.1, FN376883.1, LN908893, KF638418.1, KF772673.1, KX035076). Support for nodes on the phylogenetic tree was assessed by performing bootstrap analysis (1000 bootstrap replicates) using maximum likelihood under the T93+G model of sequence evolution, as well as by neighbour-joining using MEGA 6.0.[7] As judged by 100% 16S rRNA sequence identity *Actinomadura* sp. 5-2 (RB29) is most closely related to *Actinomadura* sp. GKU822, isolated from *Saccharum officinarum* (according to Blast, Dec. 2016).
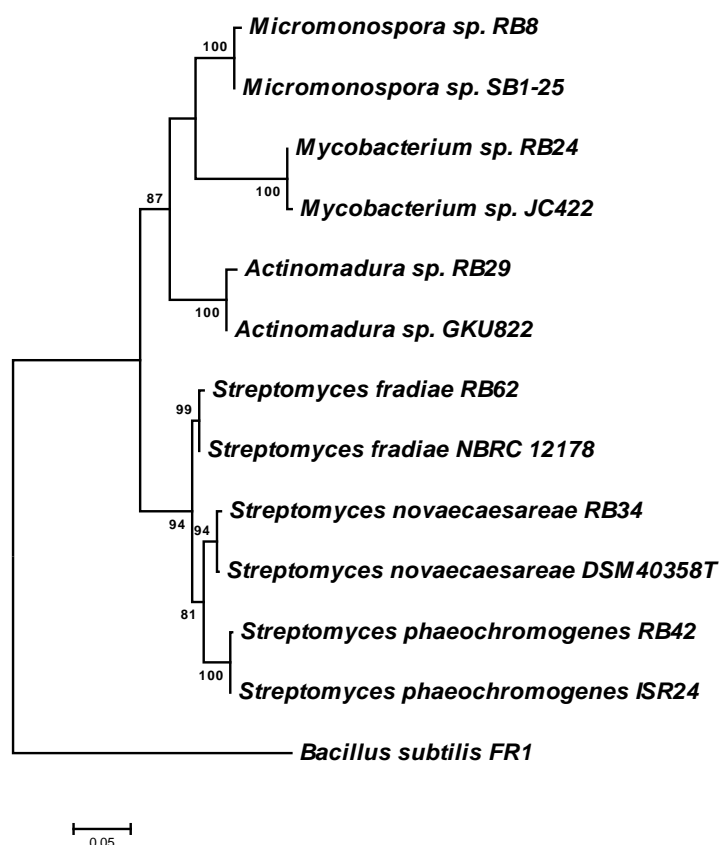
Figure S1. A rooted maximum likelihood distance tree (Substitute model: Tamura Nei, gamma distributed) is shown. The tree is rooted with *Bacillus subtilis* (GenBank accession number: AB862127) Branch values indicate bootstrap support (>70 are given) of 1000 pseudoreplicates under ML (Maximum likelihood) conditions (Blast, Dec. 2016).

Library preparation and genome sequencing

Isolated gDNA was sheared using a Covaris S220 sonication device (Covaris Inc; Massachusetts, USA) with the following settings: 55 s, 175 W, 5% Duty factor, 200 cycles of burst, 55.5 µL input volume. Sequencing libraries were prepared using the NEBNext® Ultra™ DNA Library Prep Kit for Illumina® (New England Biolabs, Frankfurt, Germany) as per the manufacturer's instructions. The libraries were then sequenced on an Illumina® MiSeq machine using v3 chemistry and a paired-end approach (300 cycles each). Read processing and assembly: Raw sequences were subjected to adapter clipping and quality trimming using Trimmomatic[8] with the following arguments: "LEADING:5 TRAILING:5 SLIDINGWINDOW:4:15 MINLEN:80". Overlapping read pairs were identified and merged using FLASH using the following arguments "-m 50 -r 200 -f 450 -s 150 -x 0.1 -z -t 8". Processed reads were assembled withSPAdes v3.6.2[9] using the "--careful" option and k-mer steps 21, 33, 55, 77, 99 and 127. The quality as well as taxonomic placement of the assembled genome were assessed checkM v1.0.4.[10] Annotations were performed using Prokka v1.11.[11] The genome draft sequence has been submitted to NCBI under project ID: PRJNA356838, sample-ID: SAMN06127924.

Table 1. Genome assembly quality statistics *Actinomadura* sp. 5-2

Number of scaffolds	7	
Total size	~6.5	Mb
smallest scaffold	5.640	bp
largest scaffold	2.582.138	bp
N50	2.134.329	bp
L50	2	
total CDS	5.700	
"hypothetical" proteins	1.559	
rRNA genes	8	
tRNA genes	80	
estimated completeness[a]	100	%
estimated contamination[a]	0	%

[a] based on checkM analyses of 104 universal bacterial markergenes ("Taxonomic-specific Workflow" for *Bacteria*)

Gene cluster analysis

The putative rubterolone biosynthetic gene cluster was identified based on its homology to the known rubrolones biosynthetic cluster and the recently published isatropolone biosynthetic gene cluster, albeit with substantial gene order rearrangement.[12] The gene cluster spans 24,607 bp and encodes 23 proteins, which we have annotated RblA−W. Interestingly, RblD has only weak homology to RubE1 from the rubrolone cluster and IstR from the isatropolone cluster, and is instead more similar to SsfN from the SF2575 cluster,[13] which has been implicated in angelic acid biosynthesis. These annotations allowed us to propose a putative biosynthetic pathway for the rubterolones in *Actinomadura* sp. 5-2.

Figure S2. Comparative gene maps of *rub* and *rbl* biosynthetic cluster and proposed biosynthetic pathway.
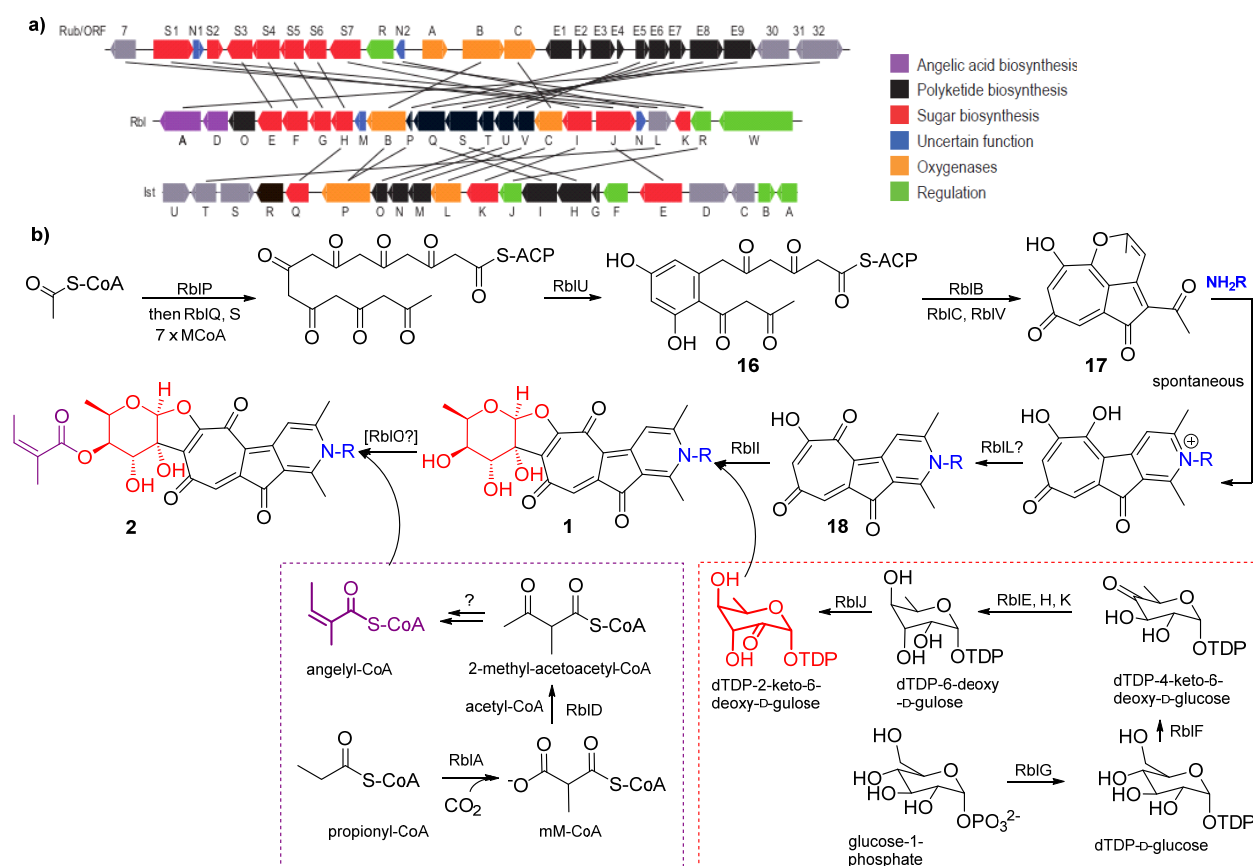
Biosynthesis of rubterolones begins by loading acetyl-CoA onto the ACP RblP. The iterative type II PKS RblS then adds seven malonyl-CoA units to this acetyl-ACP unit, with its associated chain length factor RblQ. The polyketide cyclase RblU then forms a C-C bond between carbon positions 7 and 12 and aromatises this ring. By homology to the proposed biosynthesis of rubrolones, RblB, RblC, and RblV together catalyze the oxidation and cyclization of the polyketide core, allowing it to abiotically capture ammonium or glycine during pyridine ring formation. Note that RblV is only partially homologous to its homolog in the rubrolones cluster, RubE5, which is

likely truncated. Additionally, RblB and RblP are both homologous to IstP in the isatropolone cluster, which is apparently a fusion between an oxygenase and an acyl carrier protein. The hydroxyl group at position 8 is then reduced, putatively by the oxidoreductase RblL that is homologous to ORF7 immediately upstream of the rubrolone biosynthetic gene cluster and IstT from the isatropolone biosynthetic gene cluster. The resulting product comprises the complete rubterolone aglycone.

All rubterolone aglycones are bound to the unusual sugar molecule 6-deoxygulose, whose biosynthetic enzymes are all encoded within the rubterolone biosynthetic gene cluster. Glucose-1-phosphate is thymidylated by RblG, dehydrated to d-TDP-4-keto-6-deoxy-D-glucose by RblF, and then epimerized to d-TDP-4-keto-6-deoxy-D-gulose by RblK. The conversion of d-TDP-4-keto-6-deoxy-D-glucose to dTDP-6-deoxy-D-gulose likely evolves one or more of the reductases (RblE, RblH, or RblK). This d-TDP-6-deoxy-D-gulose is then added to the rubterolone aglycone by the glycotransferase RblI, and **1** is formed by non-enzymatic aldol condensation. Compounds **2** and **4** are related to **1** by the addition of an angelic acid moiety to the hydroxyl group at position C-20. Although the biosynthesis of the angelic acid moiety remains unclear, the significant homology of RblA and RblD to SsfE and SsfN, respectively, of the SF2575 biosynthetic gene cluster, suggests a similar biosynthetic pathway. Angelic acid biosynthesis begins most likely with the carboxylation of propionyl-CoA by RblA to form methymalonyl-CoA, which is then converted to 2-methyl-acetoacyl-CoA by the type III PKS RblD. Although enzymes that might convert 2-methyl-acetoacyl-CoA to 3-hydroxyl-2-methyl-butyryl-CoA and then to anglyl-CoA are not encoded by the rubterolone biosynthetic gene cluster, homologs to the SsfK and SsfJ proteins that are proposed to perform these steps during SF2575 biosynthesis are encoded elsewhere in the *Actinomadura* sp. 5-2 genome (actino_56650 is 34% identical over 96% of its length to SsfK; actino_32760 is 61% identical over 98% of its length to SsfJ). Likewise, the enzyme that transfers anglyl-CoA to **1** remains cryptic, although RblO possess weak homology to SsfG that performs this step during SF2575 biosynthesis. Whether RblO possess this functionality along with or instead of performing the initiating step of polyketide biosynthesis requires further study.

Table S2. Rubterolone biosynthetic protein annotations based on sequence homology.

Protein Name	size (aa)	Closest Homolog(s)[a]	Annotation	Identity (%)/ Alignment length (%)[b]	Accession number
RblA		San1 SsfE ORF32	Carboxytransferase	79/74 74/95 73/95	ADG86308 ADE34513 AOZ61215
RblD	325	SsfN IstR RubE1	Ketoacyl synthase III	56/98 30/100 30/96	ADE34503 ARG41921 AOZ61205
RblO	344	ChlB3 SsfG	Ketoacyl synthase III	37/99 35/98	AAZ77676 ADE34509
RblE	313	RubS3	dTDP-glucose-4-ketoreductase	59/97	AOZ61195
RblF	333	RubS4	dTDP-glucose 4,6 dehydratase	70/98	AOZ61196
RblG	287	RubS5	Glucose-1-phosphate thymidyltransferase	63/100	AOZ61197
RblH	283	IstQ RubS6	Epimerase/dehydratase	66/99 63/99	ARG41920 AOZ61198
RblM	149	IfnL	Hypothetical protein	54/89	BAU98039
RblB	512	IstP RubB	Oxygenase	61/95 55/97	ARG41919 AOZ61203
RblP	81	IstP RubE4	Acyl carrier protein	56/89 48/93	ARG41919 AOZ61208
RblQ	407	Gra-orf2 RubE9 IstI	Chain length factor	66/99 64/98 59/98	ADO32787 AOZ61213 ARG41912
RblS	421	Erd1 RubE8 IstH	Ketoacyl synthase type II	76/100 74/100 71/98	ACX83617 AOZ61212 ARG41911
RblT	199	RubE7 IstO	Dehydrogenase	64/93 62/100	AOZ61211 ARG41918
RblU	249	IstN IfnK RubE6	Polyketide cyclase	82/100 81/99 79/100	ARG41917 BAU98038 AOZ61210
RblV	274	RubE5 IstM IfnJ	Polyketide cyclase	69/54 67/99 63/100	AOZ61209 ARG41916 BAU98037
RblC	361	IstL RubC	Hydroxylase	52/93 49/98	ARG41915 AOZ61204
RblI	383	RubS7 IstK	Glycosyltransferase	59/100 55/100	AOZ61199 ARG41914
RblJ	526	RubS1 IstE	Oxidoreductase	72/93 64/97	AOZ61192 ARG41908
RblN	130	RubN1	Hypothetical protein	62/96	AOZ61193
RblL	308	IstT ORF7	Oxidoreductase	62/100 61/100	ARG41923 AOZ61191
RblK	201	CpzDVI RubS2	dTDP-4-keto-6-deoxy-D-glucose 3,5-epimerase	55/98 45/96	ADI50280 AOZ61194
RblR	268	RubR IstJ	SARP family transcriptional regulator	56/94 53/94	AOZ61200 ARG41913
RblW	950	ADK64_28555	LuxR family transcriptional regulator	38/97	KOV61149

[a] Except for RblW, only homologs from biosynthetic gene clusters encoding for characterized compounds were considered. Origin of gene clusters: Rub = *Streptomyces* sp. KIB-H033; Ist =*Streptomyces* sp. Go66; San = *Streptomyces* sp. SANK 61196; Ssf = *Streptomyces* sp.; SF2575; Ifn = *Streptomyces* sp. RI-77; Cpz = *Streptomyces* sp. MK730-62F2; Erd = uncultured soil bacterium V167; Gra = *Streptomyces vietnamensis;* Ndb = *Synechocystis* sp.; Drr = *Streptomyces peucetius.*

[b] Percent alignment and identify were determined using BLASTp, following default parameters. Percent alignment is the proportion of the Rbl query sequence that aligns to each homolog.

3. Fermentation Procedures

Growth studies

Actinomadura sp. 5-2 was first cultivated in ISP2 broth for 10 days (30 °C, 120 rpm), and then subcultured by plating mycelium-containing broth (1 mL) onto ISP2 agar plates (20 mL each, adjusted to pH 5–10 respectively) for 13 days to monitor the growth and pigment production. Whole agar plate was then collected and cut into small pieces and extracted twice with 100 mL MeOH. After removal of MeOH under reduced pressure, the extracts were adjusted with MeOH to yield a 10 mg/mL stock solution and subjected to LC-MS analysis using a Shimadzu UHPLC-MS (gradient: 0–1 min, 10% B; 1–5 min, 10%–100% B; 5–7 min, 100% B (A: dd H_2O with 0.1% formic acid; B: MeCN with 0.1% formic acid) with the flow rate of 1.0 mL/min and analyzed using extracted ion chromatogram (EIC) mode.
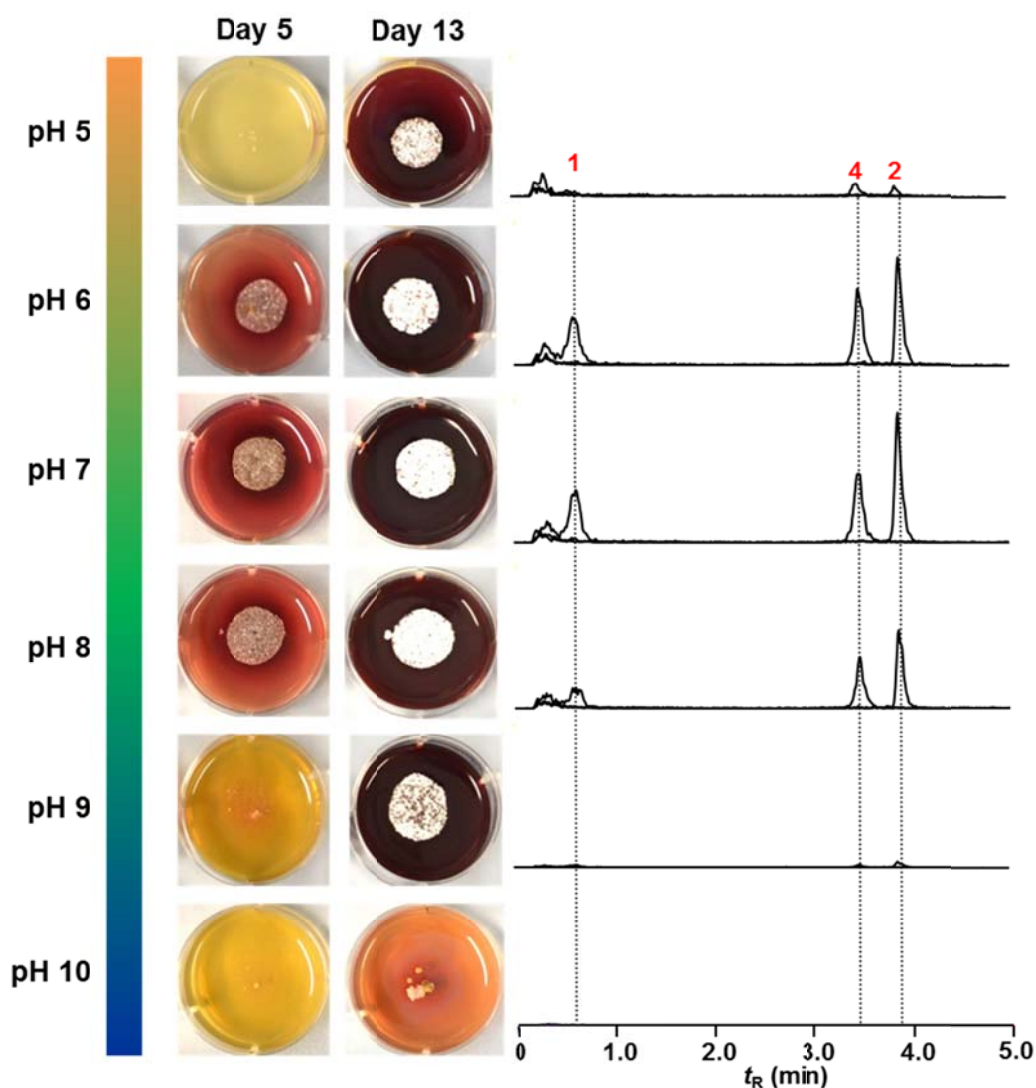
Figure S3. Representative growth and metabolite studies at different pH (left), and corresponding LC-MS chromatograms (EIC mode, **1** *m/z* 414.1; **2** *m/z* 496.1; **4** *m/z* 554.1).

Small scale cultivation for antimicrobial activity tests

Isolated Actinobacteria were cultivated in 50 mL ISP2 broth for seven days at 30 °C at 120 rpm. Each culture was separated into supernatant and cell pellet by centrifugation (4000 rpm, 10 min, RT). Cell pellet was lysed and extracted using 9 mL MeOH. Cell debris was removed by centrifugation (4000 rpm, 10 min), and methanolic cell extracts (~9 mL) were added to the previously separated culture supernatant. The combined crude extract was loaded on a pre-activated and equilibrated C18 cartridge (500 mg C18, 20% MeOH/80% ddH$_2$O). The loaded SPE column was washed with 20% MeOH, and then eluted using 100% MeOH and 100% acetone respectively. Both extracts were pooled and concentrated under reduced pressure. Finally, organic extract was dissolved with 100% MeOH to yield a 1.0 mg/mL stock solution for LC-MS analysis and antimicrobial activity test.
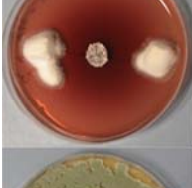
Co-cultivation studies
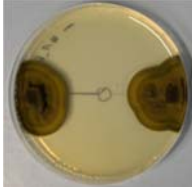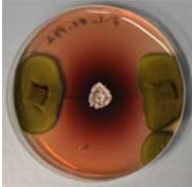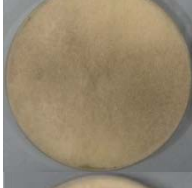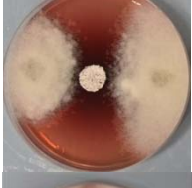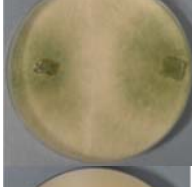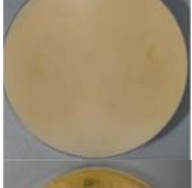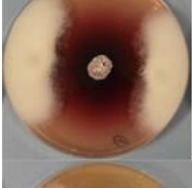
Actinomadura sp. 5-2 (RB29) was first cultivated in ISP2 broth for 10 days (30 °C, 120 rpm). Mycelium-containing ISP2 broth (250 μL) was point inoculated in the middle of a PDA or ISP2A (standard petri dish 15 x 90 mm) and incubated for seven days at 30 °C. Due to the different growth curves of the respective fungi, two different co-cultivation methods were applied.
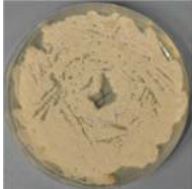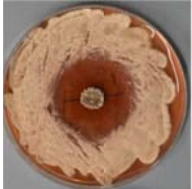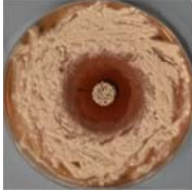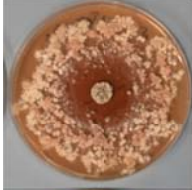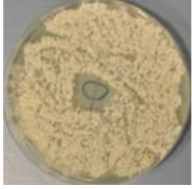
Method A was used for co-cultivation with *Termitomyces* sp. strains and *Metarhizium anisopliae*: The fungal strain was cultivated in PDB at 180 rpm for 14 days. Mycelium-containing broth (250 μL) was evenly distributed on the surface of a PDA plate (standard petri dish 15 x 90 mm).

Method B was used for fungal co-isolates and *Beauveria bassiana*: similar sized mycelium-containing agar pieces co-isolated fungi were inoculated at the same time on a PDA plate with an approximate distance of 2 cm to each other. Co-cultivations were performed at room temperature up to 14 days and the growth was monitored daily. PDA plates of individual cultures without interaction partner were cultivated as controls.

Extraction: From three interaction assays, the agar part of the zone of interaction (ZOI) was cut into squares and extracted with 100 mL of MeOH overnight at 4 °C. The mixture was filtrated and the MeOH extract concentrated under reduced pressure. The crude extract was submitted to pre-activated and equilibrated SPE-C18 (1 g) cartridge separation by 12 mL 20% MeOH (80% dH$_2$O) and 12 mL 100% MeOH, respectively. The elutent using 100% MeOH was dried under reduced pressure, dissolved in MeOH with a final concentration of 10.0 mg/mL, and analyzed by LC-MS using a Shimadzu UHPLC-MS (gradient: 0–1 min, 10% B; 1–5 min, 10%–100% B; 5–7 min, 100% B (A: dd H$_2$O with 0.1% formic acid; B: MeCN with 0.1% formic acid) with the flow rate of 1.0 mL/min and analyzed using extracted ion chromatogram (EIC) mode..

Table S3. Representative challenge assays against typical co-isolated fungi on PDA plates.

strain	inhibition	co-isolate control	co-culture	method	observation
#1 *Cladosporium perangustum* (JF499836)	moderate			B	12-day
#8 *Coriolopsis* sp. (EU863193)	weak			B	12-day
#10 *Fusarium equiseti* (HQ607811)	weak			B	7-day
#14* *Umbelopsis isabellina* (JF303862)	moderate			B	7-day
#17 *Trichoderma* sp. (HQ607860)	no			B	7-day
#22 *Trichoderma* sp. (JF831494)	moderate			B	7-day
#24 *Hypocrea virens* (HQ608079)	no			B	4-day
Beauveria bassiana	strong			B	9-day
Metarhizium anisopliae	moderate			A	4-day

Termitomyces sp**.** P5	moderate			A	12-day
Termitomyces sp**.** T112	moderate			A	12-day
Termitomyces sp. T115	moderate			A	12-day
Termitomyces sp. T153	moderate			A	12-day

* Growth on ISP2 Agar

Large scale fermentation on agar plates

Large-scale cultivation was performed by inoculation of 100 ISP2 agar plates (standard 15 mm x 90 mm, 20 mL ISP2 agar/plate) at 30 $^{\circ}$C for 10 days (until strong production of red pigment). Whole agar plates were cut into pieces and extracted twice with 2 L MeOH at 4 °C overnight. MeOH extracts were filtered and concentrated under reduced pressure. The crude extract was dissolved using 10% MeOH (unless stated otherwise: dd H_2O was used as second solvent = 90% dd H_2O) and loaded on an activated and equilibrated SPE C18 column (10 g), and fractionated by step-gradient from 10% MeOH to 100% MeOH (100 mL each). The eluent using 30% MeOH was first purified by Sephadex LH20 using 50% MeOH to obtain subfractions Fr.3.1–Fr.3.6 (20 mL/Fr.). Concentrated violet band Fr.3.5 was further separated by semi-preparative HPLC to yield pure rubterolone A (**1**, 5.50 mg, t_R = 11.19 min) using the following gradient: 0–5 min, 40% B; 5–20 min, 40%–100% B; 20–22 min, 100% B (A: dd H_2O + 0.1% formic acid; B: MeOH) with a flow rate of 2.0 mL/min. Concentrated violet band Fr.3.3 was further separated by semi-preparative HPLC to yield rubterolone D-containing subfraction (4.21 mg, t_R = 16.78 min) using the following gradient: 0–5 min, 50% B; 5–20 min, 50%–100% B; 20–22 min, 100% B (A: dd H_2O + 0.1% formic acid; B: MeOH) with a flow rate of 2.0 mL/min. This subfraction was further submitted to a second semi-preparative HPLC run to obtain rubterolone D (**4**, 3.25 mg, t_R = 10.19 min) using the following isocratic conditions: (60% MeCN, 40% ddH_2O + 0.1% formic acid). The eluent using 50% MeOH were combined, concentrated, and submitted to Sephadex LH20 column chromatography using 50%MeOH to obtain subfractions Fr.5.1 to Fr.5.5 (20 mL/Fr.). Concentrated violet band Fr. 5.4 was further separated by semi-preparative HPLC yielding rubterolone B (**2**, 5.33 mg, t_R = 13.03 min), using the following gradient: 0–5 min, 60% B; 5–20 min, 60%–100% B; 20–22 min, 100% B (A: dd H_2O + 0.1% formic acid; B: MeOH) with the flow rate of 2.0 mL/min.

Stable isotope labeling

Bacteria were cultivated in ISP2 broth for a maximum of 10 days (30 $^{\circ}$C, 120 rpm, 50 mL). Biomass was separated from culture supernatant by centrifugation (6000 rpm, RT), and washed twice using autoclaved minimal media (50 mL). The washed-biomass was added to autoclaved minimal media (1 L) and cultured for 10 days (30 $^{\circ}$C, 120 rpm). After 5 days additional labeled CH_3CO_2Na (200 mg/L) and additional biomass were added to maximize pigment production.

Minimal medium A (2 L): 1-^{13}C CH_3CO_2Na (400 mg/L)

Minimal medium B (500 mL): 2-^{13}C CH_3CO_2Na (400 mg/L)

Minimal medium C (2 L): 1, 2-^{13}C$_2$ CH_3CO_2Na (200 mg/L) + CH_3CO_2Na (200 mg/L)

Isolation of ^{13}C-labeled rubterolones A–B (1a–1c, 2a–2c): The reddish liquid culture (2 L) was centrifuged and the cell pellet separated. The obtained supernatant was mixed with activated HP20 resin (20 g/L) and stirred at 4 °C overnight. The HP20 resin was separated by filtration, washed with dd H_2O (1 L) and eluted using MeOH (1 L). The resulting MeOH eluent was dried under reduced pressure, suspended in 10% MeOH, loaded on a pre-activated and equilibrated SPE-C18 (2 g) cartridge and eluted using a step gradient to yield 30% MeOH, 50% MeOH, 80% MeOH and 100% MeOH fractions respectively. The resulting 30% MeOH eluent was dried completely and submitted on semipreparative HPLC fractionation. The ^{13}C-labeled rubterolone A was obtained by using the following gradient: 0–5 min, 40% B; 5–20 min, 40%–100% B; 20–22 min, 100% B (A: dd H_2O + 0.1% formic acid; B: MeOH) with a flow rate of 2.0 mL/min. The resulting 50% MeOH eluent was dried completely and submitted on semipreparative HPLC fractionation. The ^{13}C-labeled rubterolone B was obtained by using the following gradient: 0–5 min, 60% B; 5–20 min, 60%–100% B; 20–22 min, 100% B (A: dd H_2O + 0.1% formic acid; B: MeOH) with a flow rate of 2.0 mL/min. The ^{13}C-labeled rubterolone D was hardly detected due to limited amount. The yield of ^{13}C-labeled rubterolone A was 5.01 mg/2 L (**1a**, minimal medium A), 560 µg/500 mL (**1b**, minimal medium B), 5.57 mg/2 L (**1c**, minimal medium C). The yield of ^{13}C-labeled rubterolone B was 1.5 mg/2 L (**2a**, minimal medium A), 500 µg/500 mL (**2b**, minimal medium B), 1.43 mg/2 L (**2c**, minimal medium C).

Amine feeding

Bacteria were cultivated in ISP2 broth for a maximum of 10 days (30 $^{\circ}$C, 120 rpm, 50 mL). Biomass was separated from culture supernatant by centrifugation (6000 rpm, RT), and washed twice using autoclaved minimal media (50 mL). The washed-biomass was added to autoclaved minimal media D, E, F, G (2 L) respectively, and cultured for 10 days (30 $^{\circ}$C, 120 rpm).

Isolation of rubterolones C–L (3–6, 10–15): The reddish liquid culture (2 L) was centrifuged and the cell pellet was separated. The obtained supernatant was mixed with activated HP20 resin (20 g/L) and stirred at 4 °C overnight. The HP20 resin was separated by filtration, washed with dd H_2O (1 L) and eluted using MeOH (1 L). The resulting MeOH eluent was dried under reduced pressure, suspended in 10% MeOH, loaded on a pre-activated and equilibrated SPE-C18 (2 g) cartridge and eluted using a step gradient to yield 10% MeOH, 30% MeOH, 50% MeOH, 80% MeOH and 100% MeOH fractions respectively. The resulting 10% MeOH eluent from glycine feeding (minimal media D) culture was dried completely and submitted on semipreparative HPLC fractionation. The rubterolone C (**3**) (1.1 mg, t_R = 10.2 min) was obtained by using the following gradient: 0–5 min, 40% B; 5–20 min, 40%–100% B; 20–22 min, 100% B (A: dd H_2O + 0.1% formic acid; B: MeOH) with a flow rate of 2.0 mL/min. The resulting 10% MeOH eluent from L-alanine feeding (minimal media E) culture was dried completely and submitted on semipreparative HPLC fractionation. The rubterolone E (**5**) (2.1 mg, t_R = 12.0 min) was obtained by using the following gradient: 0–5 min, 60% B; 5–20 min, 60%–100% B; 20–22 min, 100% B (A: dd H_2O + 0.1% formic acid; B: MeOH) with a flow rate of 2.0 mL/min. The resulting 30% MeOH eluent from L-alanine feeding (minimal media E) culture was dried completely and submitted on semipreparative HPLC fractionation. The rubterolone F (**6**) (1.5 mg, t_R = 20.1 min) was obtained by using the following gradient: 0–5 min, 50% B; 5–20 min, 50%–100% B; 20–22 min, 100% B (A: dd H_2O + 0.1% formic acid; B: MeOH) with a flow rate of 2.0 mL/min. The resulting 30% MeOH eluent from β-alanine feeding (minimal media F) culture was dried completely and submitted on semipreparative HPLC fractionation. The rubterolone G (**10**) (t_R = 7.8 min) and H (**11**) (t_R = 17.7 min) were obtained by using the following gradient: 0–5 min, 40% B; 5–20 min, 40%–100% B; 20–22 min, 100% B (A: dd H_2O + 0.1% formic acid; B: MeOH) with a flow rate of 2.0 mL/min. The resulting 30% MeOH eluent from L-lysine feeding (minimal media G) culture was dried completely and submitted on semipreparative HPLC fractionation. The rubterolone I (**12**) (t_R = 7.7 min), J (**13**) (t_R = 17.6 min), K (**14**) (t_R = 7.4 min), L (**15**) (t_R = 17.4 min) were obtained by using the following gradient: 0–5 min, 30% B; 5–20 min, 30%–100% B; 20–22 min, 100% B (A: dd H_2O + 0.1% formic acid; B: MeOH) with a flow rate of 2.0 mL/min.
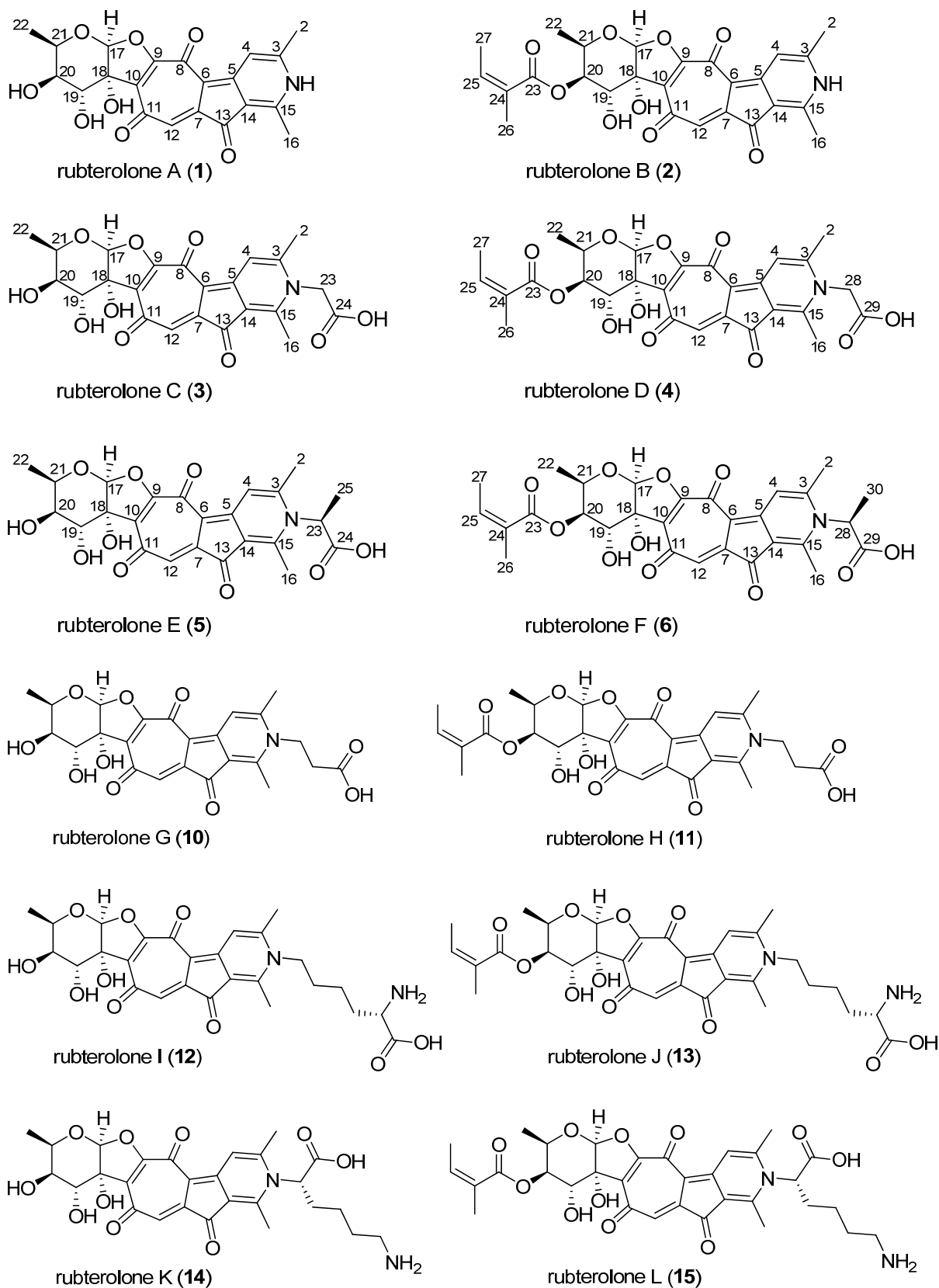
4. Structure Analysis of Rubterolones A–L (1–6, 10–15)

Figure S4. Chemical structures of rubterolones A–F (**1–6**) and proposed structures of G–L (**10–15**).

Rubterolone A (1): purple solid; $[\alpha]^{25}_D$ −149 (c 0.004 w/v%, DMSO); UV (MeCN/H$_2$O/FA) λ_{max} 216, 275, 424, 535 nm; IR (ATR) ν_{max} 3368, 3256, 2975, 2926, 2898, 1718, 1643, 1588, 1540, 1466, 1390, 1324, 1216, 1167, 1094, 1055, 1005, 943, 888, 854, 791, 762 cm^{-1}; NMR spectral data, see Table S6 and Table S7; ESI-HRMS [M+H]$^+$ m/z 414.1179 (calcd for C$_{21}$H$_{20}$O$_8$N, 414.1183).

Rubterolone B (2): purple solid; $[\alpha]^{25}_D$ −108 (c 0.004 w/v%, DMSO); UV (MeCN/H$_2$O/FA) λ_{max} 216, 275, 424, 535 nm; IR (ATR) ν_{max} 3398, 3280, 2929, 1711, 1644, 1588, 1550, 1428, 1388, 1324, 1264, 1144, 1104, 1054, 1027, 947, 890, 826, 793, 768 cm^{-1}; NMR spectral data, see Table S8 and Table S9; ESI-HRMS [M+H]$^+$ m/z 496.1596 (calcd for C$_{26}$H$_{26}$O$_9$N, 496.1602).

4-Bromobenzoyl rubterolone B (2d): purple solid; UV (MeCN/H$_2$O/FA), λ_{max} 223, 255, 274, 433, 549 nm; ^{1}H NMR spectral data, see Table S10; ESI-HRMS [M+H]$^+$ m/z 678.0974 (calcd for C$_{33}$H$_{29}$O$_{10}$N^{79}Br, 678.0969).

Rubterolone C (3): purple solid; $[\alpha]^{25}_D$ −298 (c 0.002 w/v%, DMSO); UV (MeCN/H$_2$O/FA) λ_{max} 216, 273, 430, 535 nm; IR (ATR) ν_{max} 3363, 2934, 1708, 1642, 1551, 1481, 1427, 1370, 1329, 1286, 1214, 1115, 1047, 997, 946, 910 cm^{-1}; NMR spectral data, Table S11; ESI-HRMS [M+H]$^+$ m/z 472.1229 (calcd for C$_{23}$H$_{22}$O$_{10}$N, 472.1238).

Rubterolone D (4): purple solid; $[\alpha]^{25}_D$ −412 (c 0.002 w/v%, DMSO); UV (MeCN/H$_2$O/FA) λ_{max} 216, 275, 424, 535 nm; IR (ATR) ν_{max} 3385, 2983, 2932, 1710, 1636, 1598, 1556, 1480, 1433, 1377, 1323, 1281, 1214, 1116, 1035, 992, 940, 896, 768 cm^{-1}; NMR spectral data, see Table S12; ESI-HRMS [M+H]$^+$ m/z 554.1652 (calcd for C$_{28}$H$_{28}$O$_{11}$N, 554.1657).

propargyl-rubterolone D (4a): purple solid; UV (MeCN/H$_2$O/FA), λ_{max} 228, 276, 437, 550 nm; ^{1}H NMR spectral data, see Table S13; ESI-HRMS [M+H]$^+$ m/z 591.1968 (calcd for C$_{31}$H$_{31}$O$_{10}$N$_2$, 591.1973).

Rubterolone E (5): purple solid; $[\alpha]^{25}_D$ −128 (c 0.002 w/v%, DMSO); UV (MeCN/H$_2$O/FA) λ_{max} 221, 276, 430, 536 nm; IR (ATR) ν_{max} 3359, 2983, 2940, 1707, 1644, 1600, 1549, 1481, 1427, 1368, 1317, 1236, 1121, 1026, 899 cm^{-1}; NMR spectral data, see Table S14; ESI-HRMS [M+H]$^+$ m/z 486.1388 (calcd for C$_{24}$H$_{24}$O$_{10}$N, 486.1395).

Rubterolone F (6): purple solid; $[\alpha]^{25}_D$ −236 (c 0.002 w/v%, DMSO); UV (MeCN/H$_2$O/FA) λ_{max} 220, 277, 435, 548 nm; IR (ATR) ν_{max} 3414, 2679, 1706, 1644, 1550, 1480, 1427, 1368, 1316, 1233, 1110, 1040, 891 cm^{-1}; NMR spectral data, see Table S15; ESI-HRMS [M+H]$^+$ m/z 568.1808 (calcd for C$_{29}$H$_{30}$O$_{11}$N, 568.1813).

Rubterolone G (10): purple solid; UV (MeCN/H$_2$O/FA) λ_{max} 219, 277, 430, 540 nm; ESI-HRMS [M+H]$^+$ m/z 486.1387 (calcd for C$_{24}$H$_{24}$O$_{10}$N, 486.1395).

Rubterolone H (11): purple solid; UV (MeCN/H$_2$O/FA) λ_{max} 220, 274, 436, 544 nm; ESI-HRMS [M+H]$^+$ m/z 568.1804 (calcd for C$_{29}$H$_{30}$O$_{11}$N, 568.1813).

Rubterolone I (**12**): purple solid; UV (MeCN/H$_2$O/FA) λ_{max} 232, 276, 429, 537 nm; ESI-HRMS [M+H]$^+$ *m/z* 543.1980 (calcd for C$_{27}$H$_{31}$O$_{10}$N$_2$, 543.1973).

Rubterolone J (**13**): purple solid; UV (MeCN/H$_2$O/FA) λ_{max} 233, 277, 434, 547 nm; ESI-HRMS [M+H]$^+$ *m/z* 625.2398 (calcd for C$_{32}$H$_{37}$O$_{11}$N$_2$, 625.2392).

Rubterolone K (**14**): purple solid; UV (MeCN/H$_2$O/FA) λ_{max} 232, 273, 431, 537 nm; ESI-HRMS [M+H]$^+$ *m/z* 543.1979 (calcd for C$_{27}$H$_{31}$O$_{10}$N$_2$, 543.1973).

Rubterolone L (**15**): purple solid; UV (MeCN/H$_2$O/FA) λ_{max} 235, 271, 436, 546 nm; ESI-HRMS [M+H]$^+$ *m/z* 625.2396 (calcd for C$_{32}$H$_{37}$O$_{11}$N$_2$, 625.2392).

Rubterolone A (1): The molecular formula of rubterolone A (**1**) was assigned as $C_{21}H_{19}O_8N$ based on ESI-HRMS (m/z 414.1179 $[M+H]^+$, calcd. 414.1183 $\Delta = -1.17$ ppm).

The ^1H NMR analysis revealed 15 protons as sharp signals. The ^1H chemical shifts suggested the presence of three oxymethine protons (δ_H 4.00 ppm/δ_C 70.8 ppm), δ_H 3.61 ppm/δ_C 68.4 ppm, δ_H 4.08 ppm/δ_C 70.3 ppm) and three methyl groups (δ_C 25.2 ppm/δ_H 2.41 ppm; δ_C 20.8 ppm/δ_H 2.55 ppm; δ_C 15.7 ppm/δ_H 1.09 ppm). Detailed ^{13}C NMR analysis coupled with DEPT 135 and HSQC spectra resulted in the identification of eleven quaternary carbons and two tertiary carbons (δ_C 115.1 ppm/δ_H 8.07 ppm; δ_C 114.5 ppm/δ_H 6.38 ppm) suggesting the presence of a large conjugated structure. The deoxysugar-like substructure of compound **1** was deduced from COSY correlations H-19/H-20, H-20/H-21 and H-21/H-22 and HMBC correlations of H-19 to C-17 and C-20, H-20 to C-18, C-19 and C-22, H-21 to C-17 and C-19, and H-22 to C-20 and C-21 with an anomeric proton (δ_H 5.27 ppm/δ_C 105.7 ppm). Due to the limited amount of HMBC correlations ^{13}C labeling experiment were performed to allow ^{13}C 2D-INADEQUATE experiments to establish the direct carbon-carbon connections. After successfully incorporation of 1,2-$^{13}C_2$ acetate into the molecules, comparative analysis of ^{13}C 2D-INADEQUATE spectra (compound **1c**, *vide infra*) was performed and allowed to establish the connection of four fragments as follows: C-11-C-12-C-7-C-13-C-14, C-2-C-3-C-4-C-5, C-18-C-10-C-9, and C-15-C-16. The connection between C-14 and C-15 was deduced from HMBC correlation of H-16 to C-14 and C-15. The HMBC correlation of H-4 to C-14 suggested the connection of C-5 to C-14. The C-N-C connection between C-3 and C-15 was deduced by comparison of chemical shift, which were indicative for a 2,6-dimethyl-pyridine moiety or one of its tautomeric forms (e.g. pyridinium ion). The connection of C-5-C-6-C-7 was established based on the HMBC correlation of H-4 to C-6 and H-12 to C-6 and indicative for a cyclopentenone ring. The seven-membered tropolone ring was established by the connection of C-9-C-8-C-6 due to the unsaturation requirement. The connection between the deoxysugar moiety and tropolone moiety was established by the observation of HMBC correlations of H-17 to C-9 and C-10, H-19 to C-10. The relative configuration of the deoxysugar was assigned based on the detection of nuclear Overhauser enhancements (nOe) effect between H-21 and H-17. Finally, the planar structure of **1** was confirmed by single crystal X-ray diffraction.
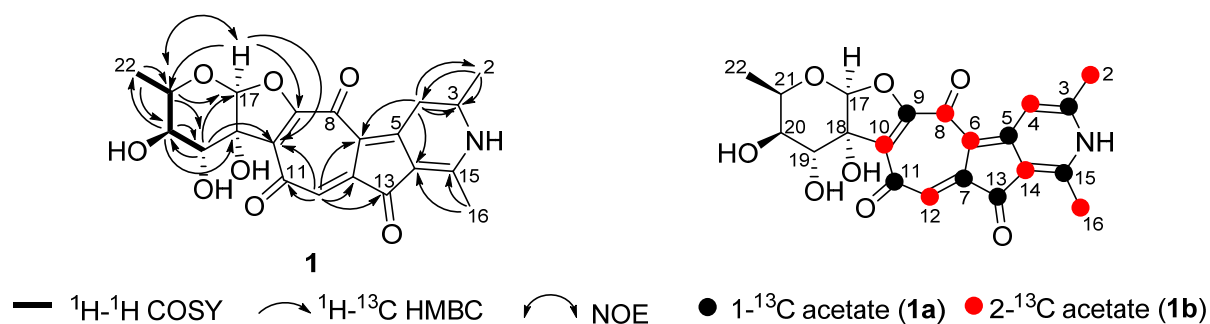
Figure S5. Key COSY, HMBC and NOE correlations and ^{13}C-acetate labeling pattern of rubterolone A (**1a,1b**).

**Rubterolone B** (**2**): ESI-HRMS analysis indicated a molecular formula of $C_{26}H_{25}O_9N$ for rubterolone B (**2**) (m/z 496.1596 [M+H]$^+$, calcd. 496.1602 $\Delta = -1.13$ ppm). Comparative analysis of ^{1}H NMR, ^{13}C NMR and HSQC spectra indicated the same core structure as compound **1** with an additional carbonyl group (δ_C 166.3 ppm), one olefinic carbon (δ_C 137.7 ppm/δ_H 6.36 ppm), one quaternary olefinic carbon (δ_C 127.7 ppm) and two methyl groups (δ_C 11.8 ppm/δ_H 1.58 ppm; δ_C 13.9 ppm/δ_H 1.44 ppm), which is in agreement with the detected molecular formula. The COSY correlation of H-27 to H-25, the corresponded HMBC correlations of H-25 to C-23, C-24, C-26 and C-27 indicated a dimethyl-α,β-unsaturated carbonyl moiety. HMBC correlations (H-20/C-23) revealed the connection between C-20 and the additional carbonyl group (δ_C 166.3 ppm) indicative for an ester bond. This conclusion was also confirmed by a deshielding effect on C-20 (δ_C 71.4 ppm/δ_H 4.71 ppm) compared to compound **1** (δ_C 68.4 ppm/δ_H 3.61 ppm). Based on a comparative analysis of the chemical shift of H-25 (δ_H 6.36 ppm, Fig. S8) and missing nOe signals in 1D and 2D NMR experiments, the additional ester moiety was assigned as an angelate ester.[14,15] The relative configuration of the deoxysugar was assigned based on the detection of nuclear Overhauser enhancements (nOE) effect between H-21 and H-17 and its similarity with compound **1**.
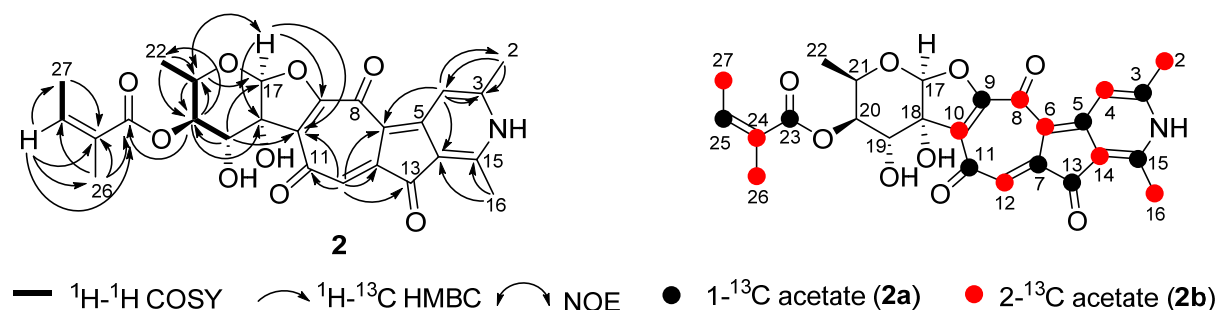
Figure S6. Key COSY, HMBC and NOE correlations and ^{13}C-acetate labeling pattern of rubterolone B (**2a, 2b**).

Rubterolone C (3): The molecular formula of rubterolone C (**3**) was assigned as $C_{23}H_{21}O_{10}N$ based on ESI-HRMS data (*m/z* 472.1229 [M+H]$^+$, calcd. 472.1238 Δ = −2.04 ppm). Comparative 1D and 2D NMR analysis indicated the same core structure as compd. **1**, but carrying CH_2CO_2H moiety (δ_C 167.0 ppm, δ_C 52.6 ppm/δ_H 4.82 ppm) at N1 based on HMBC correlation of H-23 to C-24, and NOESY correlations of H-23 to H_3-2 and H_3-16.
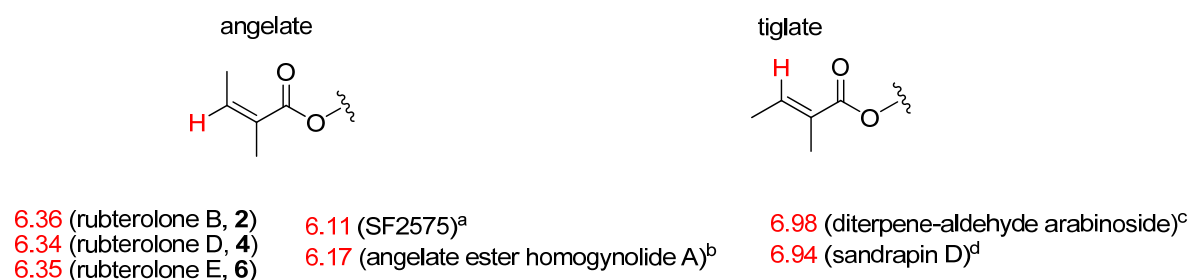
Rubterolone D (4): The molecular formula of rubterolone D (**4**) was assigned as $C_{28}H_{27}O_{11}N$ based on ESI-HRMS data (*m/z* 554.1652 [M+H]$^+$, calcd. 554.1657 Δ = −0.95 ppm). Comparative 1D and 2D NMR analysis indicated the same core structure as compound **2**, but carrying CH_2CO_2H moiety (δ_C 164.8 ppm, δ_C 54.5 ppm/δ_H 4.53 ppm) at N1 based on HMBC correlations of H-28 to C-3, C-15 and C-29.
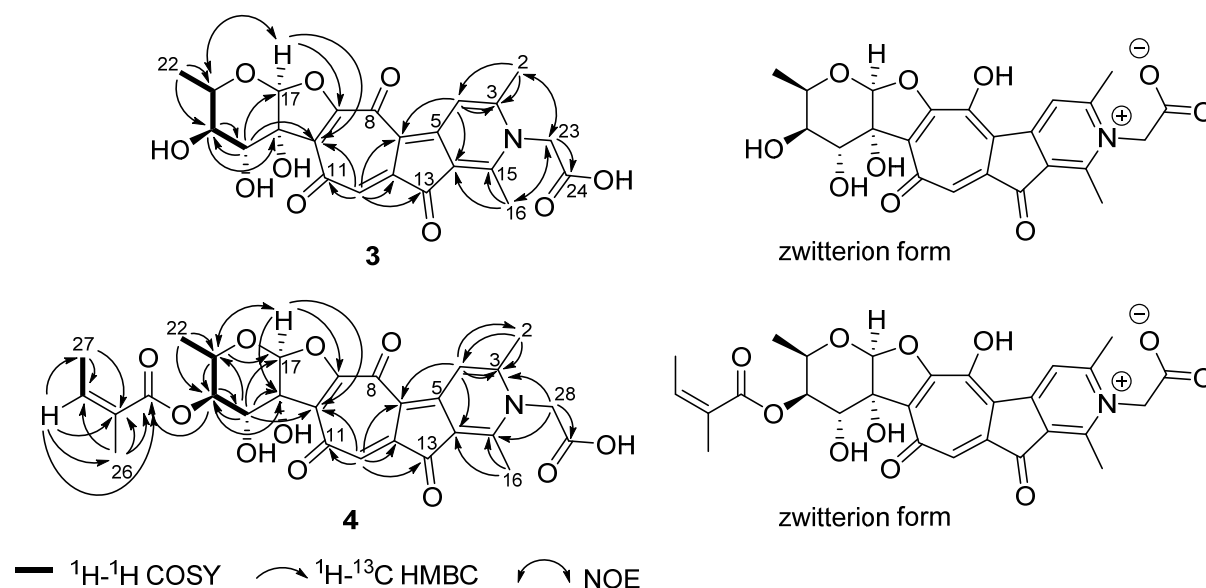
Figure S7. Key COSY, HMBC and NOE correlations of rubterolone C and D (**3** and **4**) and the pyridine inner salt tautomeric forms, respectively.

Rubterolone E (5): The molecular formula of rubterolone E (**5**) was assigned as $C_{24}H_{23}O_{10}N$ based on ESI-HRMS data (*m/z* 486.1388 [M+H]$^+$, calcd. 486.1395 Δ = −1.40 ppm). Comparative analysis of 1D and 2D NMR spectra indicated the same core structure as compd. **3**, instead the replacement of CH_2CO_2H moiety by CH_3CHCO_2H (δ_C 169.6 ppm, δ_C 60.5 ppm/δ_H 5.45 ppm, δ_C 16.2 ppm/δ_H 1.66 ppm) at N1 based on HMBC correlations of H-25 to C-23 and C-24, and NOESY correlations of H-23 and H_3-25 to H_3-2.

Rubterolone F (6): The molecular formula of rubterolone F (**6**) was assigned as $C_{29}H_{29}O_{11}N$ based on ESI-HRMS data (*m/z* 568.1808 [M+H]$^+$, calcd. 568.1813 Δ = −0.86 ppm). Comparative 1D and 2D NMR analysis

indicated the same core structure as compd. **4**, but replacing CH_2CO_2H moiety by CH_3CHCO_2H (δ_C 168.9 ppm, δ_C 63.8 ppm/δ_H 5.08 ppm, δ_C 17.2 ppm/δ_H 1.61 ppm) at N1 based on HMBC correlations of H-30 to C-28 and C-29, and NOESY correlations of H-28 to H_3-2.

angelate   tiglate

6.36 (rubterolone B, **2**)   6.11 (SF2575)[a]   6.98 (diterpene-aldehyde arabinoside)[c]
6.34 (rubterolone D, **4**)   6.17 (angelate ester homogynolide A)[b]   6.94 (sandrapin D)[d]
6.35 (rubterolone E, **6**)

Figure S8. Comparison of ^{1}H chemical shift of angelate moiety in rubterolone B (**2**), D (**4**), E (**6**) and reported angelate and tiglate moiety containing compounds (a: SF2575;[14a] b: angelate ester homogynolide A;[14b] c: diterpene-aldehyde arabinoside from Gutierrezia sphaerocephala[15a]; d: sandrapin D[15b]).

Tautomeric forms

Rubterolones contain a tropolone moiety, which is able to rapidly interconvert between keto-enol tautomers in solution. In addition, the unique 2,3,4,6-tetrasubstituted pyridine ring is able to undergo pyridine/dihydropyridine-type tautomerization (solvent-dependent color change).
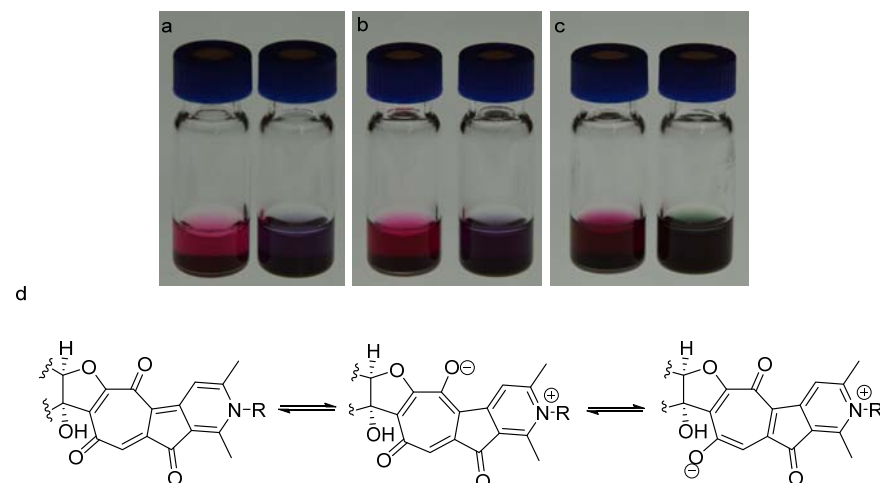
Figure S9. Solvent effect (tautomerization) on rubterolones A, B and D (**1**, **2**, **4**): a) rubterolone A (**1**), left: 50% MeOH/50% H_2O solution (0.5 mg/mL), right: DMSO solution (0.5 mg/mL); b) rubterolone B (**2**), left: 50% MeOH/50% H_2O solution (0.5 mg/mL), right: DMSO solution (0.5 mg/mL); c) rubterolone D (**4**), left: 50% MeOH/50% H_2O solution (0.5 mg/mL), right: DMSO solution (0.5 mg/mL); d) generalized drawing of possible tautomeric forms.

5. Chemical Modifications

Preparation of 4-bromo benzoyl rubterolone B (2d)
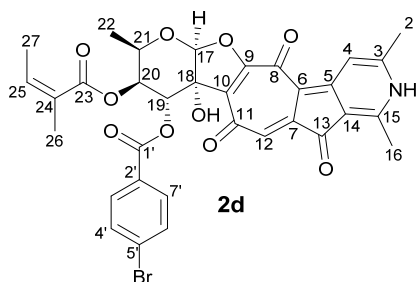
To **2** (1 mg, 2.41 µmol) was added 4-bromobenzoyl chloride in CH_2Cl_2 (10 mg, 4.56 µmol, 450 µL as 0.1 M stock solution) and DMAP (8.3 mg, 8.60 µmol) were added. The reaction was stirred at room temperature under Ar atmosphere and monitored by TLC analysis. After 3 h, the reaction was quenched by saturated NaCl solution and the mixture was extracted three times using EtOAc (3 mL each). The EtOAc extract was completely dried under reduced pressure and purified by RP-HPLC (Phenomonex C18(2) 250 x 10 mm) using the following gradient: 0–5 min, 45% B; 5–20 min, 45%–100% B; 20–25 min, 100% B (A: dd H_2O + 0.1% formic acid; B: MeCN) with a flow rate of 2.0 mL/min. The desired monoacylation product **2d** (0.2 mg, 0.3 µmol, 12%) was eluted at 17.0 min.

Preparation of propargyl-rubterolone C (4a)
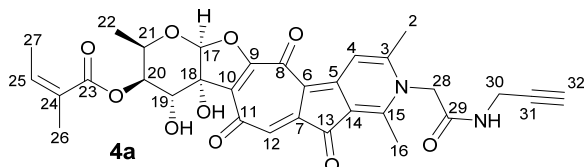
Rubterolone D (**4**, 1.0 mg, 1.81 µmol) was dissolved in DMF (70 µL) and cooled to 3 °C. To the deep green solution were subsequently added a stock solution of propargylic amine (20 µL of a 2.3 M solution, 45.2 µmol) and (1-cyano-2-ethoxy-2-oxoethylidenaminooxy)dimethylamino-morpholino-carbenium hexafluorophosphate (COMU, 1.5 mg, 3.6 µmol).[16] The mixture was shaken under a temperature below 5 °C and the reaction progress was monitored via TLC (CHCl$_3$/MeOH/AcOH 75/25/1). Additional COMU (1.5 mg, 3.6 µmol) was added every 30 min as well as additional propargylic amine (20 µl of a 2.3 M solution, 45.2 µmol) every 60 min shaking time. Upon completion or after 3 h the reaction mixture was concentrated in vacuo and submitted to semi-preparative HPLC and purified by RP-HPLC (Phenomonex C18(2) 250 x 10 mm) using the following gradient: 0–5 min, 40% B; 5–20 min, 40%–100% B; 20–25 min, 100% B (A: dd H_2O + 0.1% formic acid; B: MeCN) with a flow rate of 2.0 mL/min. The desired propargyl-rubterolone D (**4a,** 0.1 mg, 0.18 µmol, 10%) was eluted at 12.0 min.

6. Bioassays of Pure Compounds

Antimicrobial assay

The activity assay was done by the broth dilution method according to the NCCLS (National Committee for Clinical Laboratory Standards).[17]

Table S4. Antimicrobial activity of crude extracts from *Actinobacteria* isolates, ciprofloxacin (cip) and amphotericin (Amph) towards Gram (+) and Gram (–) bacteria and fungi.

strain	*B. subtilis*	*S. aureus*	*E. coli*	*P. aeruginosa*	*M. vaccae*	*S. salmonic.*	*C. albicans*	*P. notatum*
RB8	0	0	0	0	0	0	0	0
RB24.	0	0	0	0	0	0	0	0
5-2 (RB29)	14[a]	0	0	0	0	0	0	0
RB34	0	0	0	0	0	0	0	0
RB42	0	0	0	0	0	0	0	0
RB62	0	0	0	0	0	0	0	0
Cip	30	20	24/32p	28/36p	23P	-	-	-
Amph	-	-	-	-	-	18P	21	18

[a]Zone of inhibition (mm)

Antiproliferative and cytotoxic assays

Implementation of the antiproliferative and cytotoxic assays as well as information about cells and culture conditions were reported elsewhere.[18] Compounds were assayed using human umbilical vein endothelial cells HUVEC (ATCC CRL-1730), human chronic myeloid leukemia cells K-562 (DSM ACC 10) for their antiproliferative effects (GI_{50}) as well as using human cervix carcinoma cells HeLa (DSM ACC 57) for their cytotoxic effects (CC_{50}).

Table S5. Antiproliferative effect and cytotoxicity of ruterolones A, B and D (**1**, **2**, **4**)

compound	antiproliferative effect GI_{50} [µg/mL]		cytotoxicity CC_{50} [µg/mL]
	HUVEC[a]	K-562[b]	HeLa[c]
1	>50	>50	>50
2	>50	>50	>50
4	>50	>50	>50

[a]HUVEC: human umbilical vein endothelial cells; [b]K-562 cell line: human immortalized myelogenous leukemia line; [c]HeLa: human cervical cancer cell line.

7. Crystal Structure Determination

The intensity data were collected on a Nonius KappaCCD diffractometer, using graphite-monochromated Mo-K$_\alpha$ radiation. Data were corrected for Lorentz and polarization effects; absorption was taken into account on a semi-empirical basis using multiple-scans [19,20,21]

The structure was solved by direct methods (SHELXS[22]) and refined by full-matrix least squares techniques against Fo^2 (SHELXL-97[22]). All hydrogen atoms (with exception of the water molecule O3W) were located by difference Fourier synthesis and refined isotropically. ORTEP-3[23] was used for structure representations.

Crystal Data for rubterolone A (1): $C_{21}H_{22.5}NO_{9.75}$, Mr = 444.90 gmol^{-1}, red-brown prism, size 0.134 x 0.044 x 0.042 mm^3, monoclinic, space group C 2, a = 18.1189(8), b = 14.5096(5), c = 7.3114(3) Å, β = 93.922(2)°, V = 1917.65(13) Å^3 , T= -140 °C, Z = 4, $\rho_{calcd.}$ = 1.541 gcm^{-3}, μ (Mo-K$_\alpha$) = 1.23 cm^{-1}, multi-scan, transmin: 0.6826, transmax: 0.7456, F(000) = 934, 11572 reflections in h(-21/23), k(-18/18), l(-9/9), measured in the range 2.79° ≤ Θ ≤ 27.48°, completeness Θ$_{max}$ = 99.6%, 4295 independent reflections, R$_{int}$ = 0.0296, 3881 reflections with F$_o$ > 4σ(F$_o$), 378 parameters, 1 restraints, R1$_{obs}$ = 0.0392, wR$^2_{obs}$ = 0.0794, R1$_{all}$ = 0.0481, wR$^2_{all}$ = 0.0850, GOOF = 1.114, Flack-parameter 0.4(8), largest difference peak and hole: 0.178 / -0.182 e Å^{-3}.

Supporting Information Available: Crystallographic data deposited at the Cambridge Crystallographic Data Centre under CCDC-1524117 for rubterolone A contain the supplementary crystallographic data excluding structure factors; this data can be obtained free of charge via www.ccdc.cam.ac.uk/conts/retrieving.html (or from the Cambridge Crystallographic Data Centre, 12, Union Road, Cambridge CB2 1EZ, UK; fax: (+44) 1223-336-033; or deposit@ccdc.cam.ac.uk).

8. NMR Tables

Table S6. NMR Data (DMSO-d_6, at 303 K) for Rubterolone A (**1**).[a]

position	δ_C, mult.[b]	δ_H, mult. (*J* in Hz)	COSY	HMBC	NOESY	1D NOE
				rubterolone A (**1**)		
1						
2	25.2, CH$_3$	2.41, s		3, 4		
3	163.7, qC					
4	115.1, CH	8.07, s		2, 3, 6, 14		
5	159.0, qC					
6	115.4, qC					
7	137.8, qC					
8	165.2, qC					
9	164.9, qC					
10	127.8, qC					
11	182.1, qC					
12	114.5, CH	6.38, s		6, 7, 10, 11, 13		
13	196.5, qC					
14	119.8, qC					
15	155.2, qC					
16	20.8, CH$_3$	2.55, s		14, 15		
17	105.7, CH	5.27, s		9, 10, 21	21	21
18	82.2, qC					
19	70.8, CH	4.00, d, (7.9)	20	10, 17, 20		
20	68.4, CH	3.61, dd, (7.9, 5.3)	19, 21	18, 19, 22		
21	70.3, CH	4.08, q, (6.7)	20, 22	17, 19	17	17
22	15.7, CH$_3$	1.09, d, (6.7)	21	20, 21		
n.d.[c]	OH	4.81, br s				
n.d.[c]	OH	5.35, br s				
n.d.[c]	OH	7.24, br s				
n.d.[c]	NH	8.34, br s				

[a] 600 MHz for ^{1}H NMR and 150 MHz for ^{13}C NMR

[b] numbers of attached protons were determined by analysis of 2D spectra.

[c] broad singlet, can't be unambiguously assigned by analysis of 2D spectra.

Table S7. ^{13}C NMR Data Based on [^{13}C]-labeling Experiments (DMSO-d_6, at 303 K) for Rubterolone A (**1**).

position	(**1**)[b]	(**1a**) [1-^{13}C][c]	(**1b**) [2-^{13}C][d]	(**1c**) [1,2-[13]C$_2$][e]	INADEQUATE [1,2-[13]C$_2$][f]
			δ$_C$, mult.[a]		
1					
2	25.2, CH$_3$	n.d.	24.7, br s	20.6, br s	3
3	163.7, qC	157.2, br d, 64, (+)		156.4, br s	2, 4, 5
4	115.1, CH	n.d.	114.8, s	114.5, t, 62	3, 5
5	159.0, qC	161.4, s, (+)		161.7, q, 55	3, 4
6	115.4, qC	n.d.	114.8, s	111.7, m	
7	137.8, qC	137.5, d, 48, (+)		137.5, q, 62	12, 13
8	165.2, qC	n.d.	167.4, br s	169.1, m	
9	164.9, qC	163.8, s, (+)		163.7, t, 66	10
10	127.8, qC	n.d.	127.6, br s	127.1, m	9, 18
11	182.1, qC	182.8, s, (+)		182.9, t, 60	12
12	114.5, CH	n.d.	114.8, s	116.8, m	7, 11
13	196.5, qC	193.9, m, (+)		193.7, t, 58	7, 14
14	119.8, qC	n.d.	119.9, s	120.2, m	13
15	155.2, qC	150.2, br d, 52, (+)		149.4, m	16
16	20.8, CH$_3$	n.d.	20.4, br s	16.1, br s	15
17	105.7, CH	104.8, d, 40	105.6, br s	104.6, d, 41	18
18	82.2, qC	81.1, d, 42	81.8, m	80.9, q, 40	10, 17, 19
19	70.8, CH	69.0, m	70.0, m	68.9, m	18, 20
20	68.4, CH	69.0, m	68.3, m	68.0, t, 40	19, 21
21	70.3, CH	69.0, m	70.0, m	68.9, m	19, 22
22	15.7, CH$_3$	15.7, d, 42	15.5, d, 41	15.8, d, 41	21

[a] numbers of attached protons were determined by analysis of 2D spectra

[b] original compound, 150 MHz for ^{13}C NMR

[c] 1-^{13}C acetate labeled compound, 125 MHz for ^{13}C NMR

[d] 2-^{13}C acetate labeled compound, 150 MHz for ^{13}C NMR

[e] 1,2-[13]C$_2$ acetate (50%) labeled compound, 150 MHz for ^{13}C NMR

[f] INADEQUATE experiment was recorded on 150 MHz with D4 = 0.02 s/0.04 s/0.0065 s respectively.

Table S8. NMR Data (DMSO-d_6, at 303 K) for Rubterolone B (**2**).[a]

position	δ_C, mult.[b]	δ_H, mult. (J in Hz)	COSY	HMBC	NOESY	1D NOE
				rubterolone B (**2**)		
1						
2	22.5, CH$_3$	2.48, s		3, 4		
3	159.8, qC					
4	114.5, CH	8.17, s		2, 3, 6, 14		
5	168.1, qC					
6	112.1, qC					
7	137.1, qC					
8	163.1, qC					
9	164.9, qC					
10	125.9, qC					
11	182.3, qC					
12	116.6, CH	6.21, s		6, 7, 10, 11, 13		
13	195.3, qC					
14	119.9, qC					
15	152.7, qC					
16	18.7, CH$_3$	2.62, s		14, 15		
17	103.7, CH	5.31, s		9, 10, 18		21
18	80.5, qC					
19	64.8, CH	4.99, d, (4.5)	20	10, 17, 20		
20	71.7, CH	4.74, dd, (4.5, 1.5)	19, 21	18, 21, 23	22	
21	64.9, CH	4.23, qd, (6.7, 1.5)	20, 22	17, 20, 22		17
22	15.9, CH$_3$	0.97, d, (6.7)	21	20, 21	20	
23	166.3, qC					
24	127.4, qC					
25	137.8, CH	6.36, qd, (6.9, 1.5)	27	23, 24, 26, 27		26, 27
26	11.8, CH$_3$	1.58, d, (1.5)		23, 24, 25		27
27	13.9, CH$_3$	1.44, d, (6.9)	25	23, 24, 25		25, 26
n.d.[c]	OH	4.11, br s				
n.d.[c]	OH	5.88, br s				
n.d.[c]	NH	8.13, br s				

[a] 600 MHz for ^{1}H NMR and 150 MHz for ^{13}C NMR

[b] numbers of attached protons were determined by analysis of 2D spectra.

[c] broad singlet, can't be unambiguously assigned by analysis of 2D spectra.

Table S9. ^{13}C NMR Data Based on [^{13}C]-labeling Experiments (DMSO-d_6, at 303 K) for Rubterolone B (**2**).

position	(2)[b]	(2a) [1-^{13}C][c]	(2b) [2-^{13}C][d]	(2c) [1,2-^{13}C][e]	INADEQUATE [1,2-^{13}C] [f]
			δ_C, mult.[a]		
1					
2	22.5, CH$_3$	n.d.	25.1, d, 8	21.0, br s	
3	159.8, qC	156.0, s	n.d.	157.0, br s	
4	114.5, CH	n.d.	114.6, d, 8	114.5, t, 60	5
5	163.1, qC	161.7, s	n.d.	161.4, t, 52	4
6	112.1, qC	n.d.	113.4, d, 72	111.3, br s	
7	137.1, qC	136.9, d, 48	n.d.	136.8, d, 68	
8	168.1, qC	n.d.	166.7, d, 72	169.0, t, 64	
9	164.9, qC	164.1, s	n.d.	164.2, t, 67	
10	125.9, qC	n.d.	126.0	126.0, m	18
11	182.3, qC	182.7, s	n.d.	182.6, t, 58	
12	116.6, CH	n.d.	115.3, d, 17	117.4, m	
13	195.3, qC	193.8, d, 48	n.d.	194.3, t, 57	14
14	119.9, qC	n.d.	119.7, s	120.0, m	13
15	152.7, qC	149.4, s	n.d.	150.0, br s	16
16	18.7, CH$_3$	n.d.	20.7, d, 5	16.6, d, 41	15
17	103.7, CH	103.0, d, 42	103.6, d, 41	103.0, d, 41	18
18	80.5, qC	80.2, d, 42	80.7, m	80.3, q, 43	10, 17, 19
19	64.8, CH	64.3, d, 42	65.2, m	64.2, q, 43	18, 20
20	71.7, CH	71.6, d, 42	71.6, m	71.7, d, 43	19, 21
21	64.9, CH	64.3, d, 42	65.2, m	64.7, q, 43	20, 22
22	15.9, CH$_3$	15.9, s	16.7, d, 42	15.9, d, 41	21
23	166.3, qC	165.9, s	n.d.	166.0, d, 72	24
24	127.4, qC	n.d.	127.2, d, 46	127.4, m	23, 26
25	137.8, CH	137.4, s	n.d.	137.6, t, 72	27
26	11.8, CH$_3$	11.7	11.7, d, 46	11.7, d, 43	24
27	13.9, CH$_3$	n.d.	13.9, s	13.9, d, 43	25

[a] numbers of attached protons were determined by analysis of 2D spectra.

[b] original compound, 150 MHz for ^{13}C NMR

[c] 1-^{13}C acetate labeled compound, 125 MHz for ^{13}C NMR

[d] 2-^{13}C acetate labeled compound, 150 MHz for ^{13}C NMR

[e] 1,2-[13]C$_2$ acetate (50%) labeled compound, 150 MHz for ^{13}C NMR

[f] INADEQUATE experiment was recorded on 150 MHz with D4 = 0.02 s/0.04 s/0.0065 s respectively.

Table S10. Comparison of ^{1}H NMR Data (DMSO-d_6, at 303 K) of 4-Bromobenzoyl rubterolone (**2d**) and Rubterolone B (**2**).[a]

	δ_H, mult. (*J* in Hz)	
position	4-bromobenzoyl rubterolone B (**2d**)	rubterolone B (**2**)
1		
2	2.41, s	2.48, s
3		
4	8.08, s	8.17, s
5		
6		
7		
8		
9		
10		
11		
12	6.19, s	6.21, s
13		
14		
15		
16	2.56, s	2.62, s
17	5.49, s	5.31, s
18		
19	6.81, d, (4.5)	4.99, d, (4.5)
20	4.90, dd, (4.5, 1.5)	4.74, dd, (4.5, 1.5)
21	4.32, qd, (6.7, 1.5)	4.23, qd, (6.7, 1.5)
22	0.99, d, (6.7)	0.97, d, (6.7)
23		
24		
25	6.33, qd, (7.2, 1.5)	6.36, qd, (6.9, 1.5)
26	1.59, d, (1.5)	1.58, d, (1.5)
27	1.40, dd, (7.2)	1.44, d, (6.9)
1'		
2'		
3'	8.01, dt, (8.5, 2.4)	
4'	7.76 dt, (8.5, 2.4)	
5'		
6'	7.76 dt, (8.5, 2.4)	
7'	8.01, dt, (8.5, 2.4)	
n.d. [b]		4.11, br s
n.d. [b]	5.78, br s	5.88, br s
n.d. [b]	8.30, br s	8.13, br s

[a] 500 MHz for ^{1}H NMR of **2b**; 600 MHz for ^{1}H NMR of **2**

[b] broad singlet, can't be unambiguously assigned by analysis of 2D spectra.

Table S11. NMR Data (DMSO-d_6, at 303 K) for Rubterolone C (**3**).[a]

position	δ_C, mult.[b]	δ_H, mult. (J in Hz)	COSY	HMBC	NOESY
1					
2	21.9, CH$_3$	2.59, br s		3, 4	4, 23
3	157.7, qC				
4	116.1, CH	8.37, s		3, 4, 14	2
5	160.2, qC				
6	110.3, qC				
7	137.4, qC				
8	169.8, qC				
9	163.6, qC				
10	127.2, qC				
11	183.2, qC				
12	117.6, CH	6.37, s		6, 7, 10, 11, 13, 18	
13	193.7, qC				
14	121.6, qC				
15	151.5, qC				
16	14.2, CH$_3$	2.77, s		14, 15	23
17	104.4, CH	5.27, s		9, 10	21
18	80.7, qC				
19	68.5, CH	4.57, d, (5.4)	20	10, 17, 18, 20, 21	20
20	69.1, CH	3.48, dd, (5.4, 2.7)	19, 21	18, 19	19, 21
21	67.6, CH	4.03, qd, (6.6, 2.7)	20, 22	22	17, 20
22	15.8, CH$_3$	1.06, d, (6.6)	21	20, 21	
23	52.6, CH$_2$	4.82, br s		24	2, 16
24	167.0, qC				
n.d. [c]	OH	4.54, br s			
n.d. [c]	OH	5.52, br s			
n.d. [c]	OH	6.37, br s			

[a] 600 MHz for ^{1}H NMR and 150 MHz for ^{13}C NMR

[b] numbers of attached protons were determined by analysis of 2D spectra.

[c] broad singlet, can't be unambiguously assigned by analysis of 2D spectra.

Table S12. NMR Data (DMSO-d_6, at 303 K) for Rubterolone D (**4**).[a]

position	δ_C, mult.[b]	δ_H, mult. (*J* in Hz)	COSY	HMBC	NOESY
			rubterolone D (4)		
1					
2	22.0, CH$_3$	2.58, s		3, 4	
3	157.6, qC				
4	116.0, CH	8.39, s		2, 3, 6, 14	
5	159.9, qC				
6	109.8, qC				
7	136.8, qC				
8	169.5, qC				
9	164.1, qC				
10	126.2, qC				
11	182.9, qC				
12	117.9, CH	6.28, s		6, 7, 10, 11, 13	
13	194.1, qC				
14	121.3, qC				
15	151.7, qC				
16	14.2, CH$_3$	2.78, s		14, 15	
17	102.9, CH	5.34, s		9, 10, 18	21
18	80.2, qC				
19	64.2, CH	5.08, d, (4.2)	20	10, 17, 18, 20, 21	
20	71.2, CH	4.70, dd, (4.2, 1.2)	19, 21	18, 19, 23	
21	64.4, CH	4.24, qd, (6.7, 1.2)	20, 22	17, 20	17
22	15.9, CH$_3$	0.97, d, (6.7)	21	20, 21	
23	165.9, qC				
24	127.4, qC				
25	137.4, CH	6.34, qd, (6.3, 1.7)	27	23, 24, 26, 27	
26	11.7, CH$_3$	1.56, d, (1.7)		23, 24, 25	
27	13.9, CH$_3$	1.49, d, (6.3)	25	23, 24, 25	
28	54.5, CH$_2$	4.53, br s		3, 15, 29	
29	164.8, qC				
n.d. [c]	OH	5.38, br s			
n.d. [c]	OH	5.80, br s			
n.d. [c]	OH	8.44, br s			

[a] 600 MHz for ^{1}H NMR and 150 MHz for ^{13}C NMR

[b] numbers of attached protons were determined by analysis of 2D spectra.

[c] broad singlet, can't be unambiguously assigned by analysis of 2D spectra.

Table S13. Comparison of ^{1}H NMR Data (DMSO-d_6, at 303 K) of Propargyl-rubterolone D (**4a**) and Rubterolone D (**4**).[a]

position	δ$_H$, mult. (*J* in Hz)	
	propargyl-rubterolone D (**4a**)	rubterolone D (**4**)
1		
2	2.59, s	2.58, s
3		
4	8.41, s	8.39, s
5		
6		
7		
8		
9		
10		
11		
12	6.23, s	6.28, s
13		
14		
15		
16	2.78, s	2.78, s
17	5.35, s	5.34, s
18		
19	5.07, d, (4.3)	5.08, d, (4.2)
20	4.70, dd, (4.3, 1.3)	4.70, dd, (4.2, 1.2)
21	4.24, qd, (6.5, 1.3)	4.24, qd, (6.7, 1.2)
22	0.97, d, (6.5)	0.97, d, (6.7)
23		
24		
25	6.35, qd, (7.2, 1.5)	6.34, qd, (6.3, 1.7)
26	1.56, br s	1.56, d, (1.7)
27	1.44, dd, (7.2, 1.5)	1.49, d, (6.3)
28	5.08, br s	4.53, br s
29		
30	3.97, br d, (2.1)	
31		
32	3.22, t, (2.1)	
n.d.[b]		5.38, br s
n.d.[b]		5.80, br s
n.d.[b]	9.10, br s	8.44, br s

[a] 600 MHz for **4** and 500 MHz for **4a**

[b] broad singlet, can't be unambiguously assigned.

Table S14. NMR Data (DMSO-d_6, at 303 K) for Rubterolone E (**5**).[a]

position	δ_C, mult.[b]	δ_H, mult. (J in Hz)	COSY	HMBC	NOESY
1					
2	23.2, CH_3	2.71, br s[d]			23, 25
3	158.0, qC				
4	116.6, CH	8.35, s		2, 3, 14	
5	159.9, qC				
6	110.3, qC				
7	137.4, qC				
8	169.8, qC				
9	163.5, qC				
10	127.1, qC				
11	183.2, qC				
12	117.6, CH	6.36, s		6, 7, 10, 11, 13	
13	193.4, qC				
14	122.4, qC				
15	152.2, qC				
16	22.1, CH_3	2.62, br s[d]			
17	104.5, CH	5.27, s		9, 10, 18, 21	
18	80.8, qC				
19	68.6, CH	4.55, d, (5.4)	20	10, 17, 18, 20, 21	
20	69.1, CH	3.49, dd, (5.4, 3.1)	19, 21	17, 18, 22	
21	67.8, CH	4.04, qd, (6.3, 3.1)	20, 22	17, 22	
22	15.9, CH_3	1.07, d, (6.3)	21		
23	60.5, CH	5.43, br s	25		2
24	169.6, qC				
25	16.2, CH_3	1.66, br d	23	23, 24	2
n.d.[c]	OH	4.69, br s			
n.d.[c]	OH	5.42, br s			
n.d.[c]	OH	5.56, br s			
n.d.[c]	OH	7.21, br s			

[a] 600 MHz for ^{1}H NMR and 150 MHz for ^{13}C NMR

[b] numbers of attached protons were determined by analysis of 2D spectra.

[c] broad singlet, can't be unambiguously assigned by analysis of 2D spectra.

[d] broad signals caused by rotation.

Table S15. NMR Data (DMSO-d_6, at 303 K) for Rubterolone F (**6**).[a]

position	δ_C, mult.[b]	δ_H, mult. (J in Hz)	COSY	HMBC	NOESY
			rubterolone F (**6**)		
1					
2	22.8, CH$_3$	2.67, br s[d]		3	2
3	156.3, qC				
4	116.6, CH	8.38, s		5	
5	158.0, qC				
6	109.9, qC				
7	137.0, qC				
8	169.5, qC				
9	164.5, qC				
10	124.4, qC				
11	185.0, qC				
12	117.6, CH	6.23, s		6, 7, 10, 13	
13	193.9, qC				
14	124.3, qC				
15	151.9, qC				
16	16.1, CH$_3$	2.78, br s[d]			
17	104.5, CH	5.38, s		9, 10	
18	83.7, qC				
19	69.6, CH	4.53, d, (3.3)	20	18, 21	
20	70.8, CH	4.82, d, (3.3)	19, 21	18, 19, 21, 23	
21	63.6, CH	4.15, q, (6.6)	20, 22	17, 20, 22	
22	16.1, CH$_3$	1.01, d, (6.6)	21	20, 21	
23	166.1, qC				
24	127.6, qC				
25	137.1, CH	6.35, q, 7.8	27	23	
26	11.8, CH$_3$	1.53, s		23, 24, 25, 27	
27	14.1, CH$_3$	1.42, d, 7.8	25	24, 25	
28	63.8, CH	5.08, br s	30		2
29	168.3, qC				
30	17.2, CH$_3$	1.61, br d, 6.6	28	28, 29	
n.d.[c]	OH	5.33, br s			
n.d.[c]	OH				
n.d.[c]	OH	8.20, br s			

[a] 600 MHz for ^{1}H NMR and 150 MHz for ^{13}C NMR

[b] numbers of attached protons were determined by analysis of 2D spectra.

[c] broad singlet, can't be unambiguously assigned by analysis of 2D spectra.

[d] broad signals caused by rotation.

Table S16. Comparison of ^{1}H NMR Data (DMSO-d_6, at 303 K) of **1**–**6**

position	A (**1**)	C (**3**)	E (**5**)	B (**2**)	D (**4**)	F (**6**)
			δ_H, mult. (J in Hz)			
1						
2	2.41, s	2.59, br s	2.71, br s[d]	2.48, s	2.58, s	2.67, br s[d]
3						
4	8.07, s	8.37, s	8.35, s	8.17, s	8.39, s	8.38, s
5						
6						
7						
8						
9						
10						
11						
12	6.38, s	6.37, s	6.36, s	6.21, s	6.28, s	6.23, s
13						
14						
15						
16	2.55, s	2.77, s	2.62, br s[d]	2.62, s	2.78, s	2.78, br s[d]
17	5.27, s	5.27, s	5.27, s	5.31, s	5.34, s	5.38, s
18						
19	4.00, d, (7.9)	4.57, d, (5.4)	4.55, d, (5.4)	4.99, d, (4.5)	5.08, d, (4.2)	4.53, d, (3.3)
20	3.61, dd, (7.9, 5.3)	3.48, dd, (5.4, 2.7)	3.49, dd, (5.4, 3.1)	4.74, dd, (4.5, 1.5)	4.70, dd, (4.2, 1.2)	4.82, d, (3.3)
21	4.08, q, (6.7)	4.03, qd, (6.6, 2.7)	4.04, qd, (6.3, 3.1)	4.23, qd, (6.7, 1.5)	4.24, qd, (6.7, 1.2)	4.15, q, (6.6)
22	1.09, d, (6.7)	1.06, d, (6.6)	1.07, d, (6.3)	0.97, d, (6.7)	0.97, d, (6.7)	1.01, d, (6.6)
23		4.82, br s	5.43, br s			
24						
25			1.66, br d	6.36, qd, (6.9, 1.5)	6.34, qd, (6.3, 1.7)	6.35, q, 7.8
26				1.58, d, (1.5)	1.56, d, (1.7)	1.53, s
27				1.44, d, (6.9)	1.49, d, (6.3)	1.42, d, 7.8
28					4.53, br s	5.08, br s
29						
30						1.61, br d, 6.6
OH	4.81, br s	4.54, br s	4.69, br s	4.11, br s	5.38, br s	5.33, br s
OH	5.35, br s	5.52, br s	5.42, br s	5.88, br s	5.80, br s	
OH	7.24, br s	6.37, br s	5.56, br s			
NH	8.34, br s		7.21, br s	8.13, br s	8.44, br s	8.20, br s

Table S17. Comparison of ^{13}C NMR Data (DMSO-d_6, at 303 K) of **1–6**

position	δ_C, mult.					
	A (**1**)	C (**3**)	E (**5**)	B (**2**)	D (**4**)	F (**6**)
1						
2	25.2, CH$_3$	21.9, CH$_3$	23.2, CH$_3$	22.5, CH$_3$	22.0, CH$_3$	22.8, CH$_3$
3	163.7, qC	157.7, qC	158.0, qC	159.8, qC	157.6, qC	156.3, qC
4	115.1, CH	116.1, CH	116.6, CH	114.5, CH	116.0, CH	116.6, CH
5	159.0, qC	160.2, qC	159.9, qC	168.1, qC	159.9, qC	158.0, qC
6	115.4, qC	110.3, qC	110.3, qC	112.1, qC	109.8, qC	109.9, qC
7	137.8, qC	137.4, qC	137.4, qC	137.1, qC	136.8, qC	137.0, qC
8	165.2, qC	169.8, qC	169.8, qC	163.1, qC	169.5, qC	169.5, qC
9	164.9, qC	163.6, qC	163.5, qC	164.9, qC	164.1, qC	164.5, qC
10	127.8, qC	127.2, qC	127.1, qC	125.9, qC	126.2, qC	124.4, qC
11	182.1, qC	183.2, qC	183.2, qC	182.3, qC	182.9, qC	185.0, qC
12	114.5, CH	117.6, CH	117.6, CH	116.6, CH	117.9, CH	117.6, CH
13	196.5, qC	193.7, qC	193.4, qC	195.3, qC	194.1, qC	193.9, qC
14	119.8, qC	121.6, qC	122.4, qC	119.9, qC	121.3, qC	124.3, qC
15	155.2, qC	151.5, qC	152.2, qC	152.7, qC	151.7, qC	151.9, qC
16	20.8, CH$_3$	14.2, CH$_3$	22.1, CH$_3$	18.7, CH$_3$	14.2, CH$_3$	16.1, CH$_3$
17	105.7, CH	104.4, CH	104.5, CH	103.7, CH	102.9, CH	104.5, CH
18	82.2, qC	80.7, qC	80.8, qC	80.5, qC	80.2, qC	83.7, qC
19	70.8, CH	68.5, CH	68.6, CH	64.8, CH	64.2, CH	69.6, CH
20	68.4, CH	69.1, CH	69.1, CH	71.7, CH	71.2, CH	70.8, CH
21	70.3, CH	67.6, CH	67.8, CH	64.9, CH	64.4, CH	63.6, CH
22	15.7, CH$_3$	15.8, CH$_3$	15.9, CH$_3$	15.9, CH$_3$	15.9, CH$_3$	16.1, CH$_3$
23		52.6, CH	60.5, CH	166.3, qC	165.9, qC	166.1, qC
24		167.0, qC	169.6, qC	127.4, qC	127.4, qC	127.6, qC
25			16.2, CH$_3$	137.8, CH	137.4, CH	137.1, CH
26				11.8, CH$_3$	11.7, CH$_3$	11.8, CH$_3$
27				13.9, CH$_3$	13.9, CH$_3$	14.1, CH$_3$
28					54.5, CH$_2$	63.8, CH
29					164.8, qC	168.3, qC
30						17.2, CH$_3$

9. NMR and MS Spectra
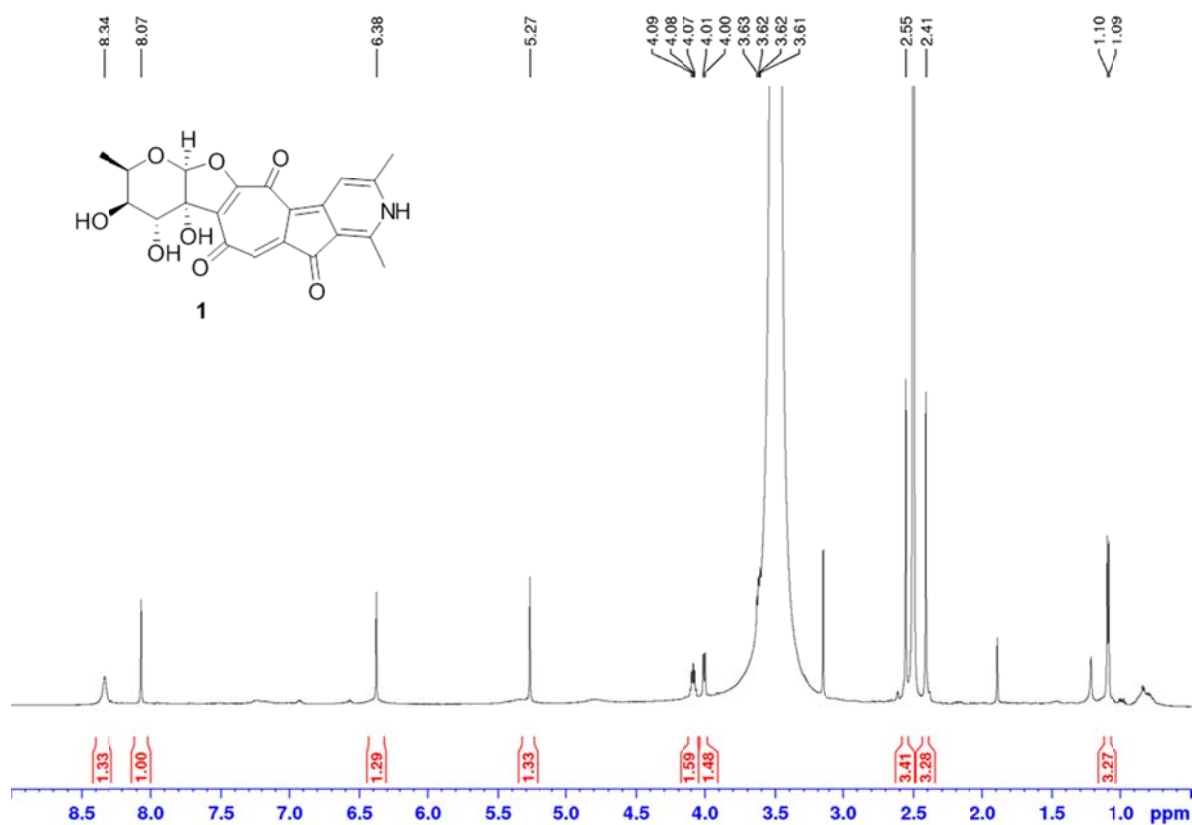
Figure S10. ^{1}H NMR spectrum of rubterolone A **(**1**)** (DMSO-d$_6$, 303K, 600 MHz).
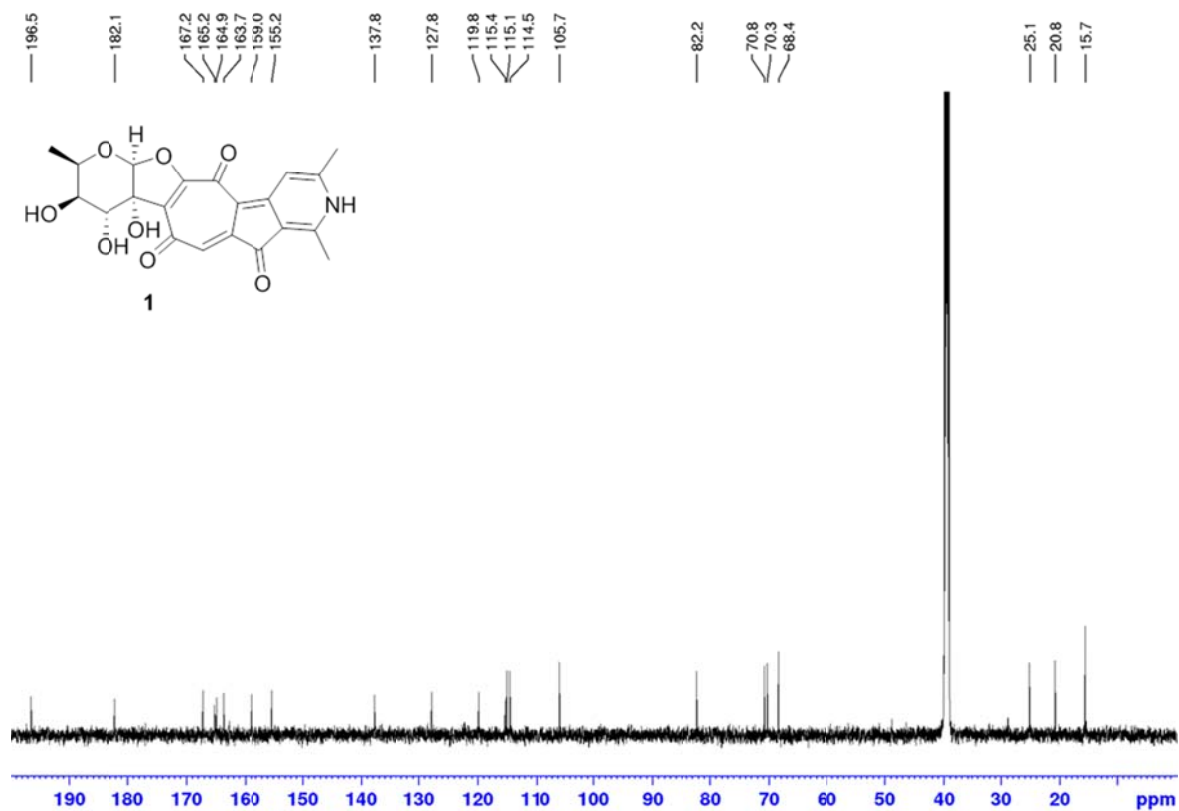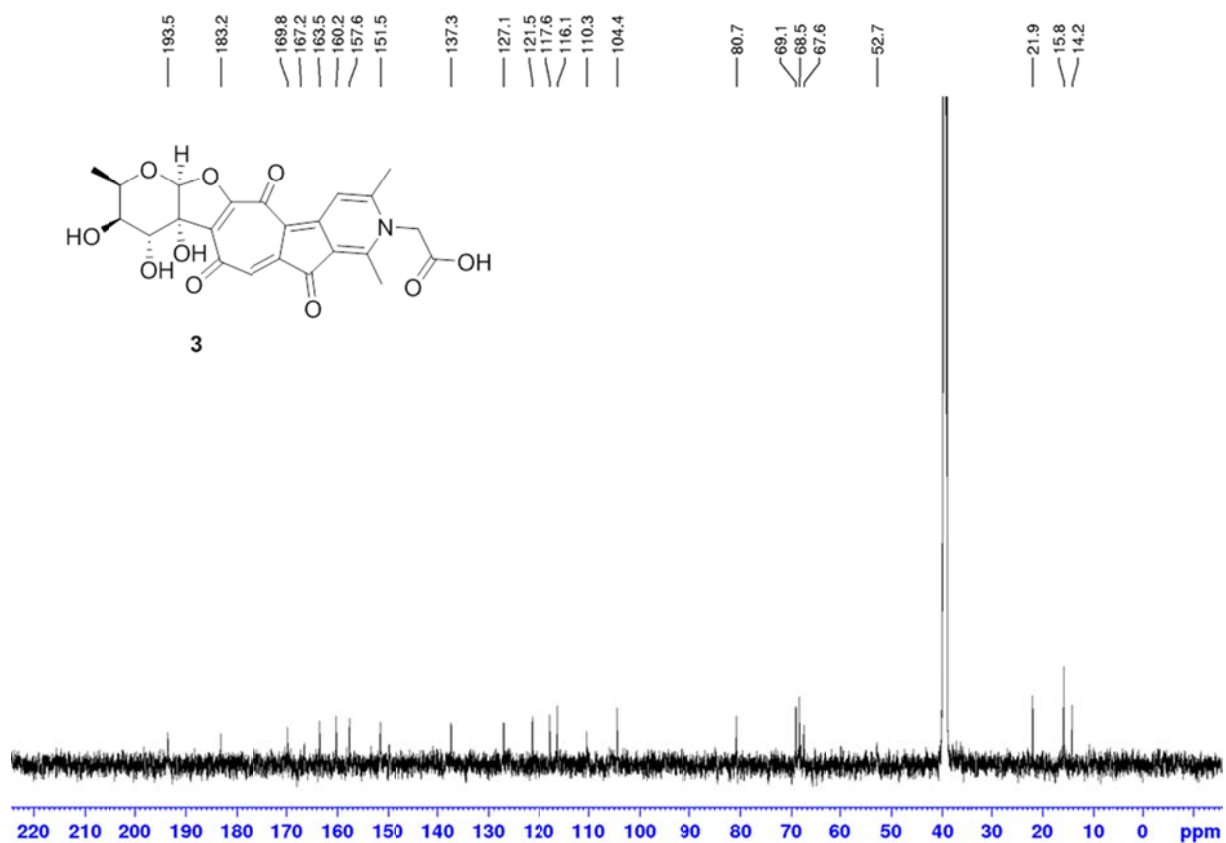

Figure S11. ^{13}C NMR spectrum of rubterolone A (1) (DMSO-d$_6$, 303K, 150 MHz).
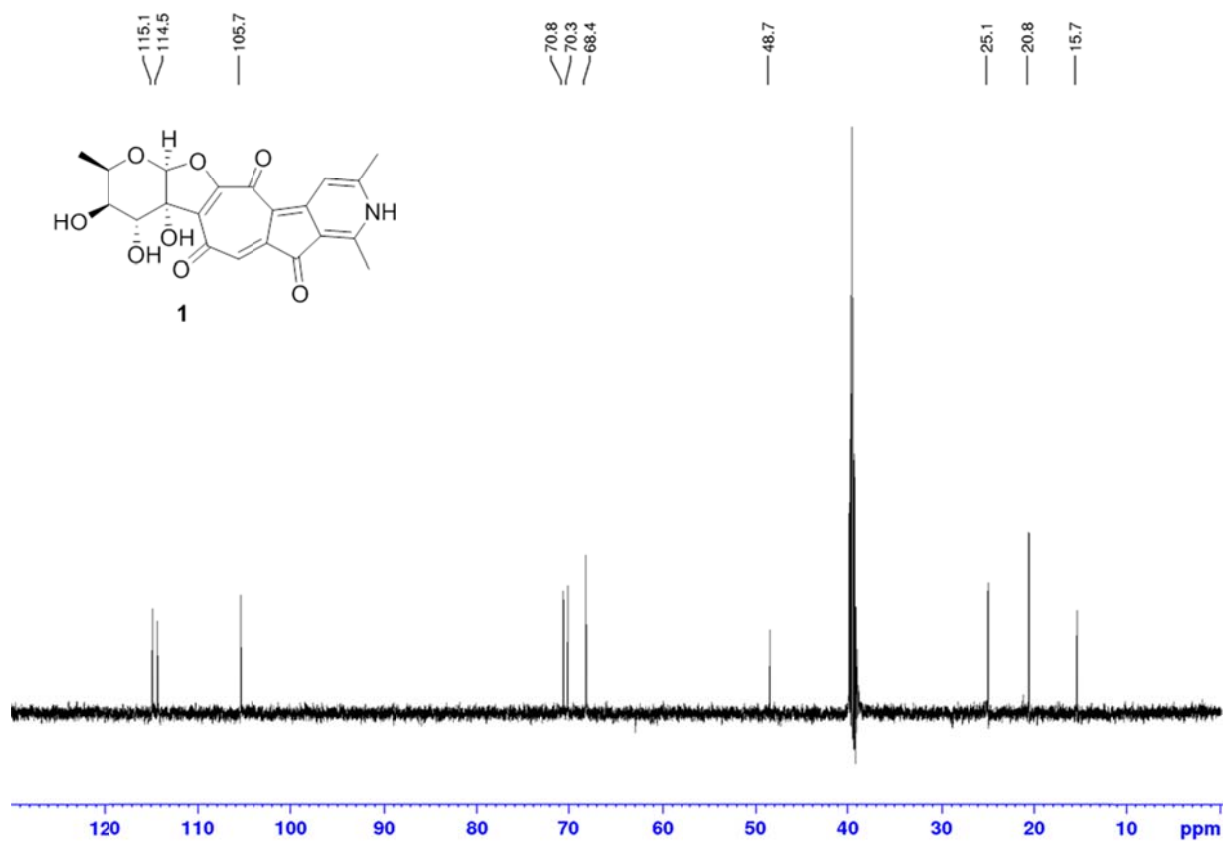
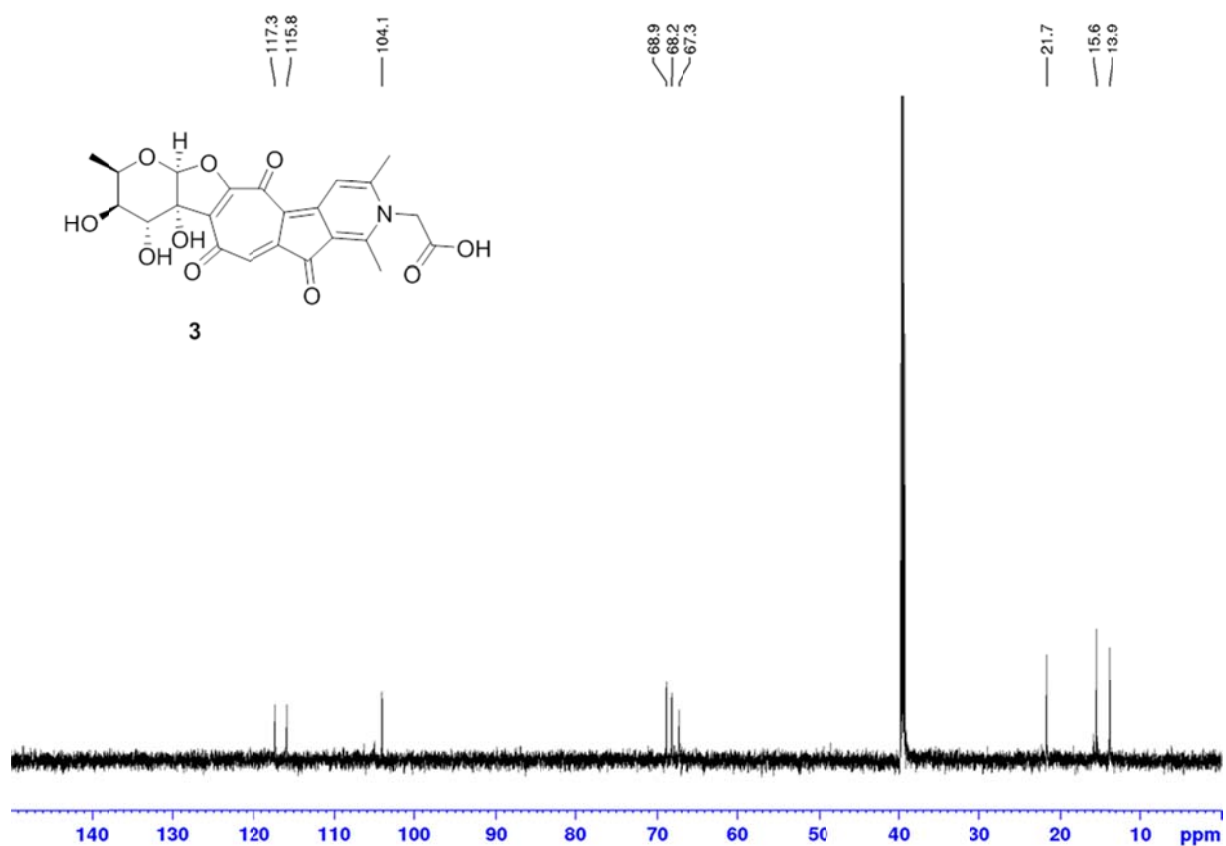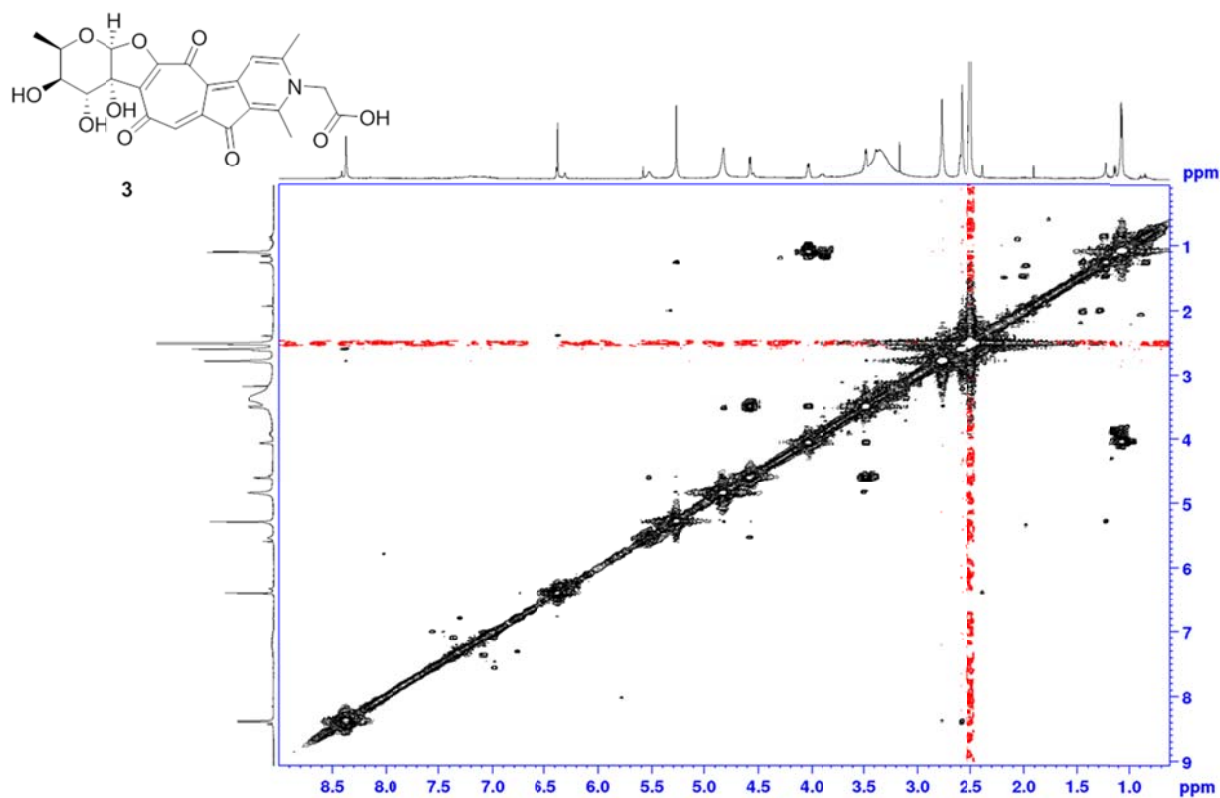**Figure S12.** DEPT135 spectrum of rubterolone A (1) (DMSO-d$_6$, 303K, 150 MHz).
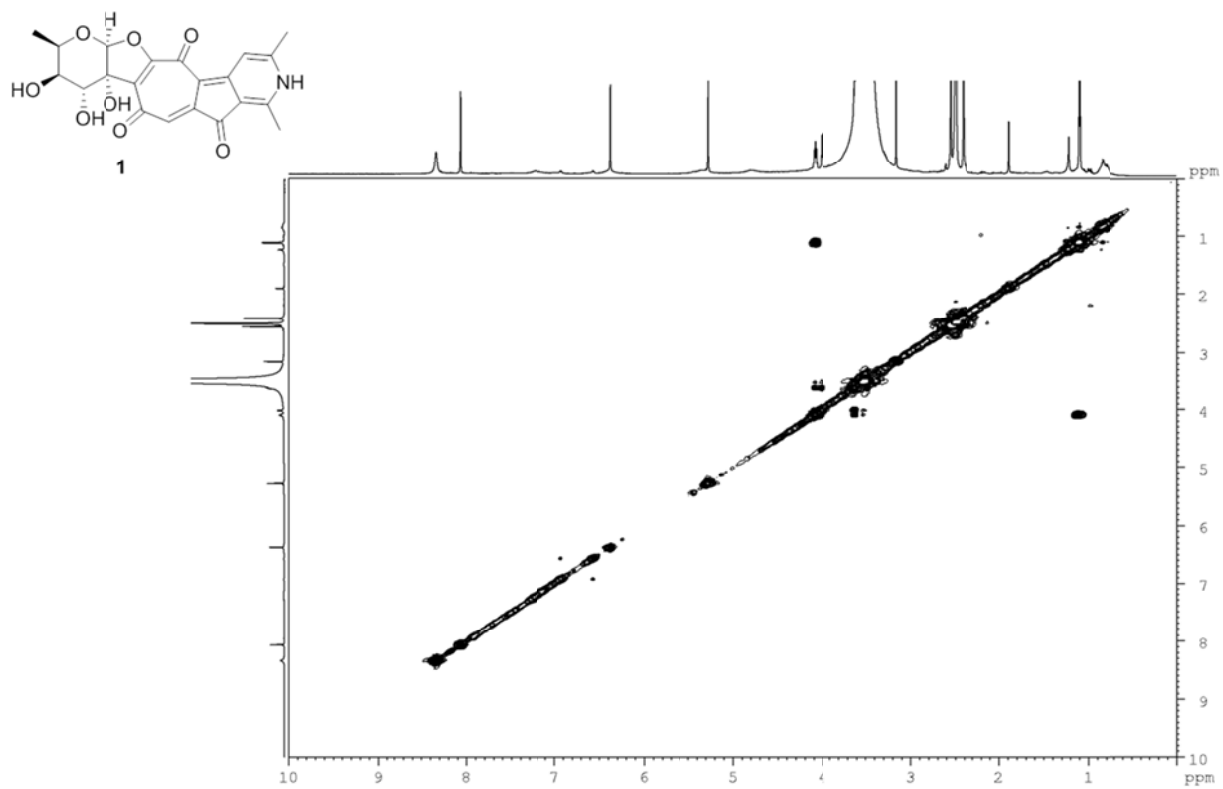
Figure S13. ^{1}H-^{1}H COSY spectrum of rubterolone A (1) (DMSO-d$_6$, 303K, 600 MHz).
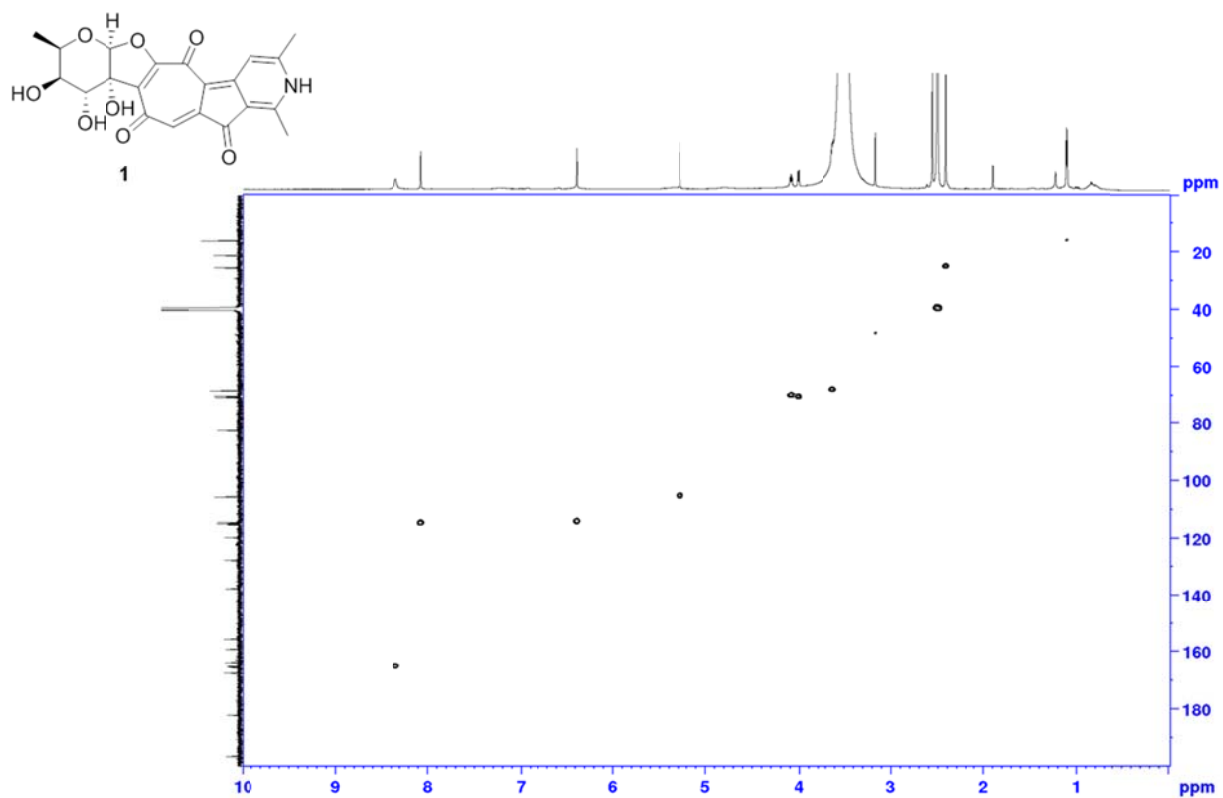
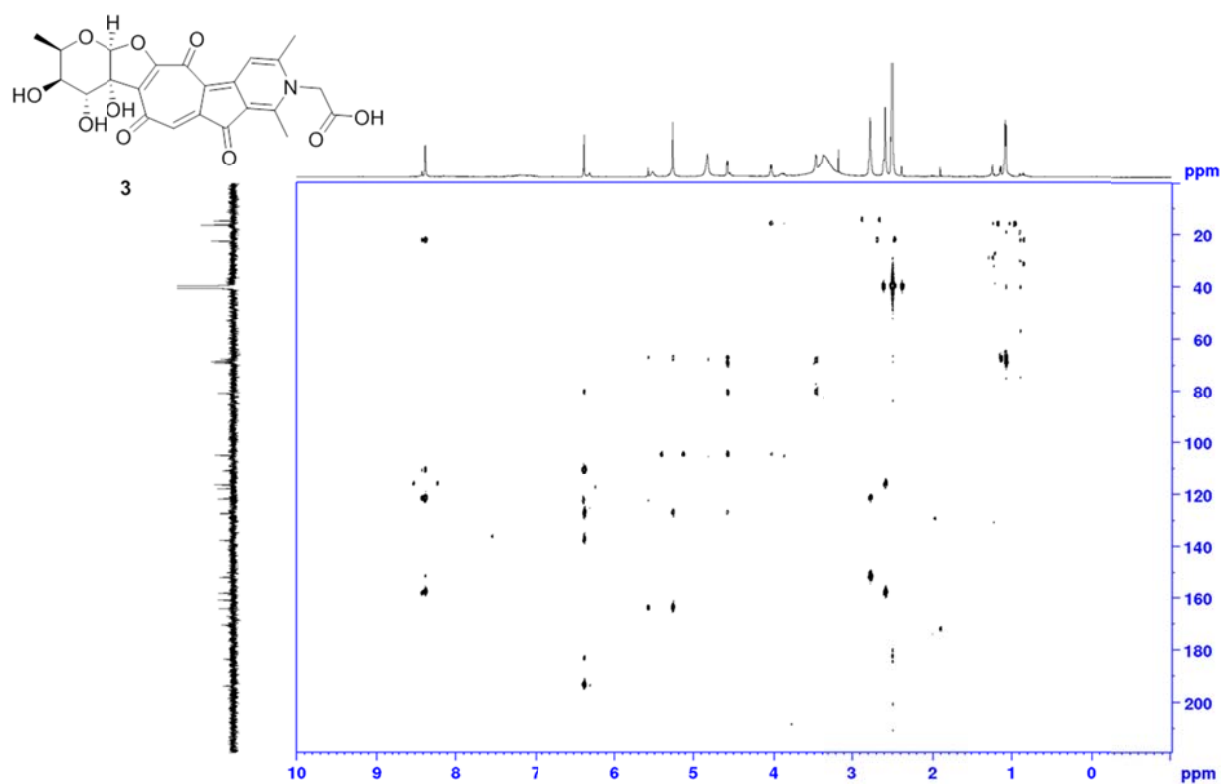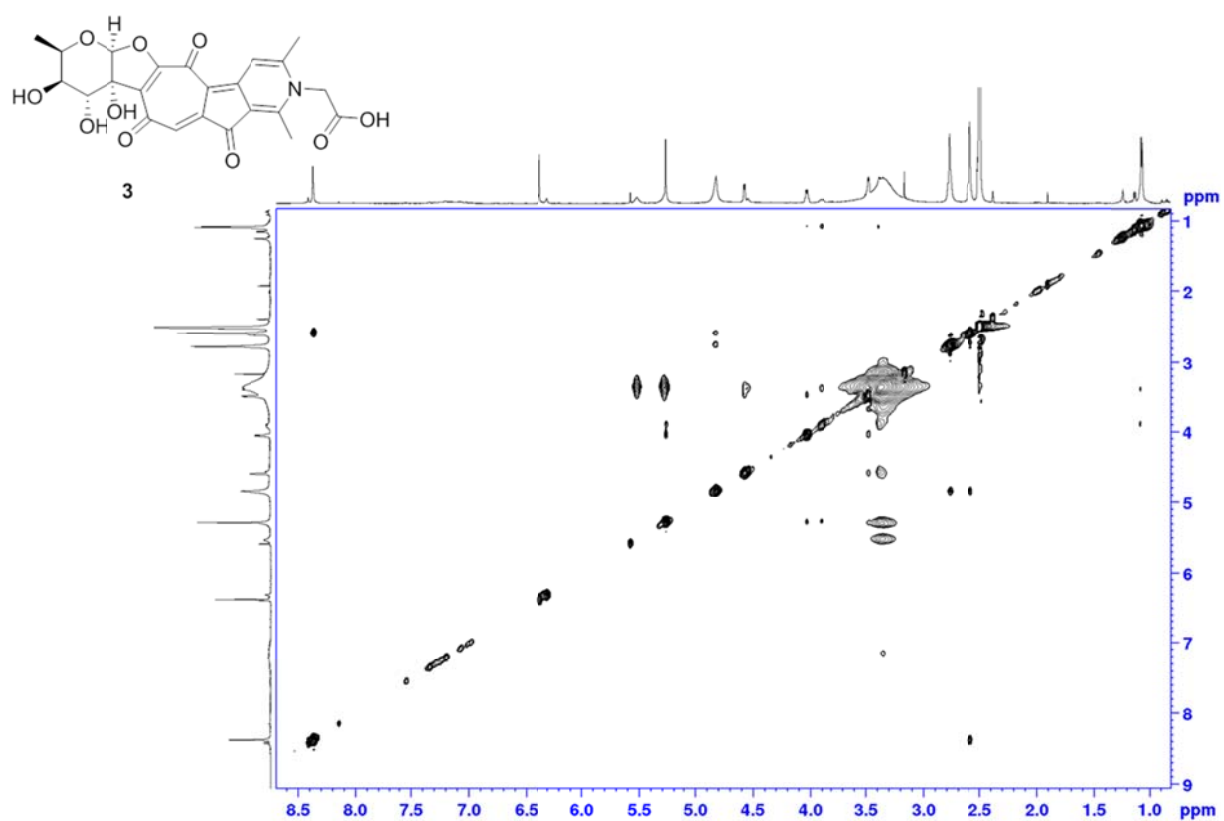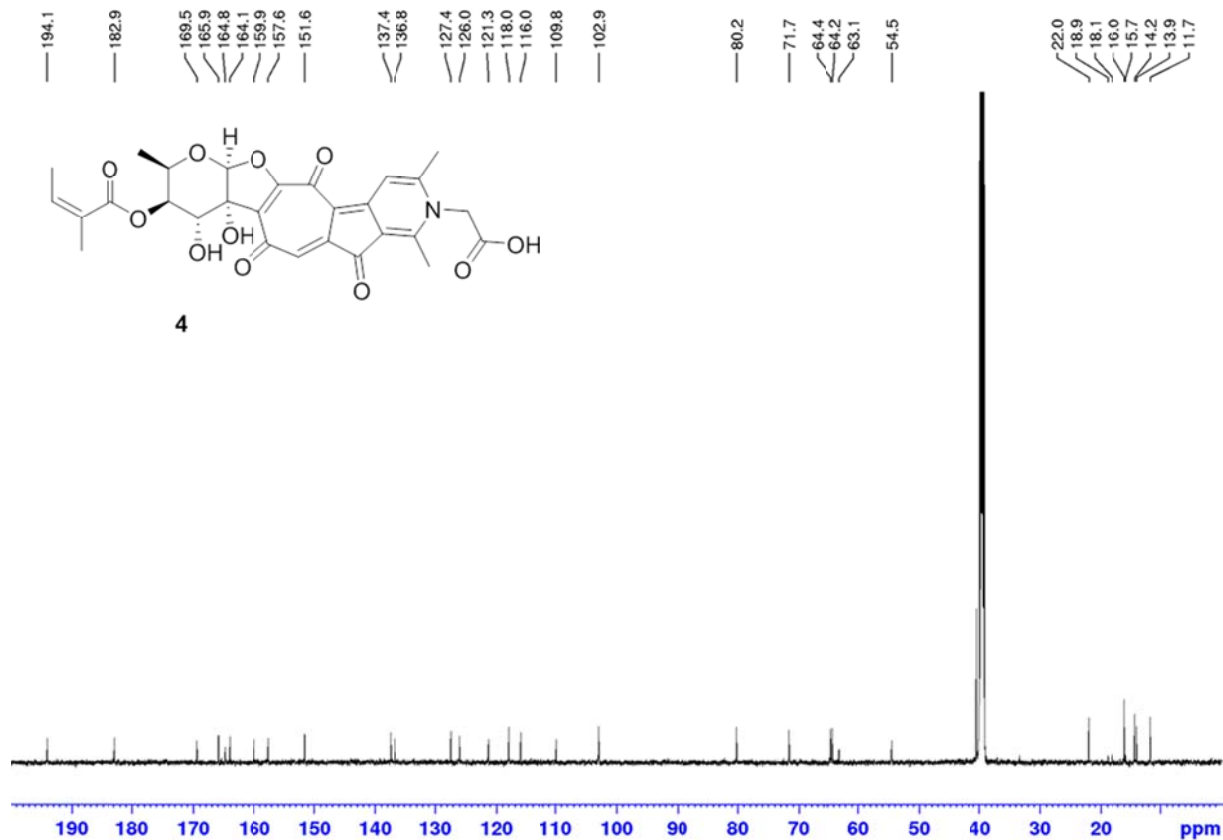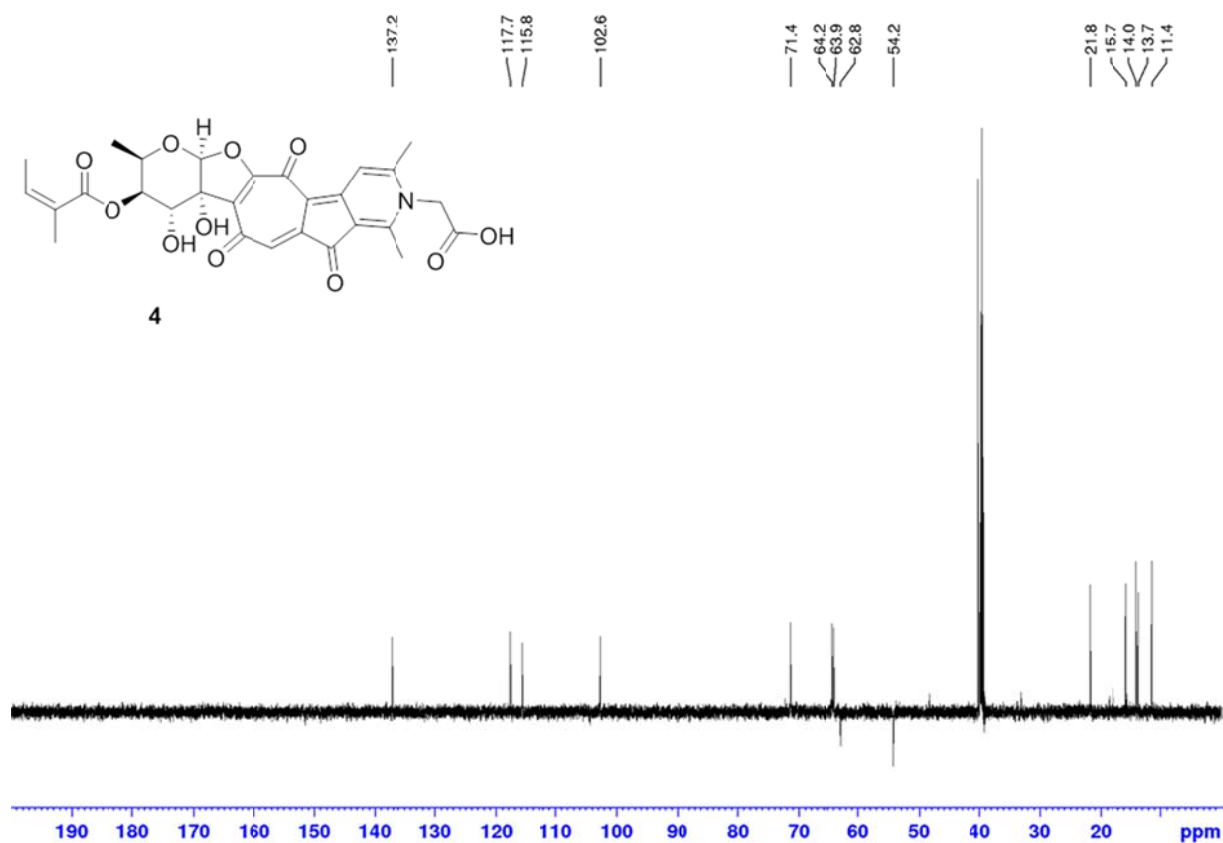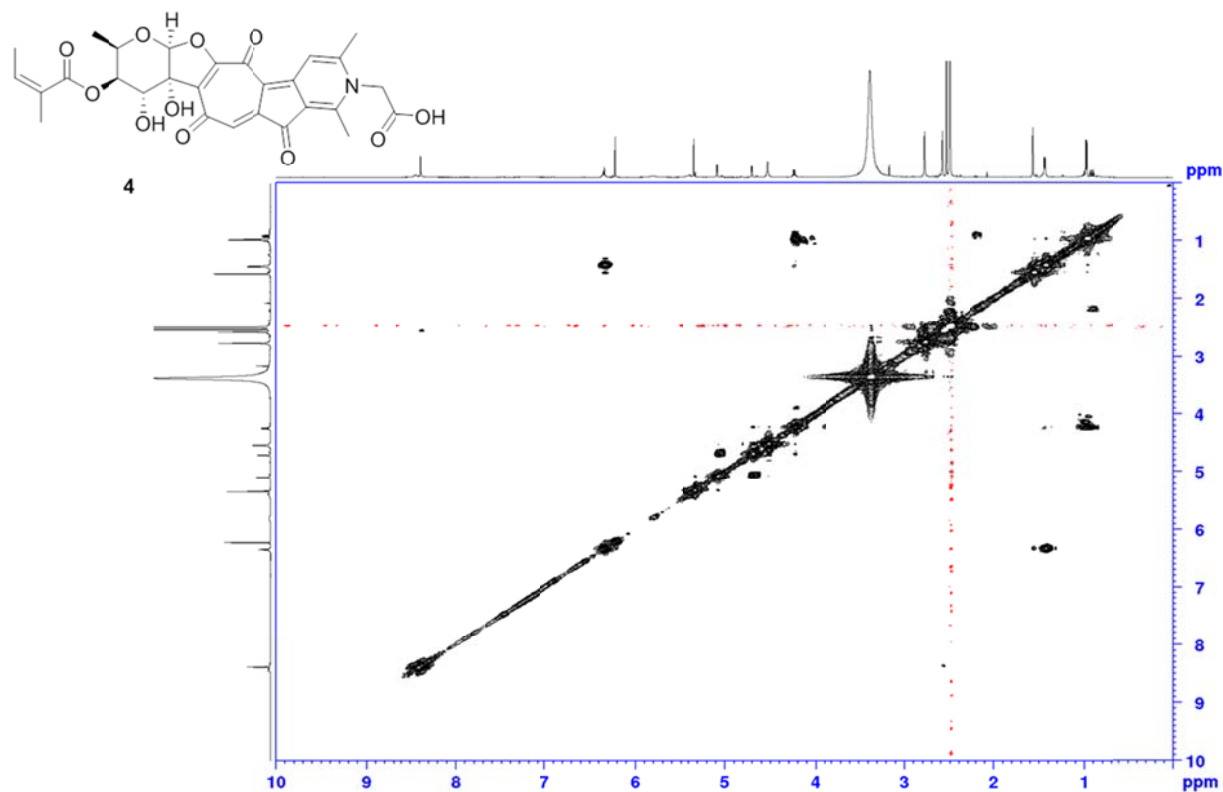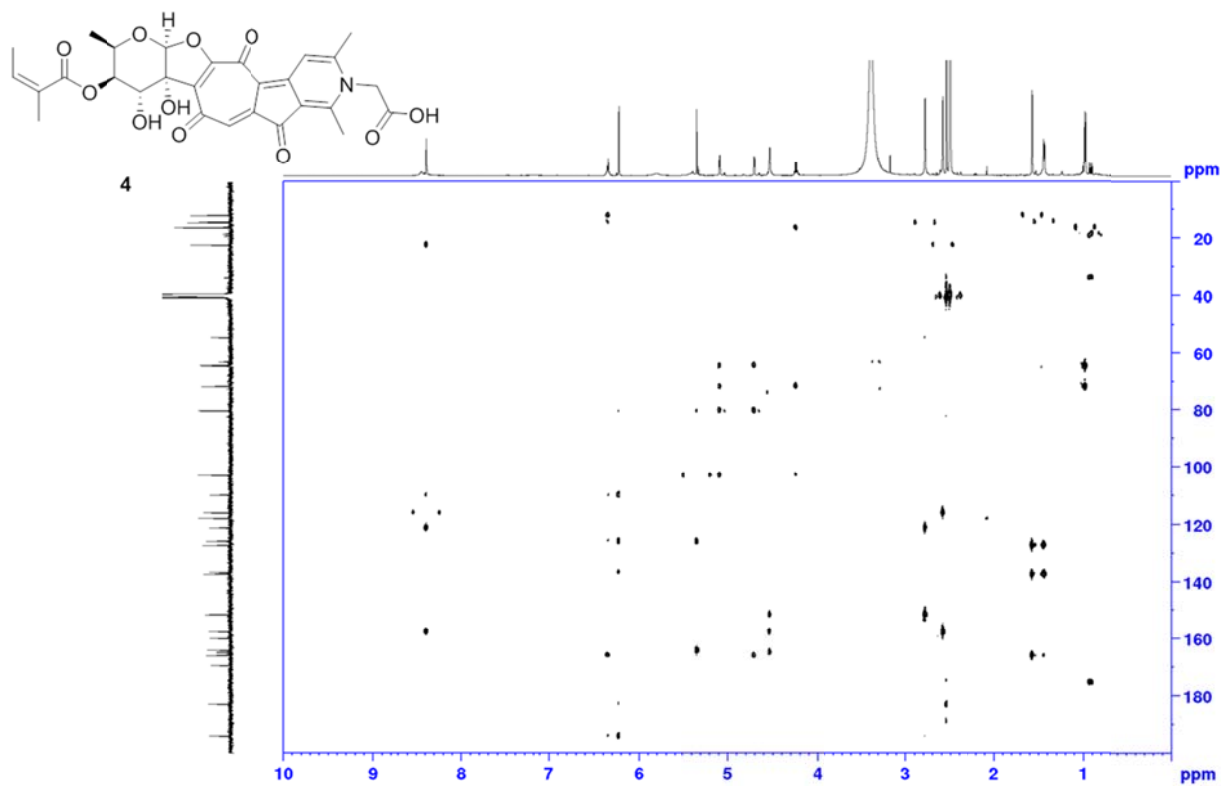**Figure S14.** HSQC spectrum of rubterolone A (1**)** (DMSO-d$_6$, 303K, 600 MHz).
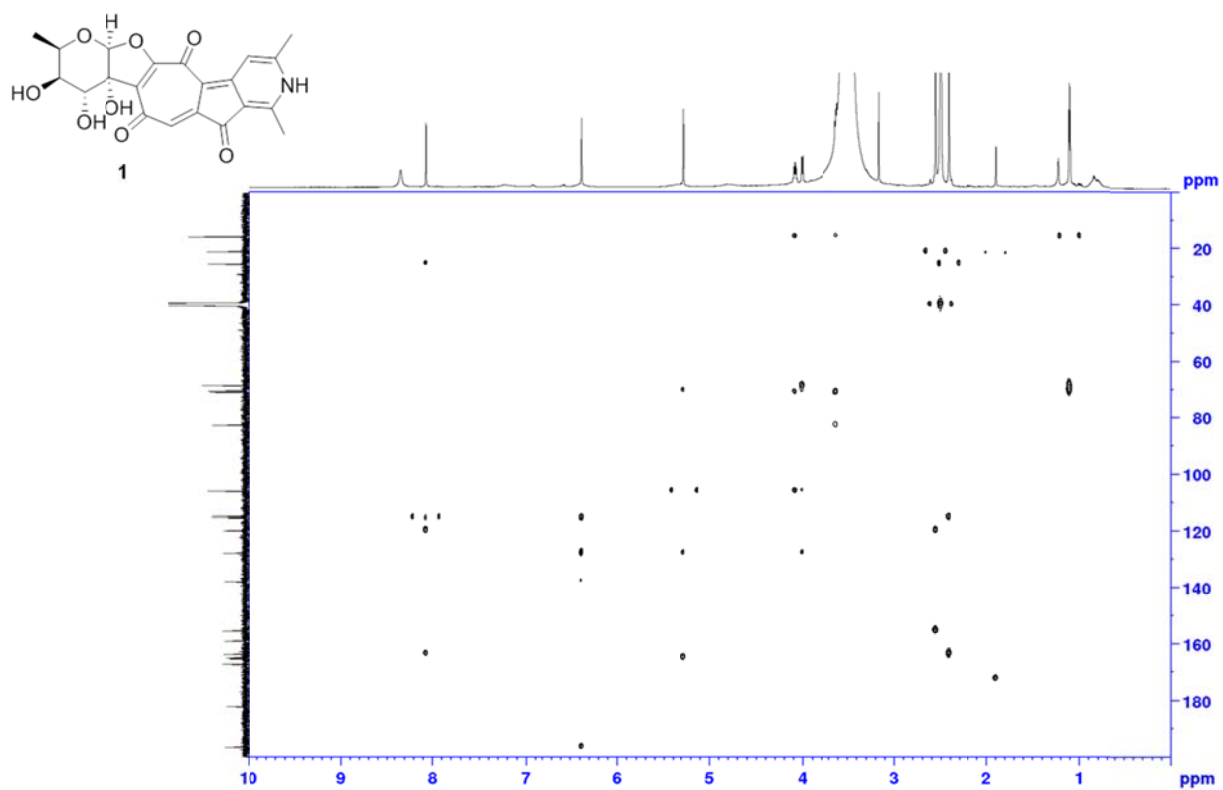
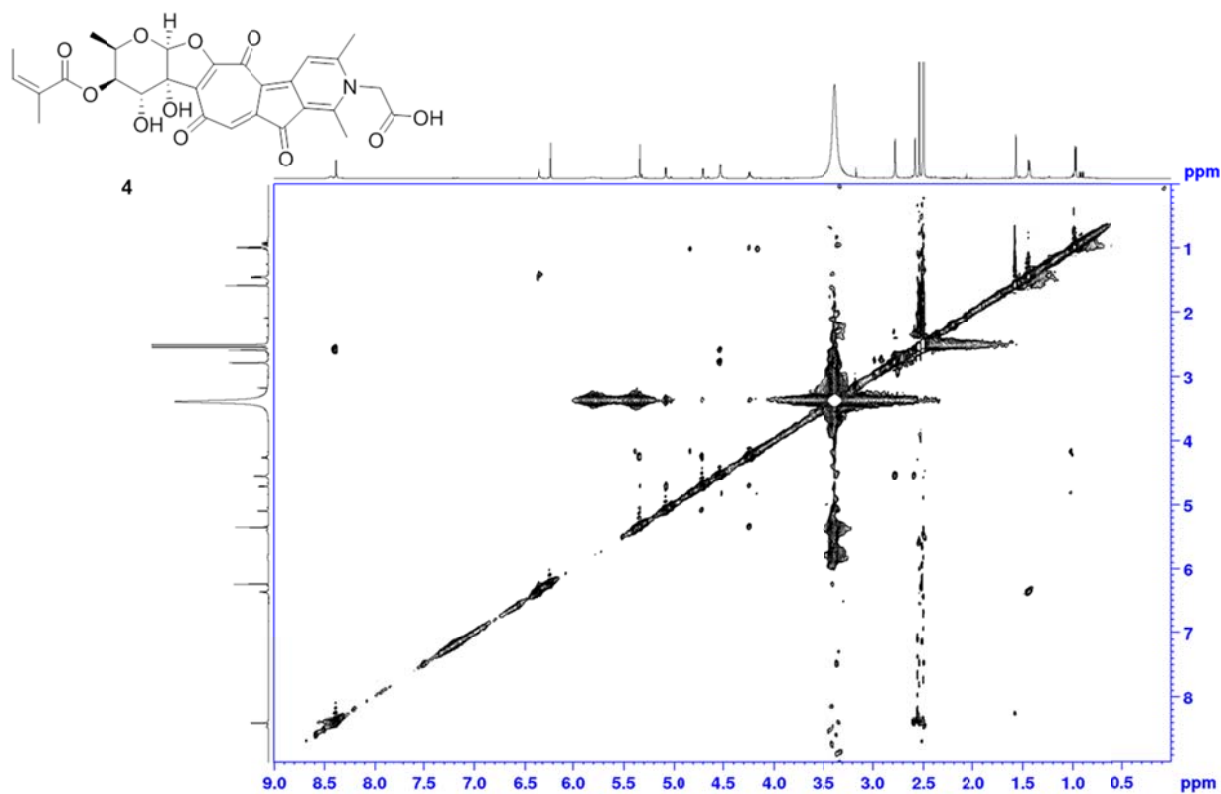**Figure S15.** HMBC spectrum of rubterolone A (1) (DMSO-d$_6$, 303K, 600 MHz).
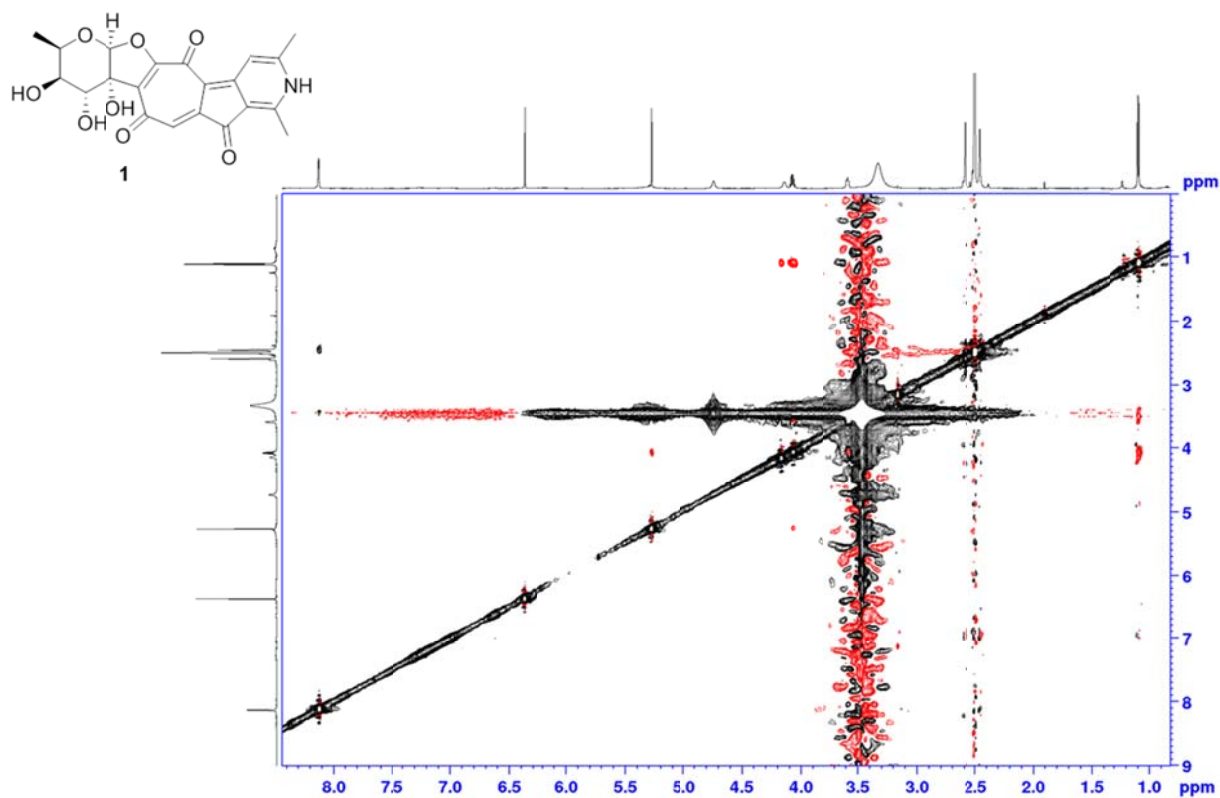
**Figure S16.** NOESY spectrum of rubterolone A (1) (DMSO-d$_6$, 303K, 500 MHz).
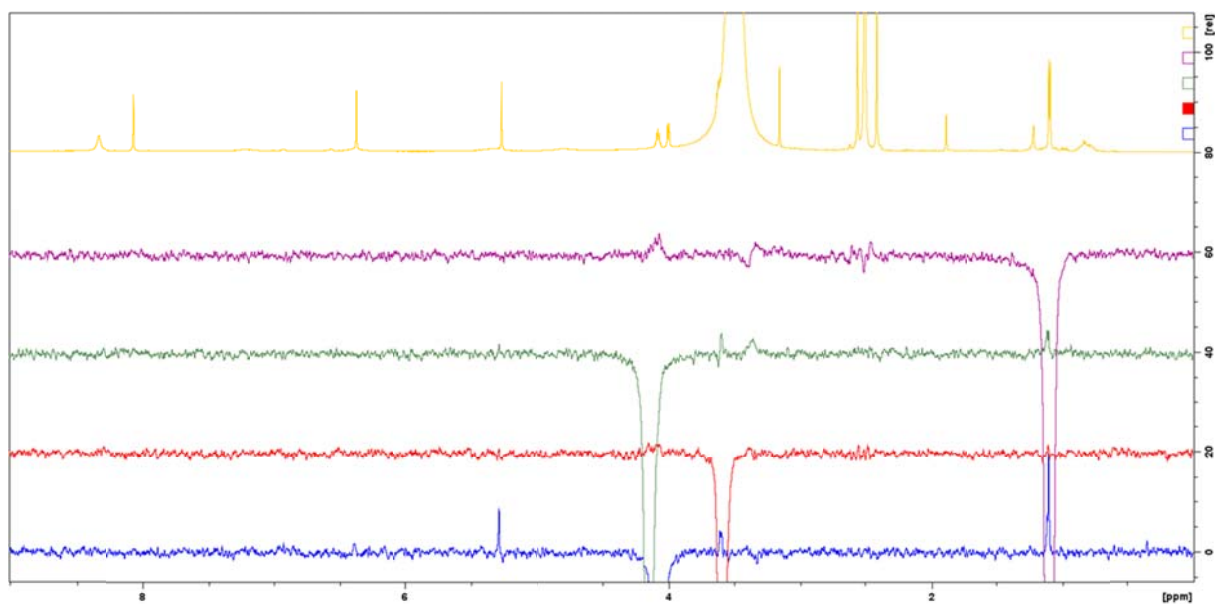
Figure S17. 1D selNOE spectrum of rubterolone A (1) (DMSO-d$_6$, 303K, 600 MHz).
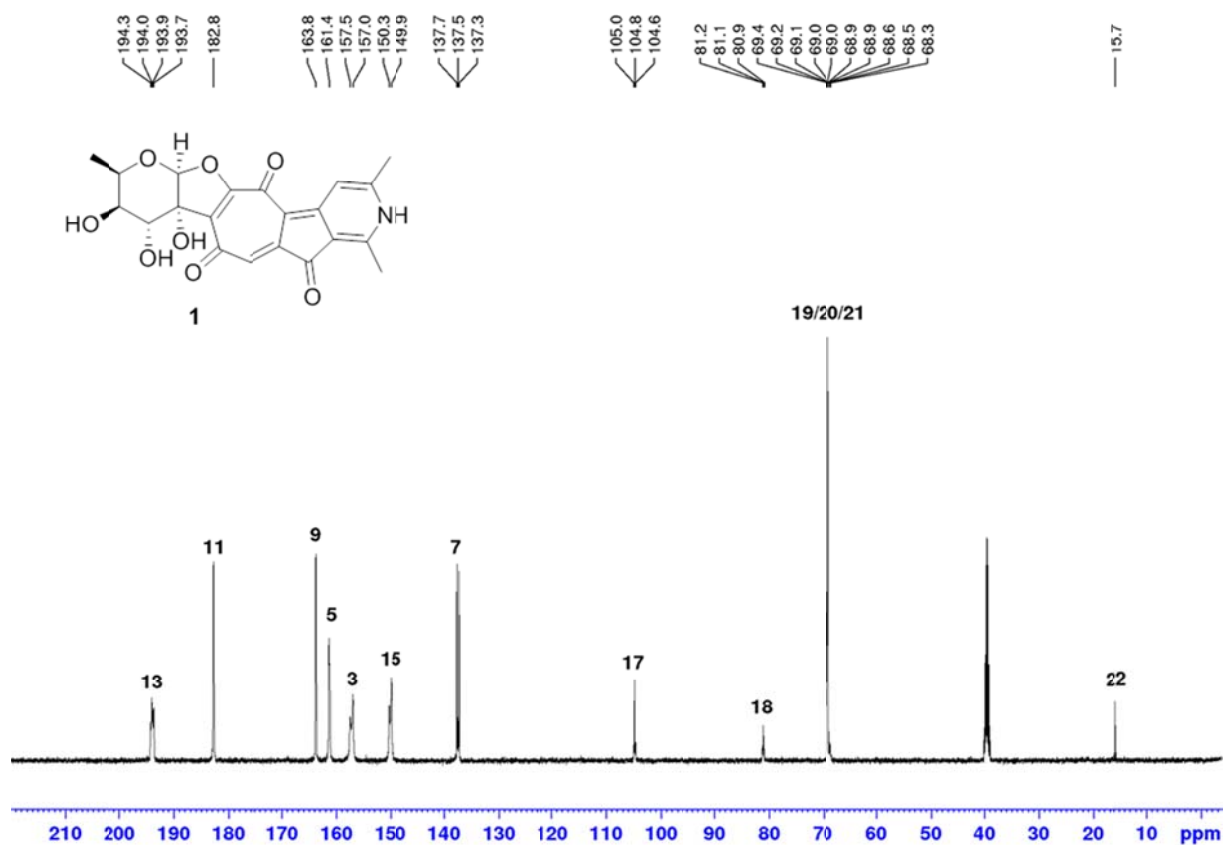
Figure S18. ^{13}C NMR spectrum of [1-^{13}C] acetate labeled rubterolone A (1a) (DMSO-d$_6$, 303K, 600 MHz).
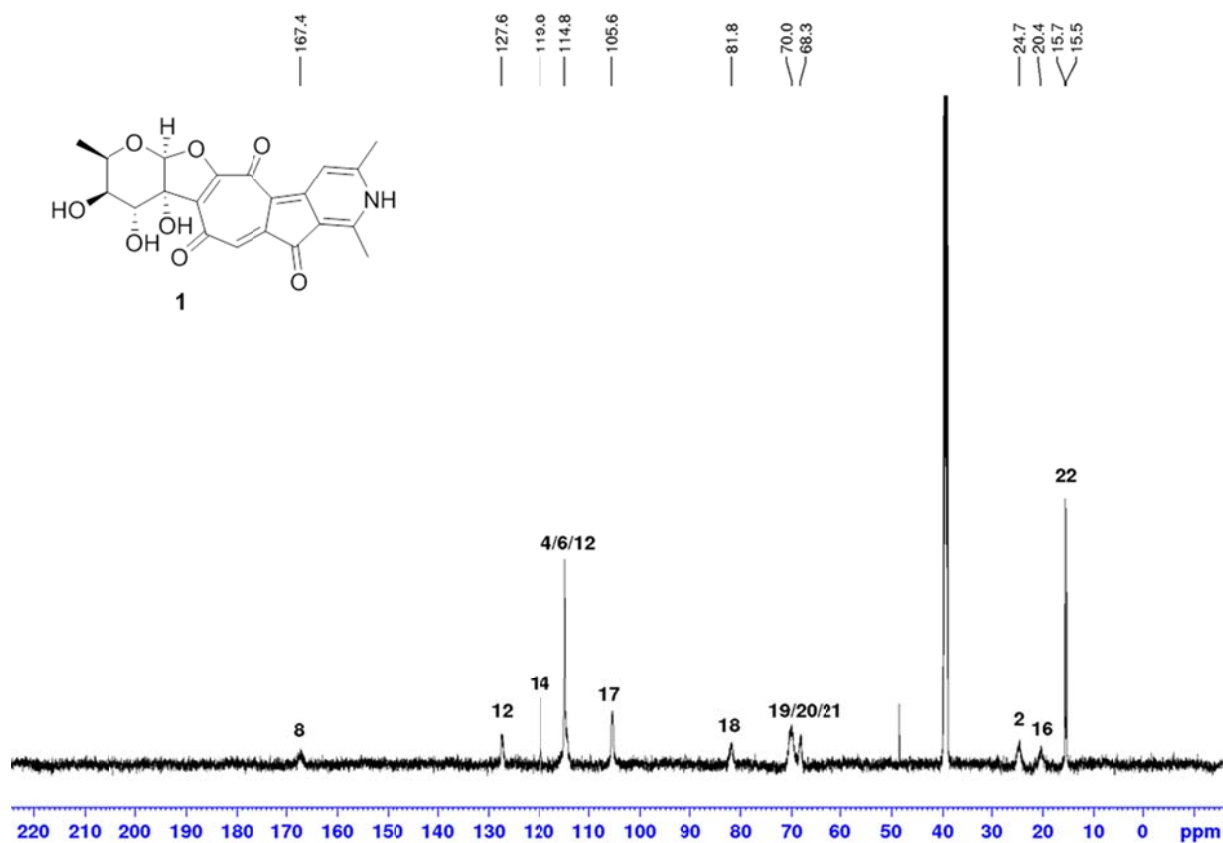
Figure S19. ^{13}C NMR spectrum of [2-^{13}C] acetate labeled rubterolone A (1b) (DMSO-d$_6$, 303K, 600 MHz).
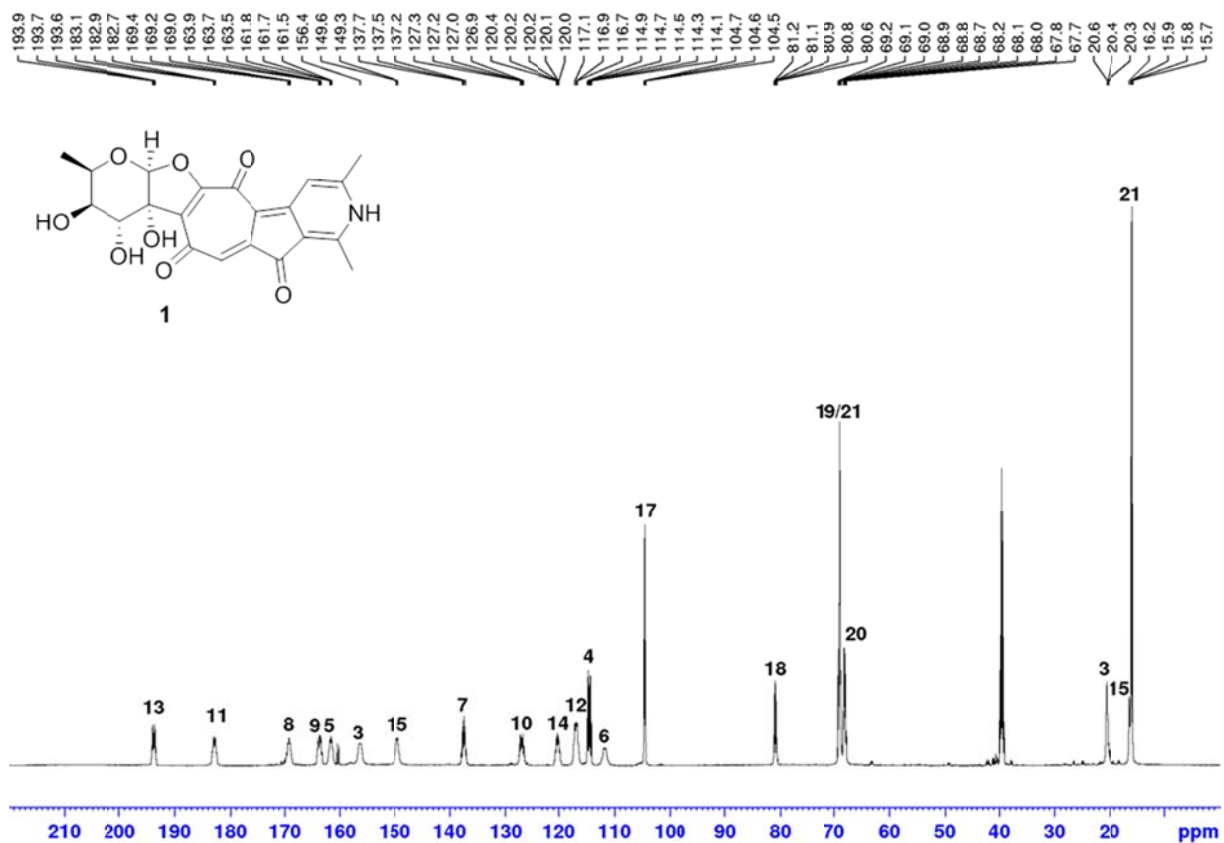
Figure S20. ^{13}C NMR spectrum of [1,2-^{13}C$_2$] acetate labeled rubterolone A (1c) (DMSO-d$_6$, 303K, 600 MHz).
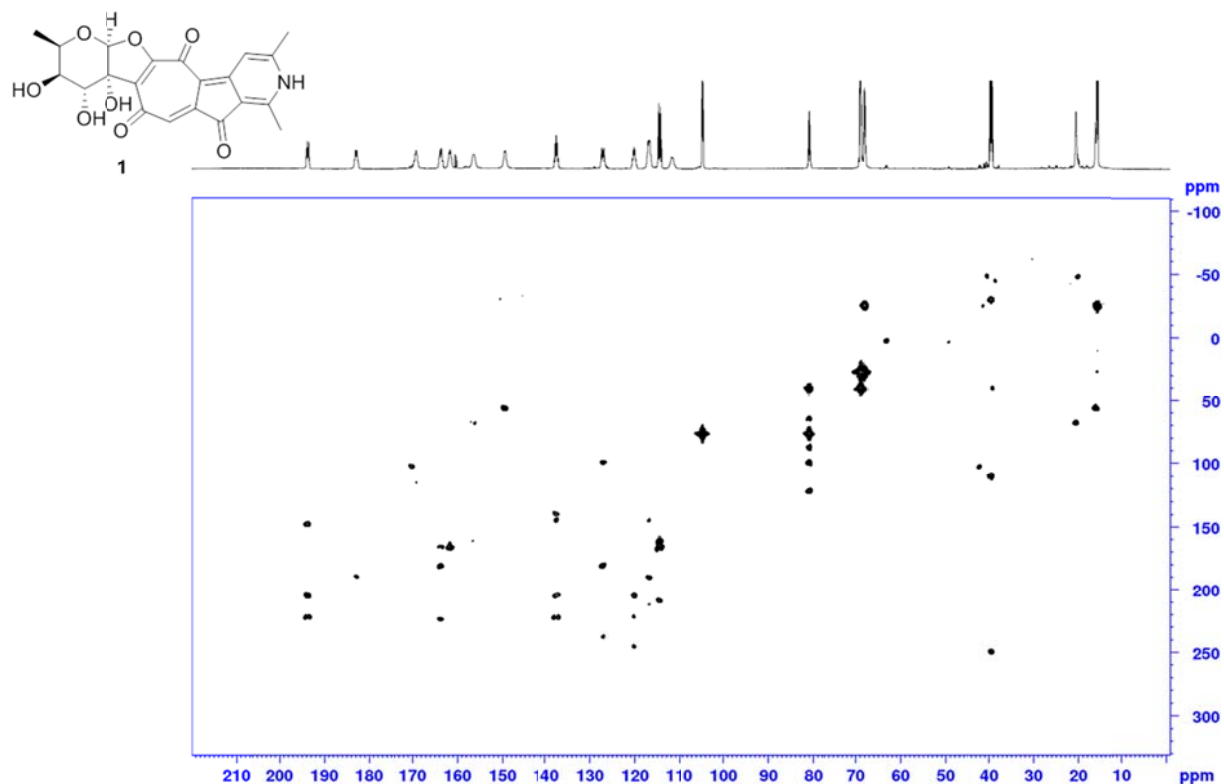
Figure S21. ^{13}C 2D INADEQUATE spectrum of [1,2-^{13}C$_2$] acetate labeled rubterolone A (1c) (DMSO-d$_6$, 303K, 600 MHz, D4 0.0065 s).
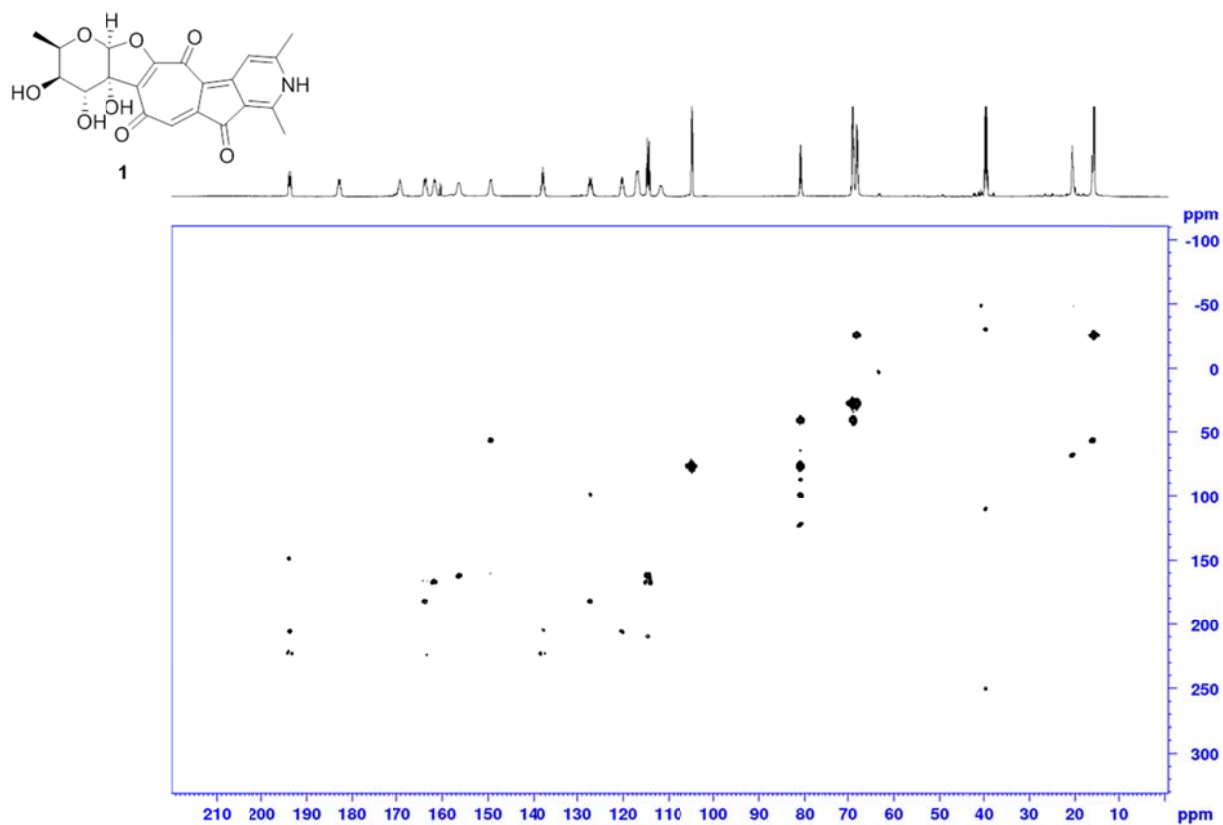
Figure S22. ^{13}C 2D INADEQUATE spectrum of [1,2-^{13}C$_2$] acetate labeled rubterolone A (1c) (DMSO-d$_6$, 303K, 600 MHz, D4 0.02 s).
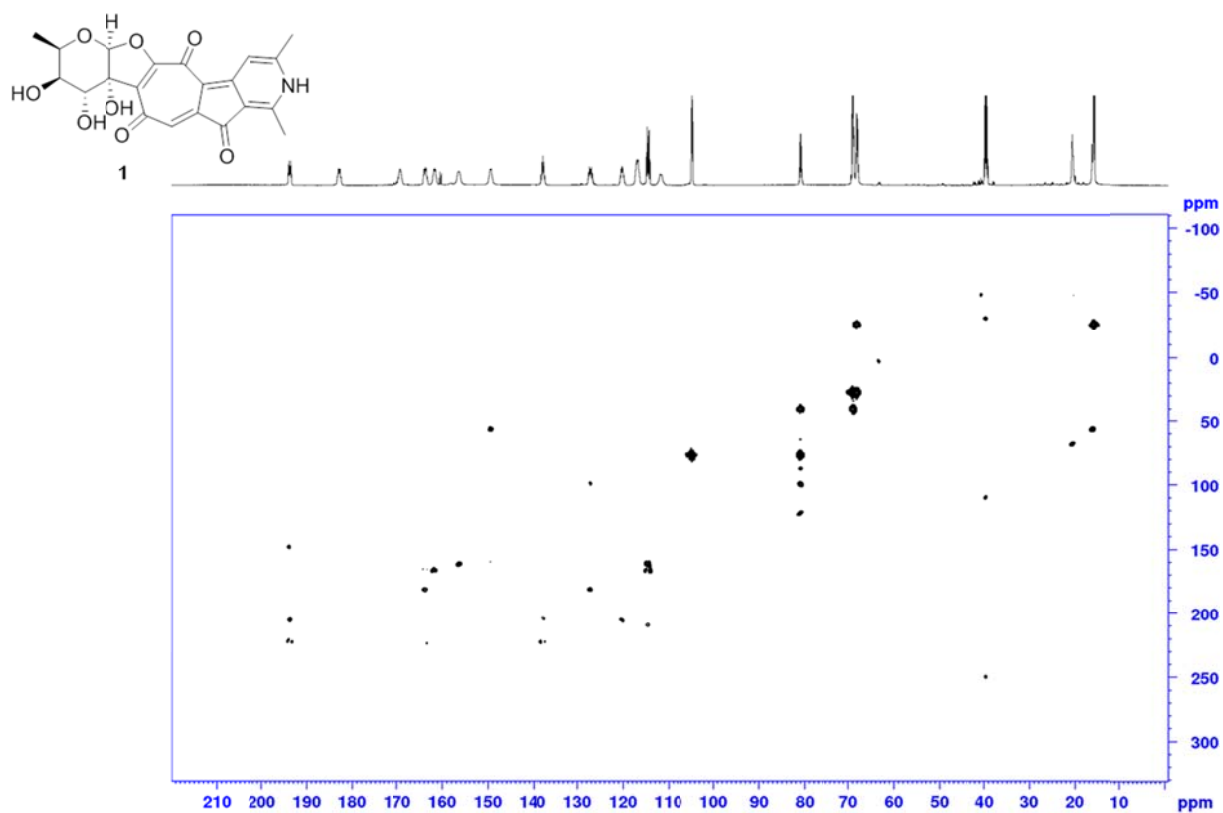
Figure S23. ^{13}C 2D INADEQUATE spectrum of [1,2-^{13}C$_2$] acetate labeled rubterolone A (1c) (DMSO-d$_6$, 303K, 600 MHz, D4 0.04 s).
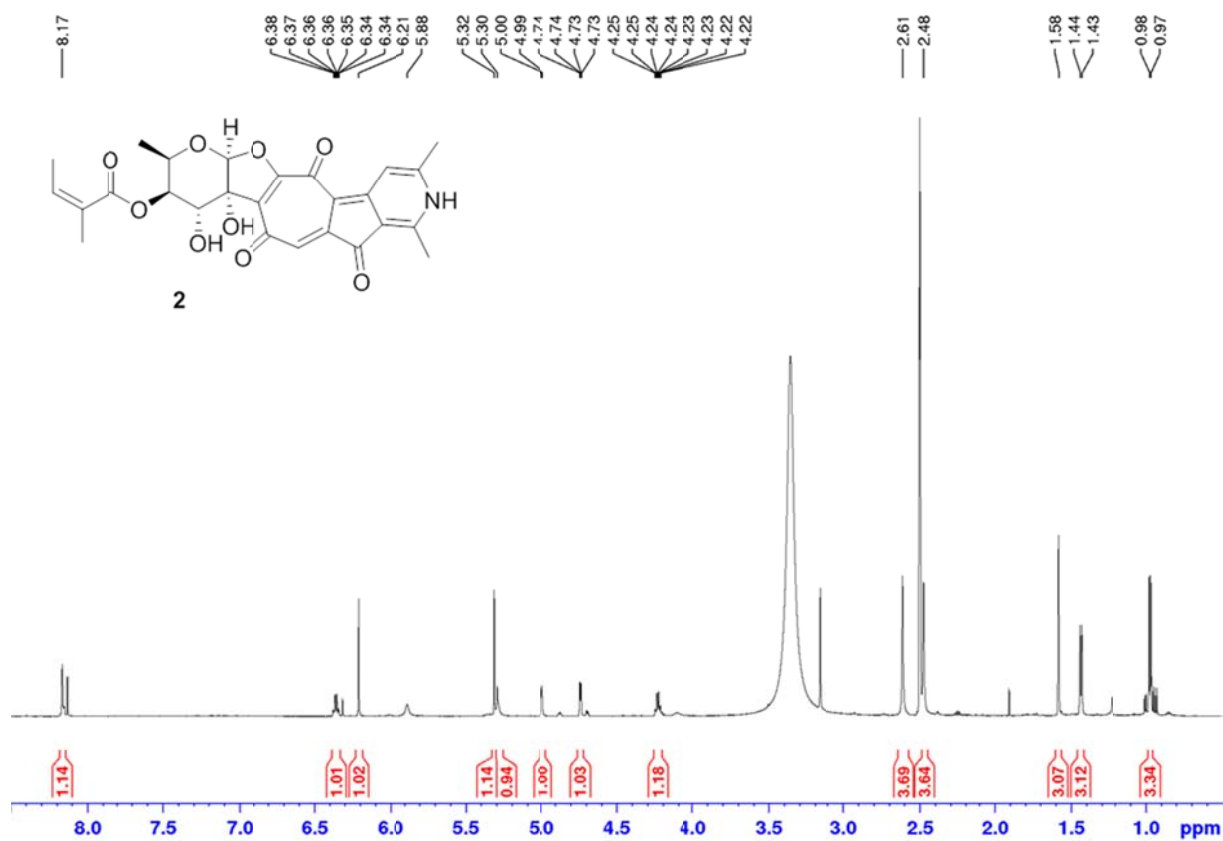
Figure S24. ^{1}H NMR spectrum of rubterolone B (2) (DMSO-d$_6$, 303K, 600 MHz).
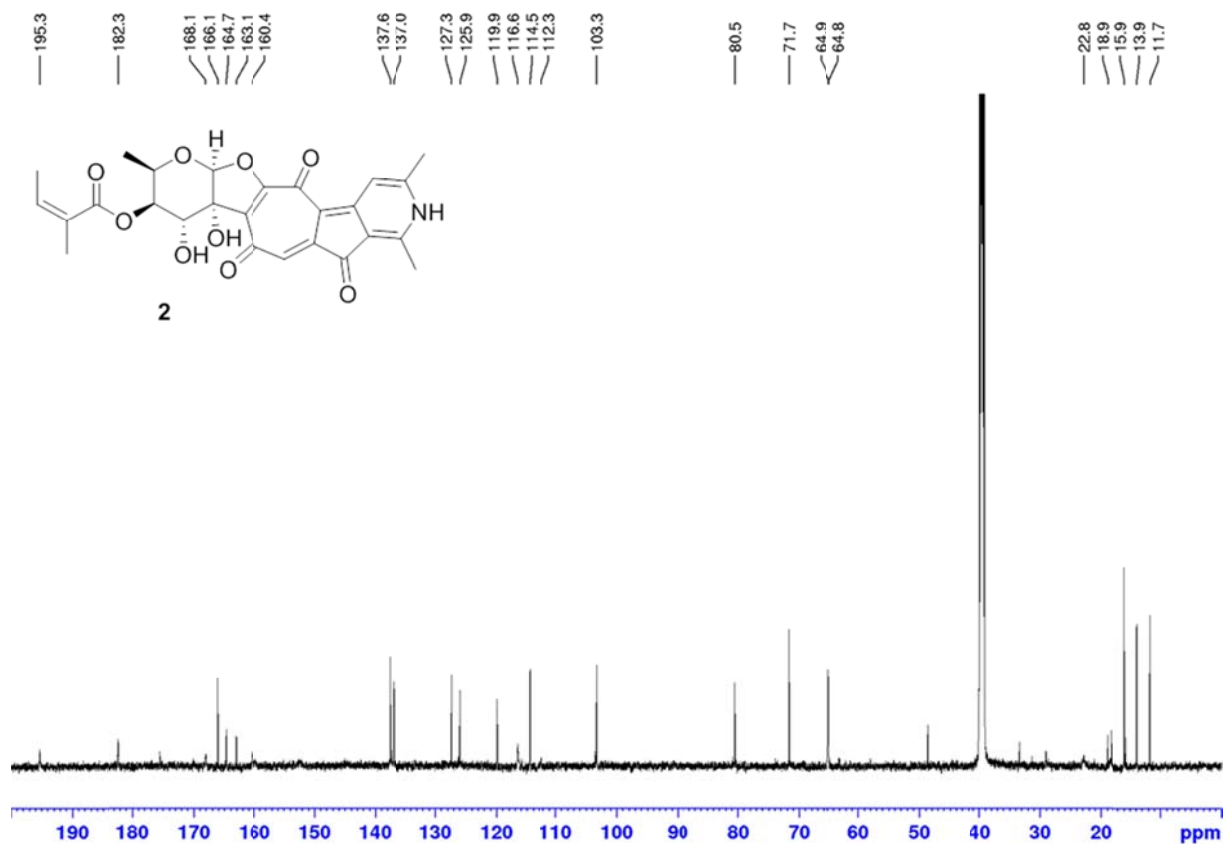
Figure S25. ^{13}C NMR spectrum of rubterolone B (2) (DMSO-d$_6$, 303K, 150 MHz).
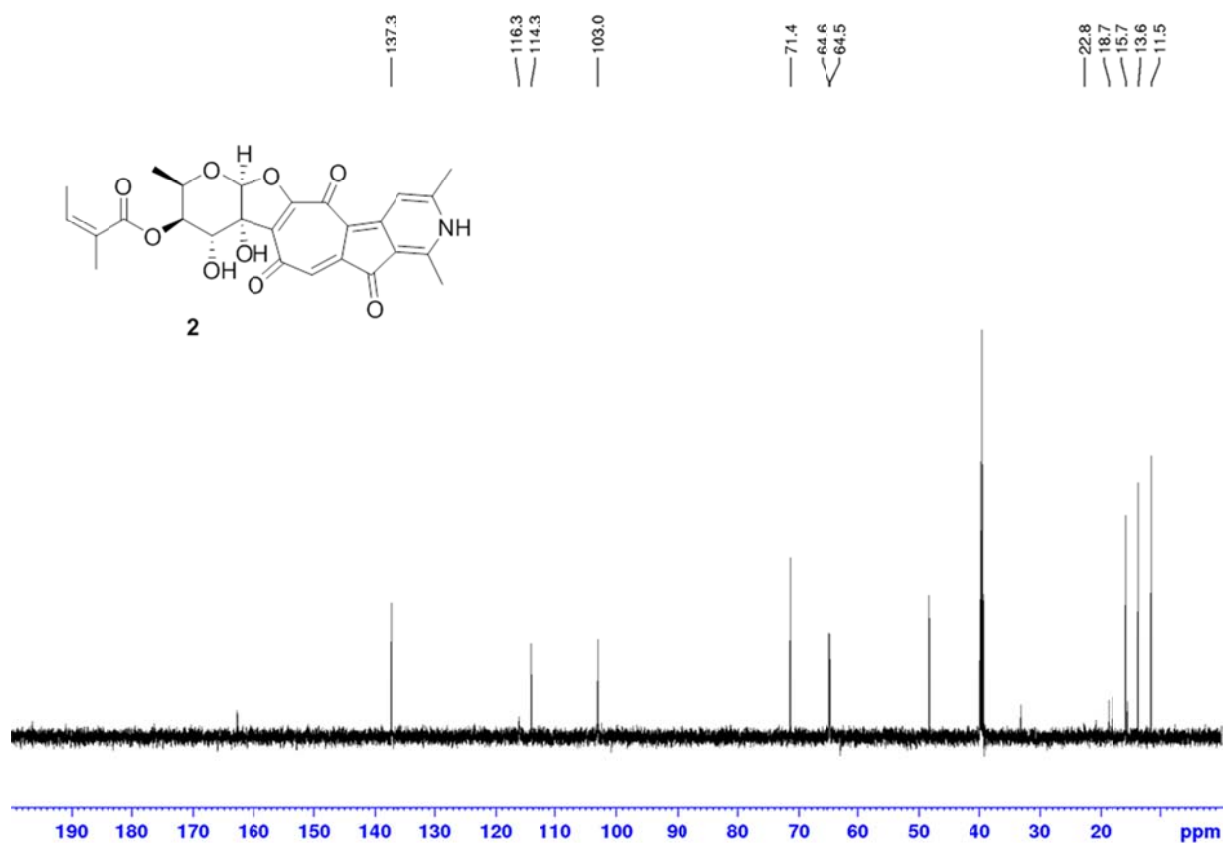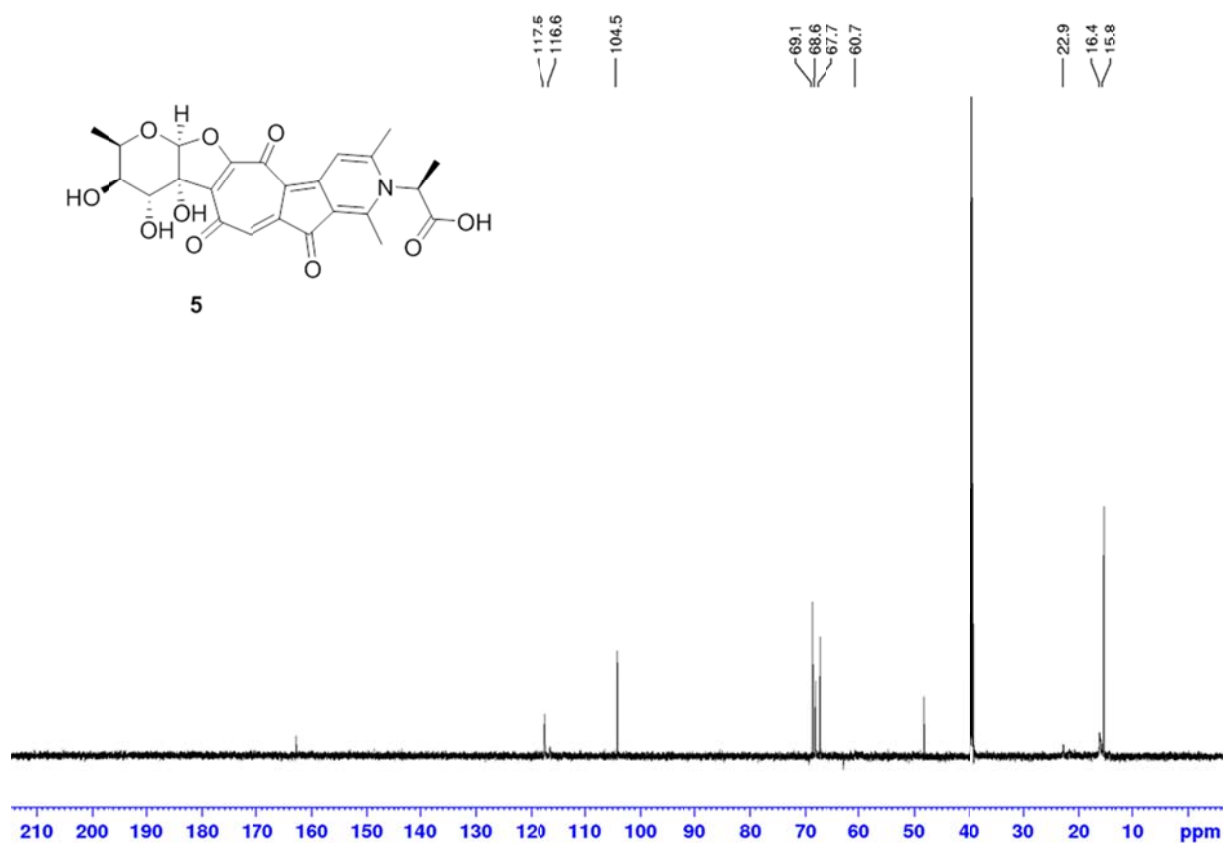
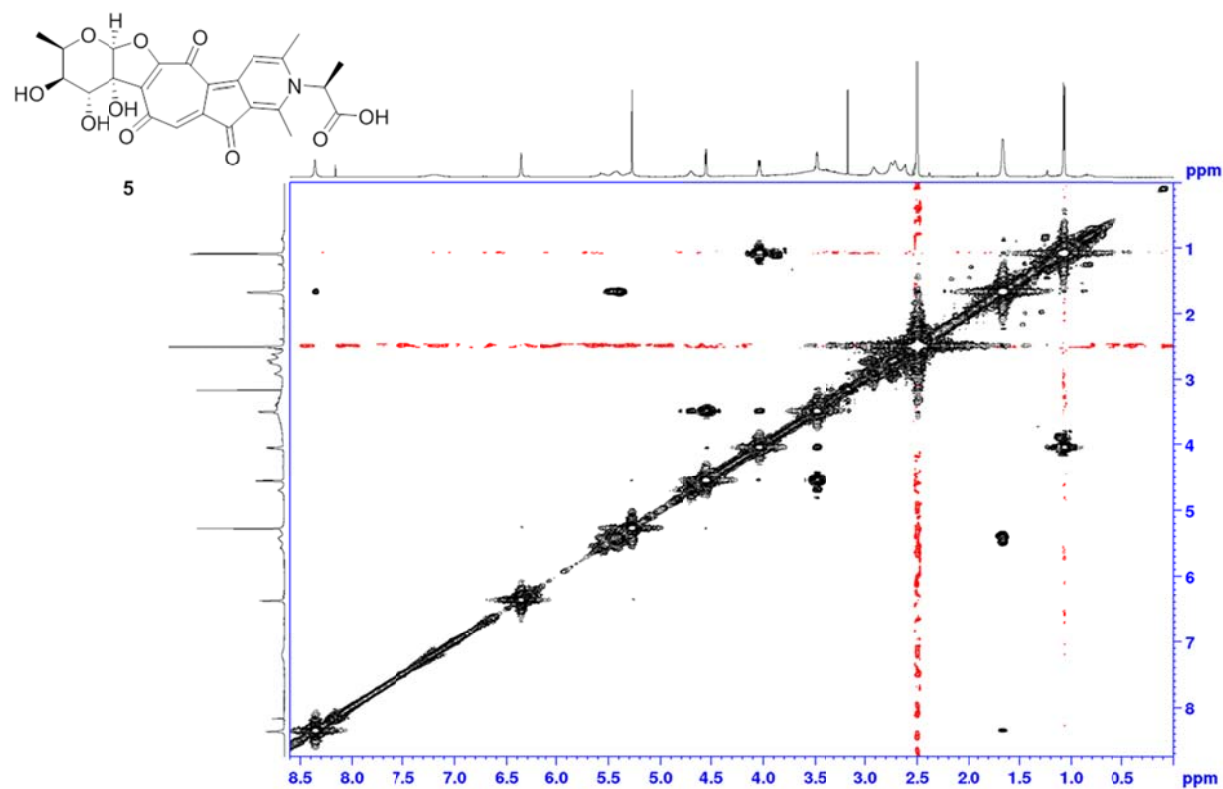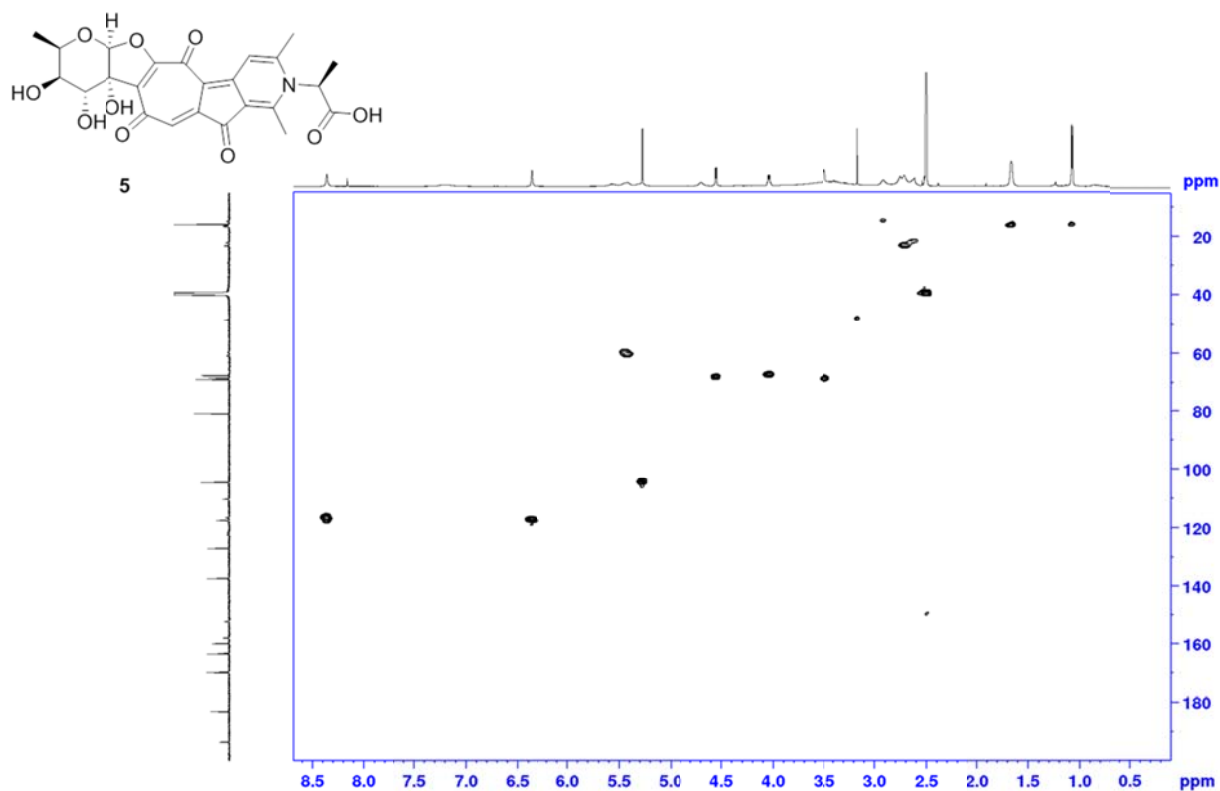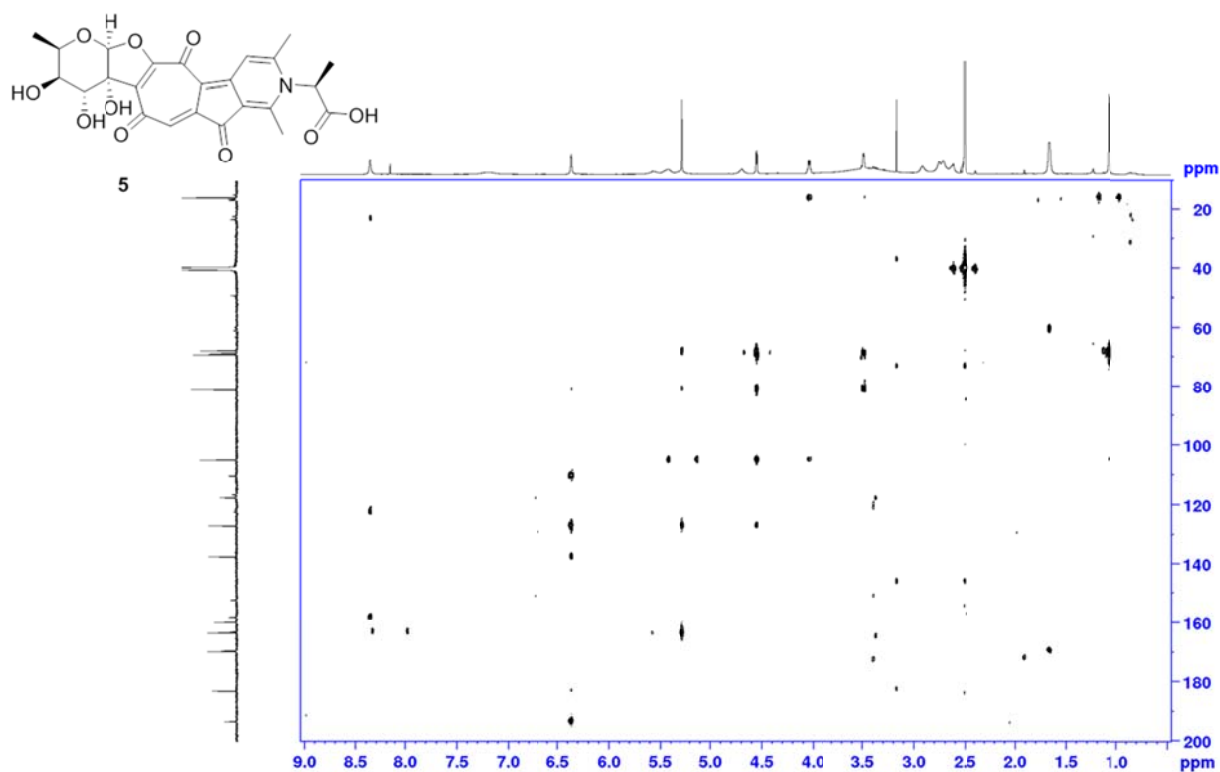**Figure S26**. DEPT135 spectrum of rubterolone B (**2**) (DMSO-*d*₆, 303K, 150 MHz).
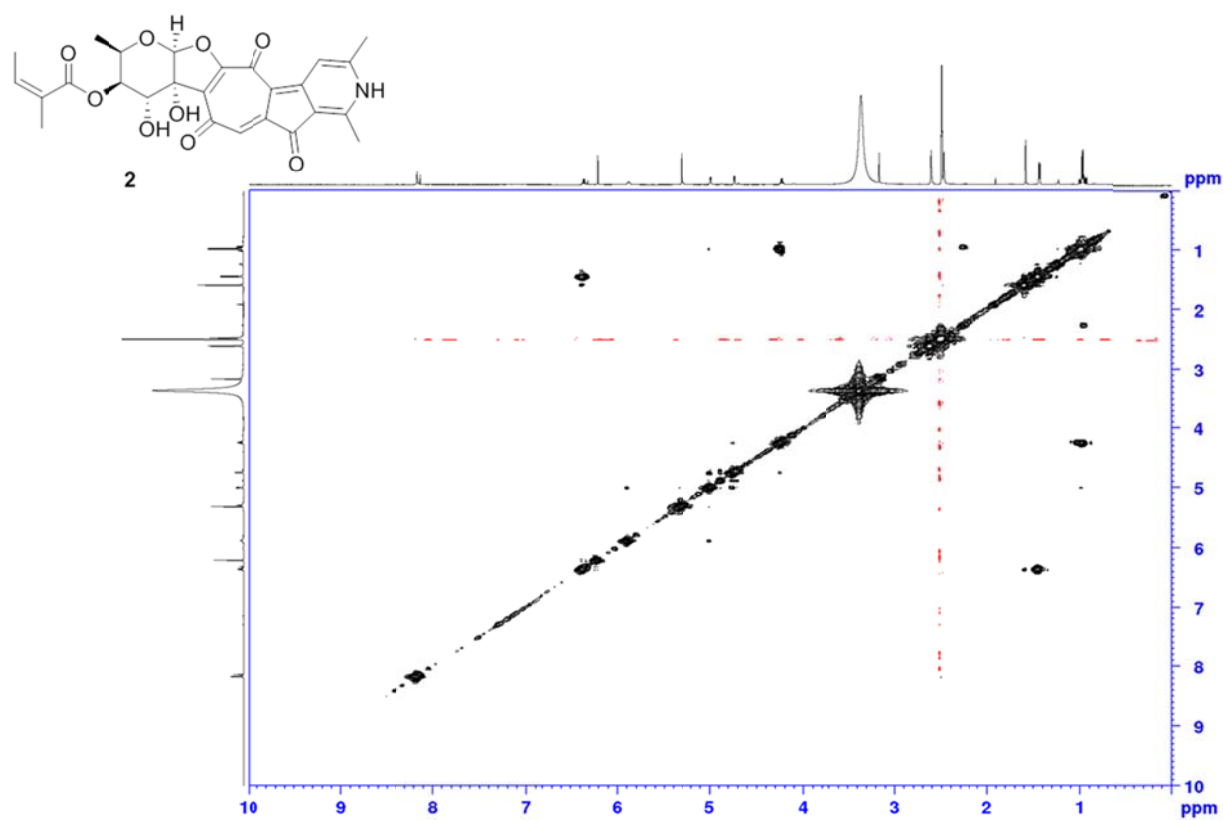
Figure S27. ¹H-¹H COSY spectrum of rubterolone B (2) (DMSO-d₆, 303K, 600 MHz).
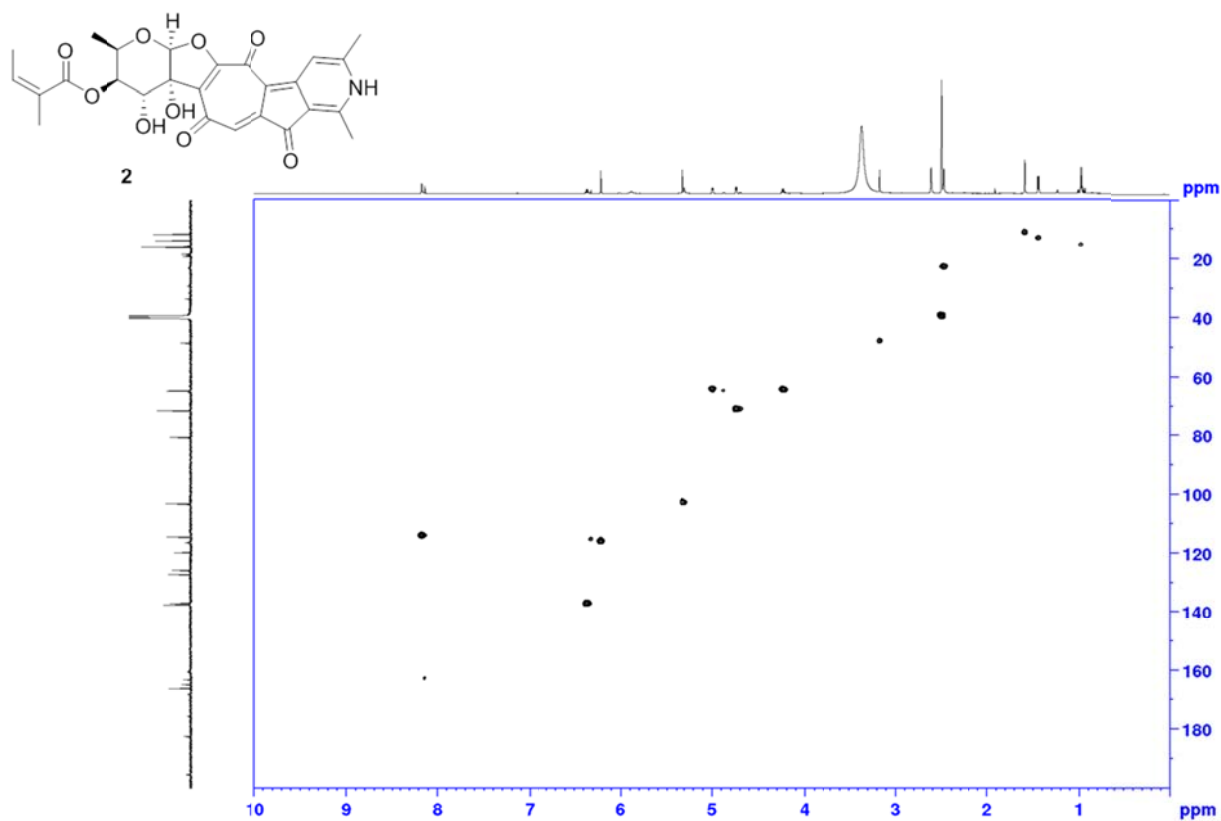
Figure S28. HSQC spectrum of rubterolone B (**2**) (DMSO-d$_6$, 303K, 600 MHz).
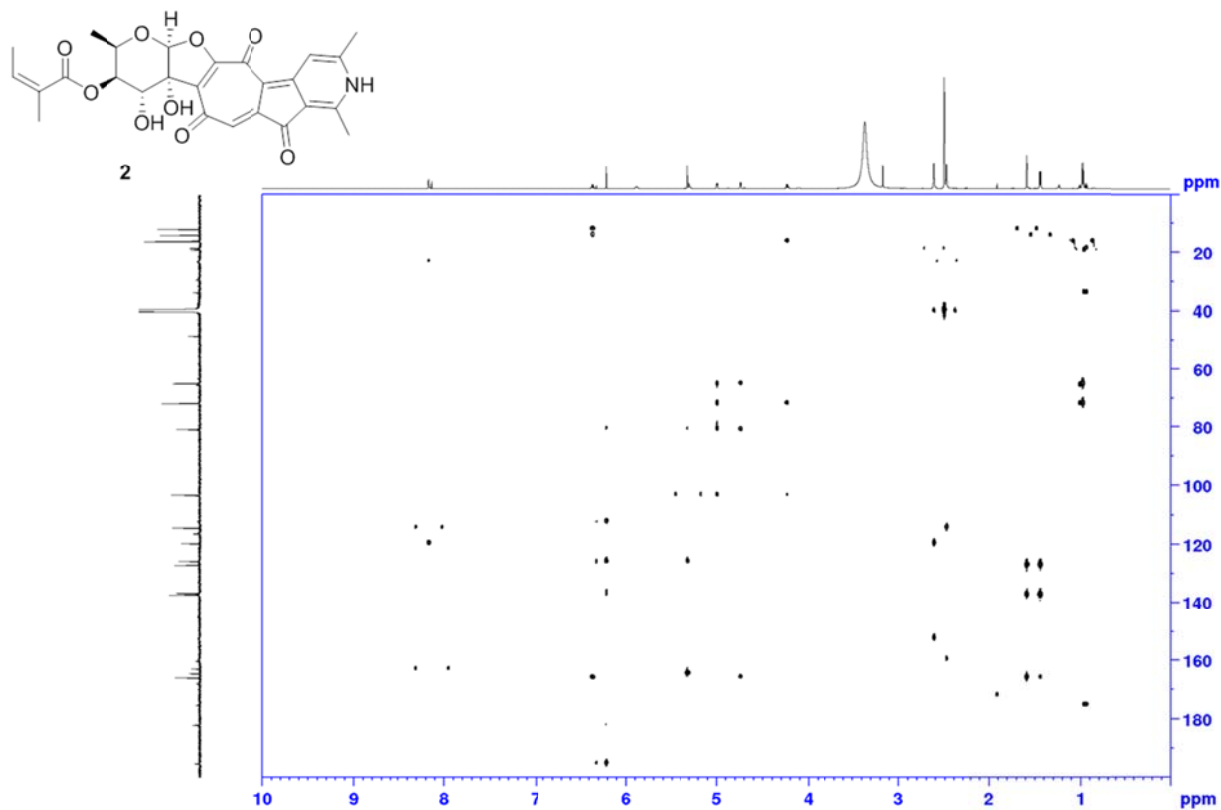
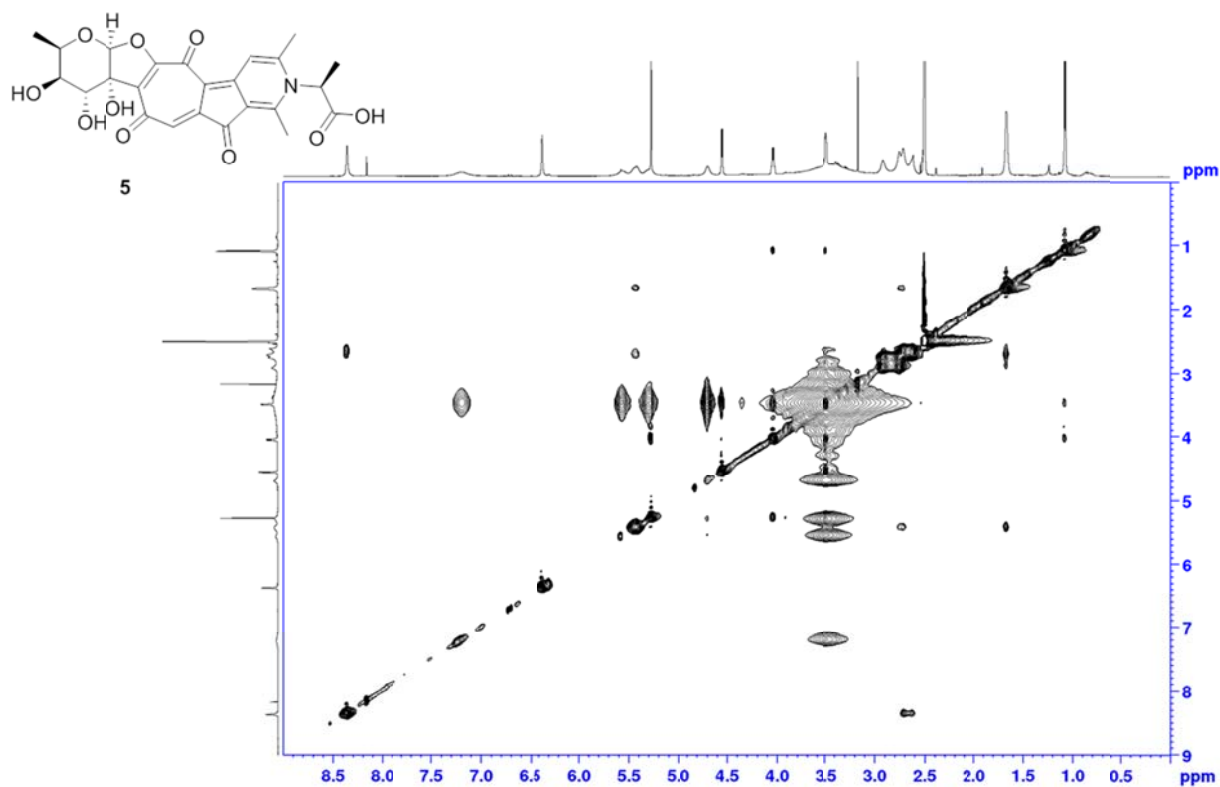**Figure S29.** HMBC spectrum of rubterolone B (**2**) (DMSO-d$_6$, 303K, 600 MHz).
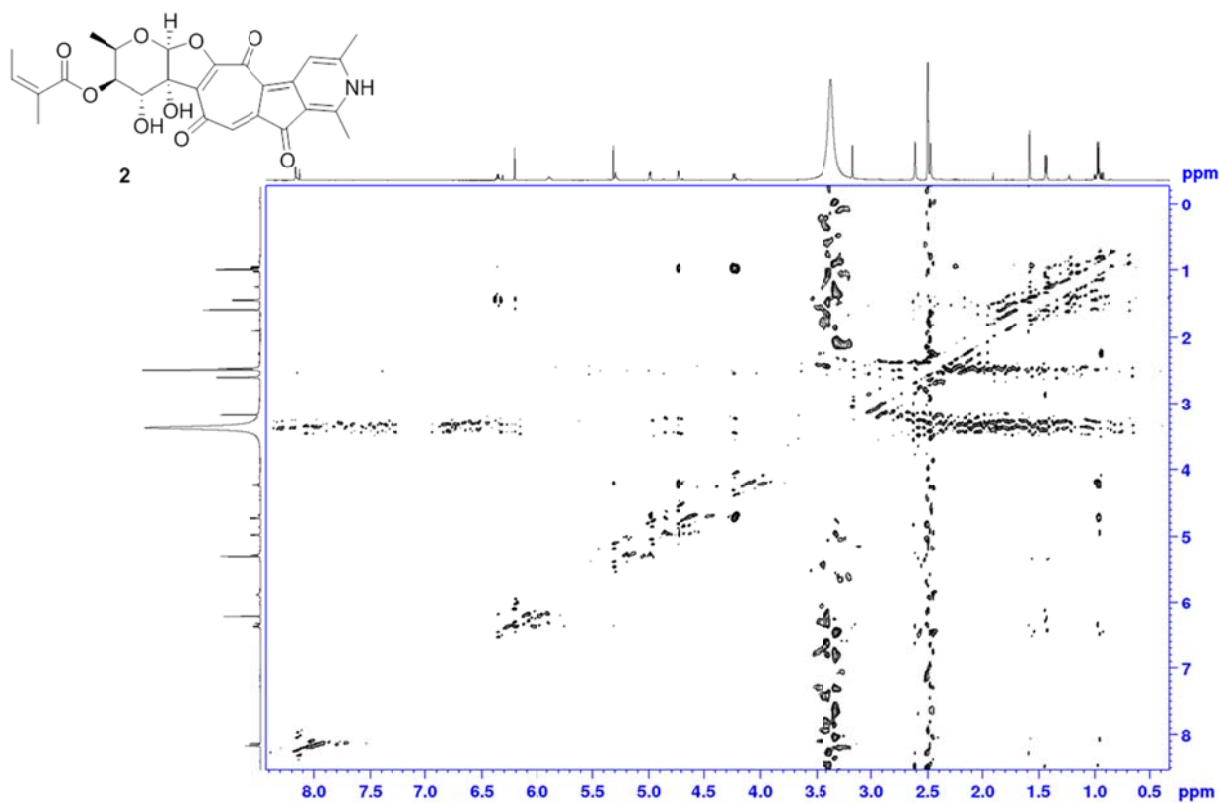
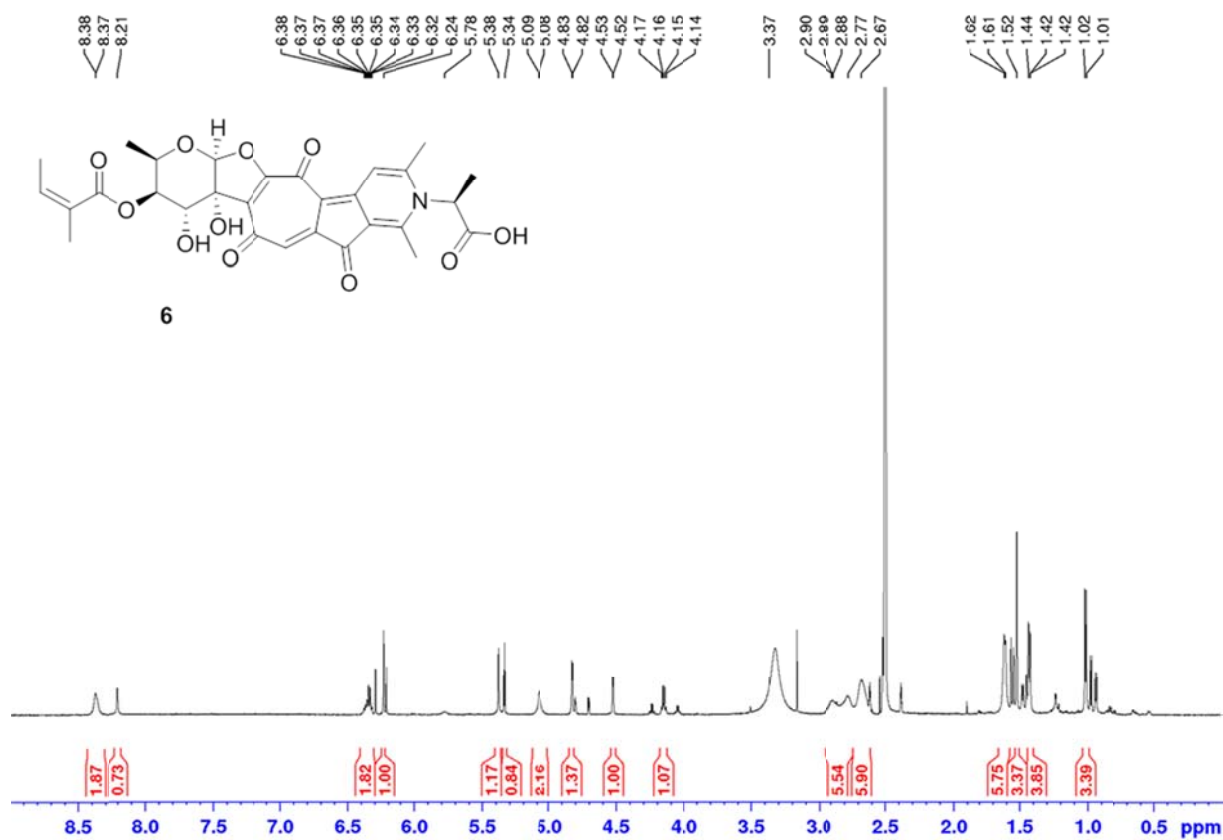**Figure S30.** NOESY spectrum of rubterolone B (2) (DMSO-d$_6$, 303K, 500 MHz).
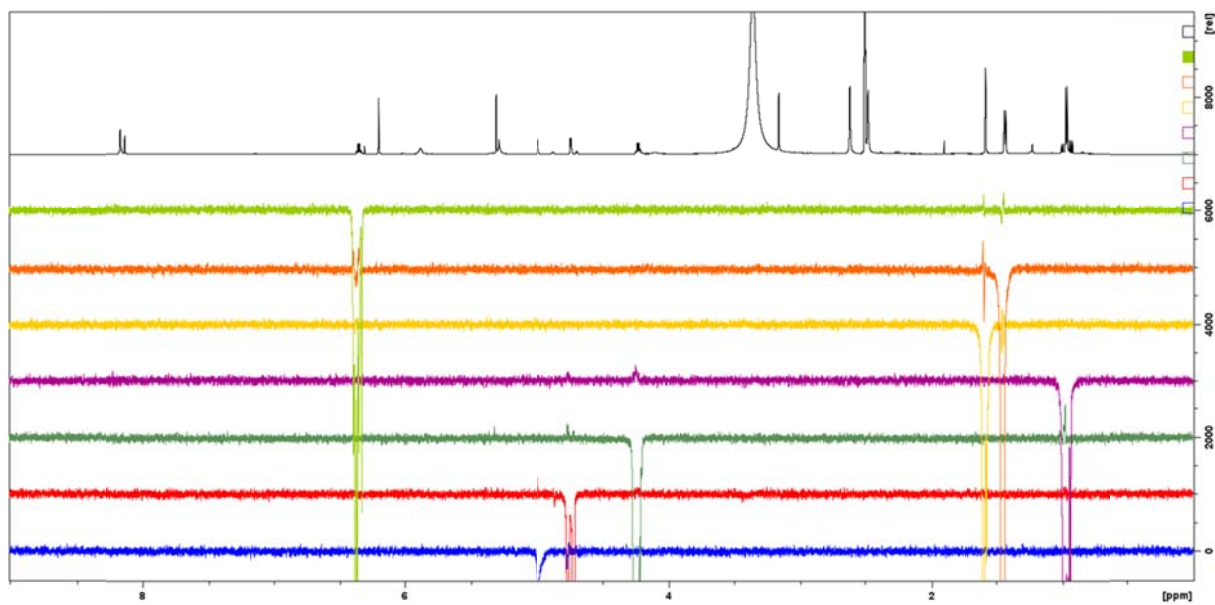
Figure S31. 1D selNOE spectrum of rubterolone B (2) (DMSO-d$_6$, 303K, 600 MHz).
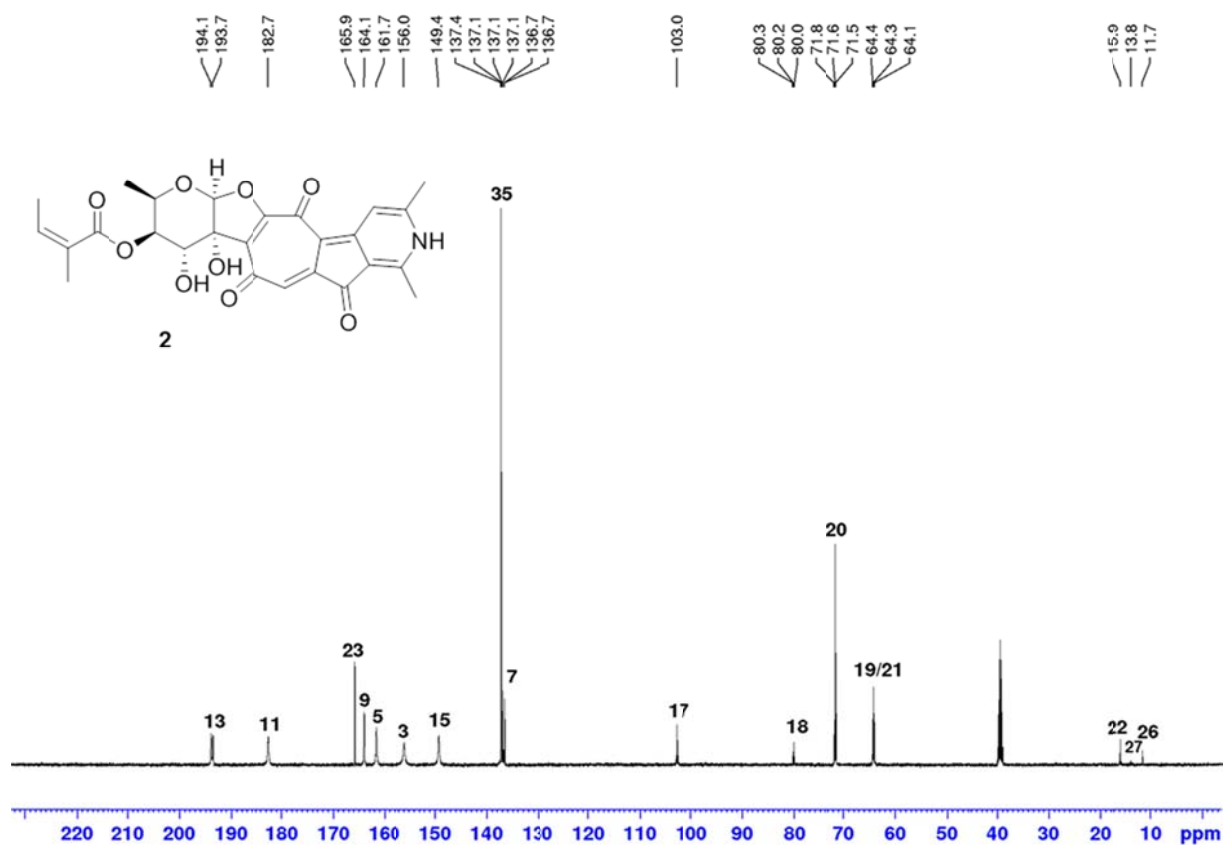
Figure S32. ^{13}C NMR spectrum of [1-^{13}C] acetate labeled rubterolone B (2a) (DMSO-d$_6$, 303K, 600 MHz).
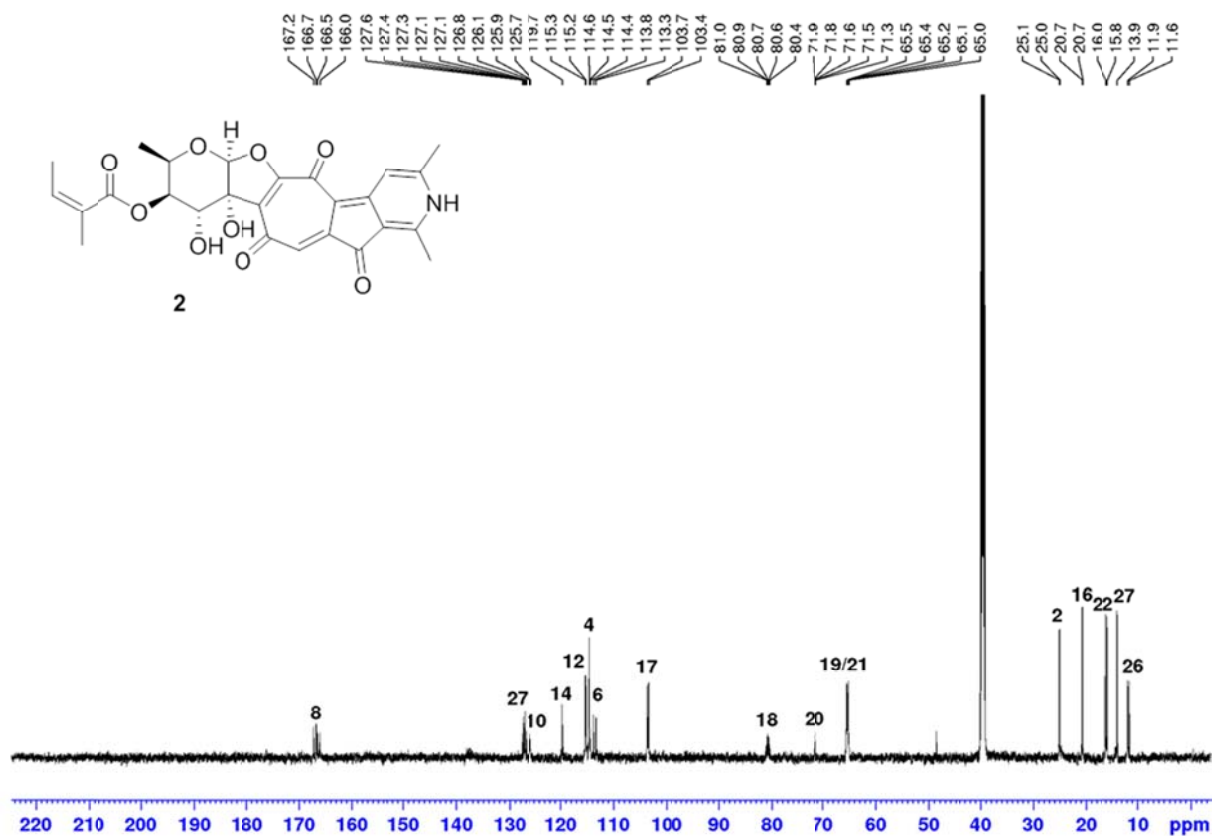
Figure S33. ^{13}C NMR spectrum of [2-^{13}C] acetate labeled rubterolone B (2b) (DMSO-d$_6$, 303K, 600 MHz).
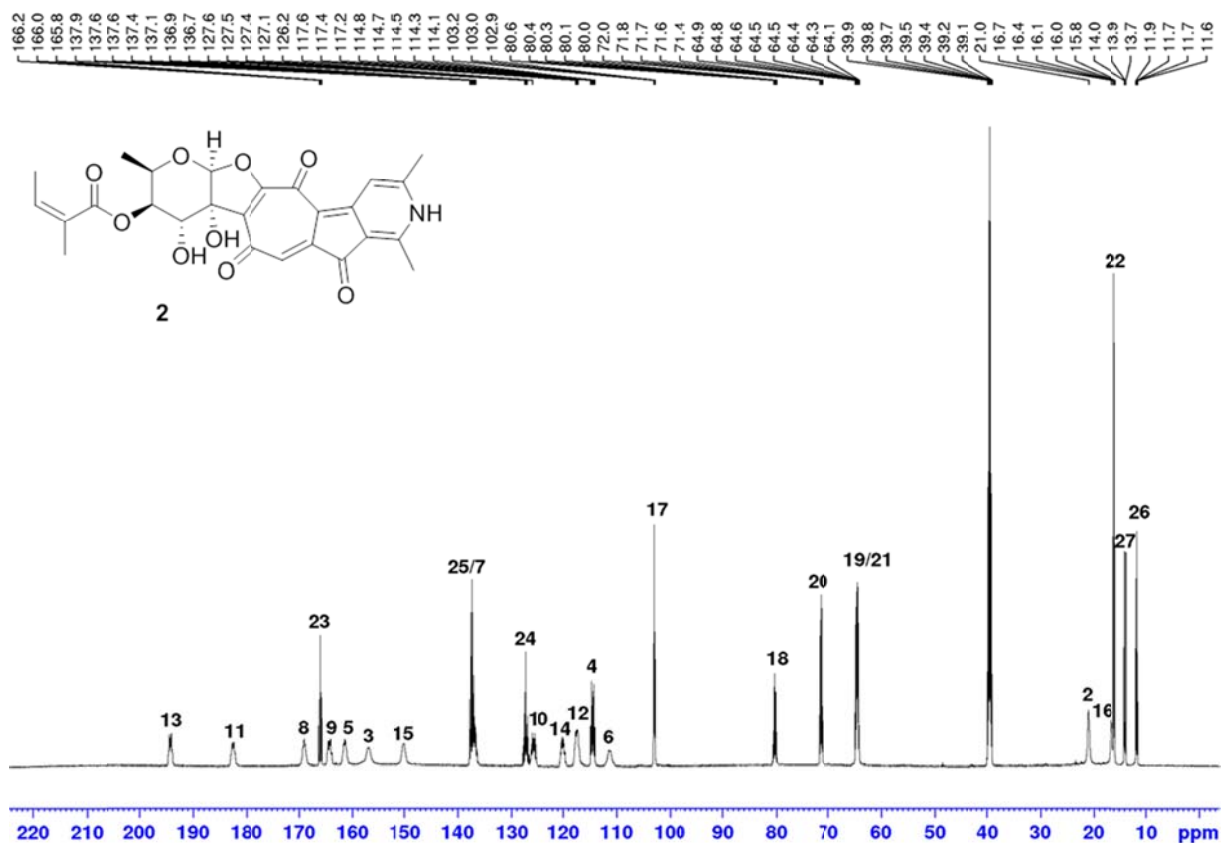
Figure S34. ^{13}C NMR spectrum of [1,2-^{13}C$_2$] acetate labeled rubterolone B (2c) (DMSO-d$_6$, 303K, 600 MHz).
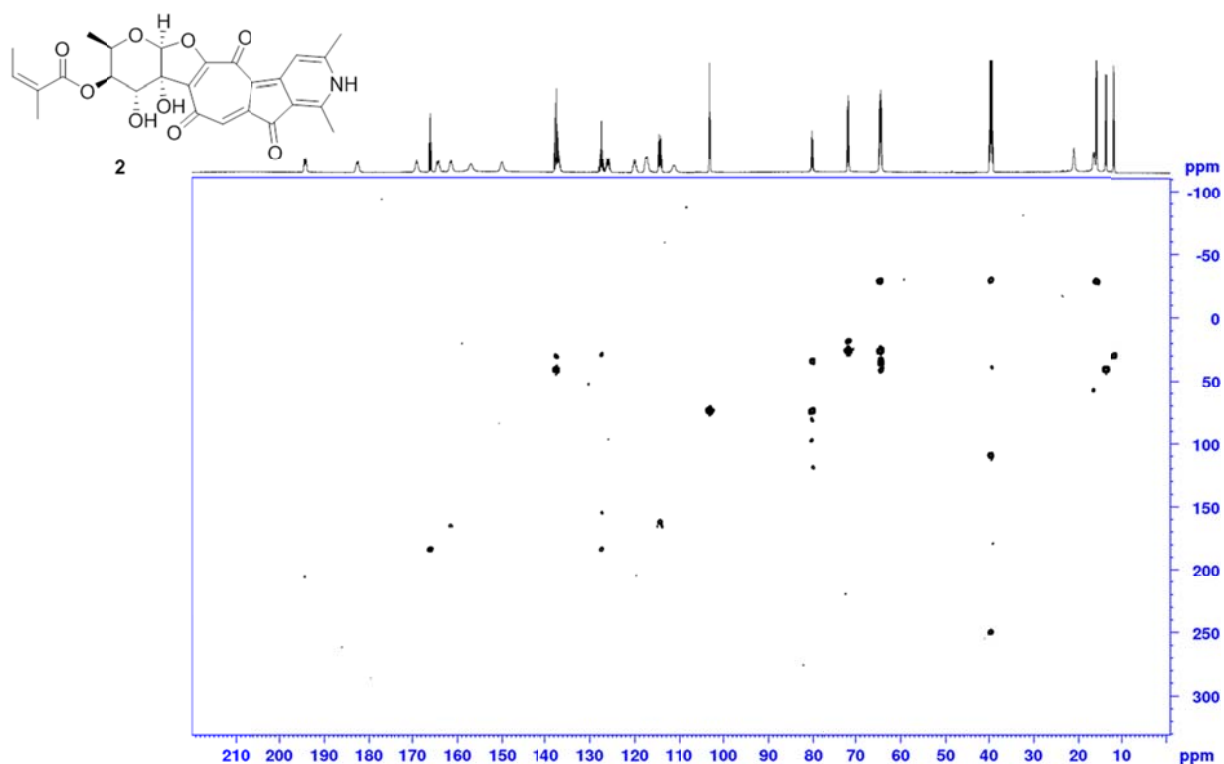
Figure S35. ^{13}C 2D INADEQUATE spectrum of [1,2-^{13}C$_2$] acetate labeled rubterolone B (2c) (DMSO-d$_6$, 303K, 600 MHz, D4 0.0065 s).
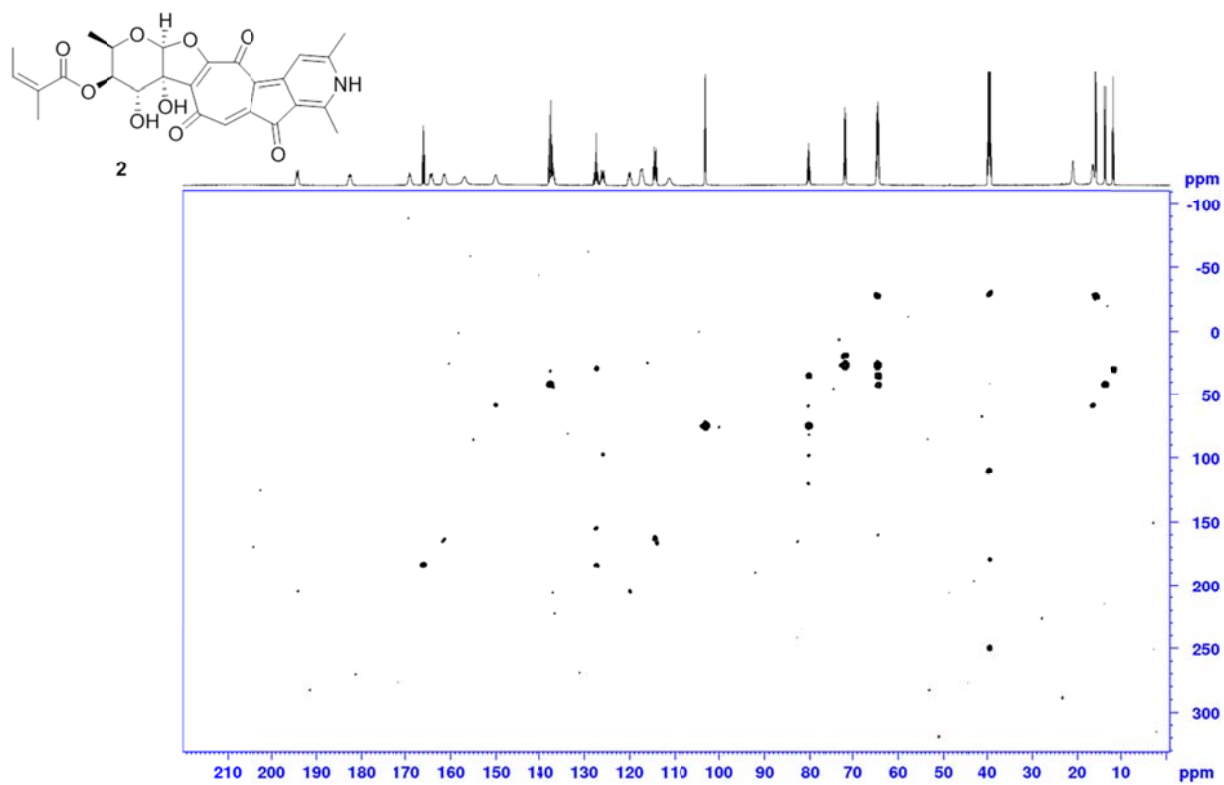
Figure S36. ^{13}C 2D INADEQUATE spectrum of [1,2-^{13}C$_2$] acetate labeled rubterolone B (2c) (DMSO-d$_6$, 303K, 600 MHz, D4 0.02 s).
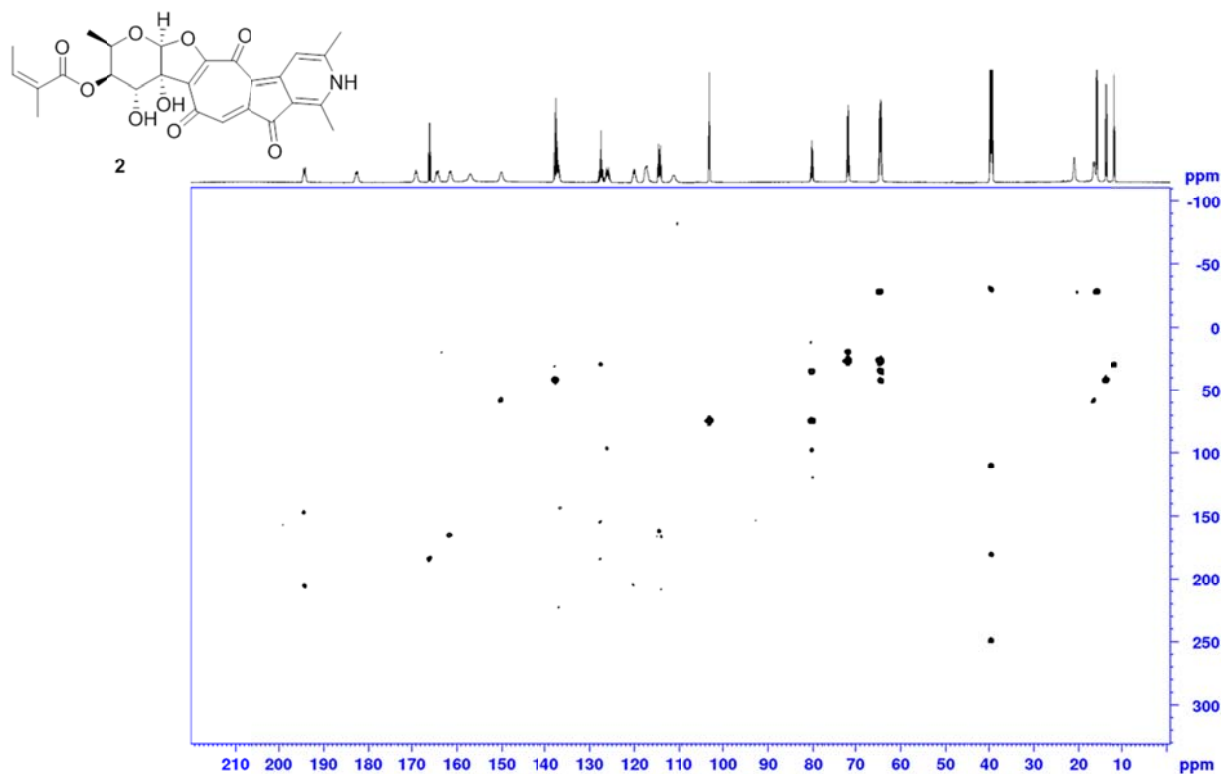
Figure S37. ^{13}C 2D INADEQUATE spectrum of [1,2-^{13}C$_2$] acetate labeled rubterolone B (2c) (DMSO-d$_6$, 303K, 600 MHz, D4 0.04 s).
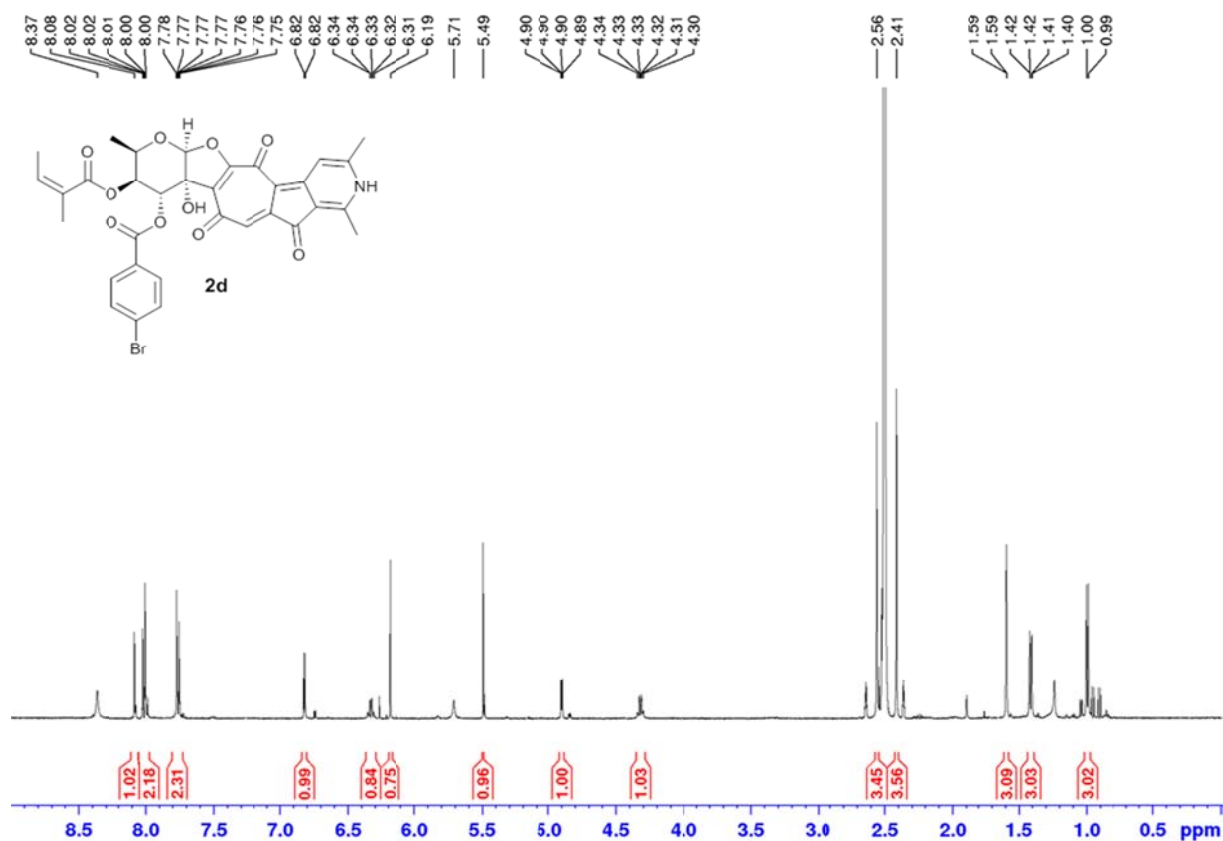
Figure S38. ^{1}H NMR spectrum of 4-bromobenzoyl rubterolone B (**2d**) (DMSO-d_6, 303K, 600 MHz).
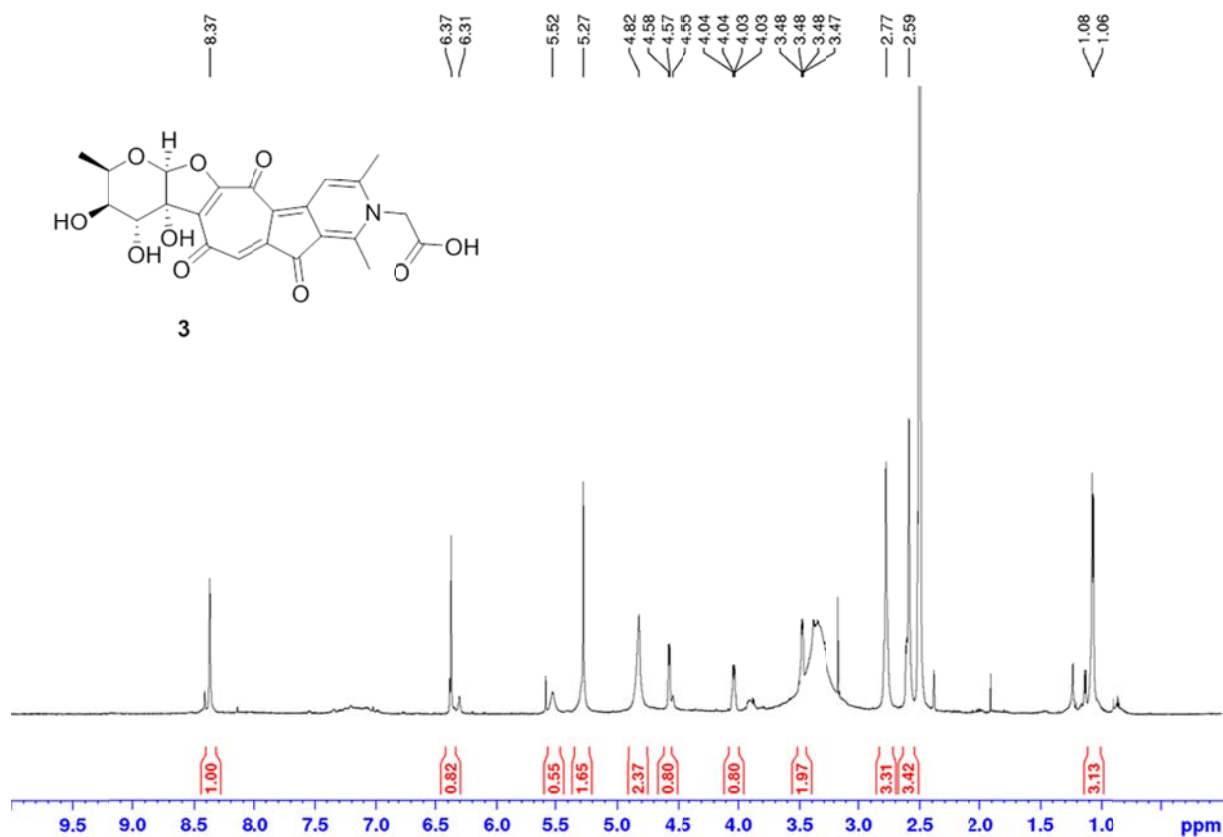
Figure S39. ^{1}H NMR spectrum of rubterolone C (**3**) (DMSO-d$_6$, 303K, 600 MHz).

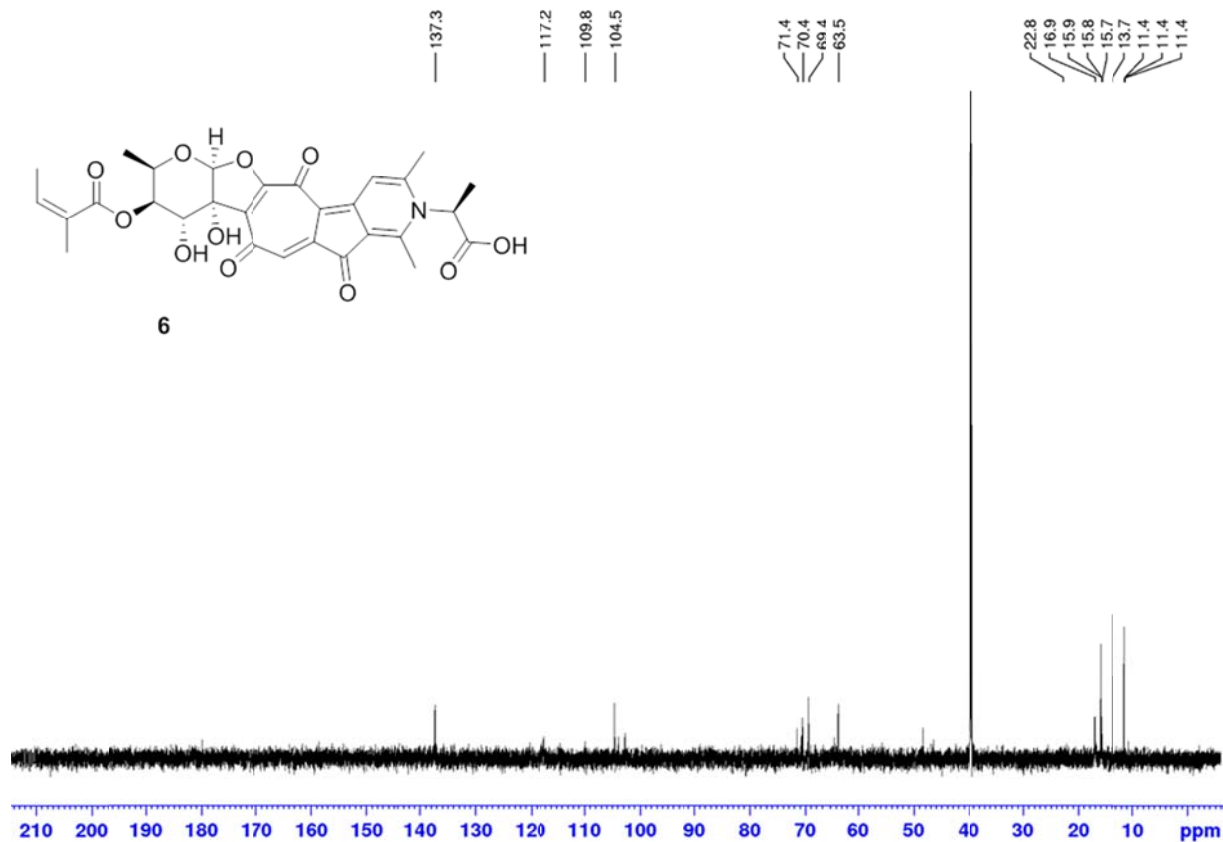**Figure S40.** ^{13}C NMR spectrum of rubterolone C (3) (DMSO-d_6, 303K, 150 MHz).

**Figure S41.** DEPT135 spectrum of rubterolone C (3) (DMSO-d_6, 303K, 150 MHz).

Figure S42. ^{1}H-^{1}H COSY spectrum of rubterolone C (3) (DMSO-d$_6$, 303K, 600 MHz).
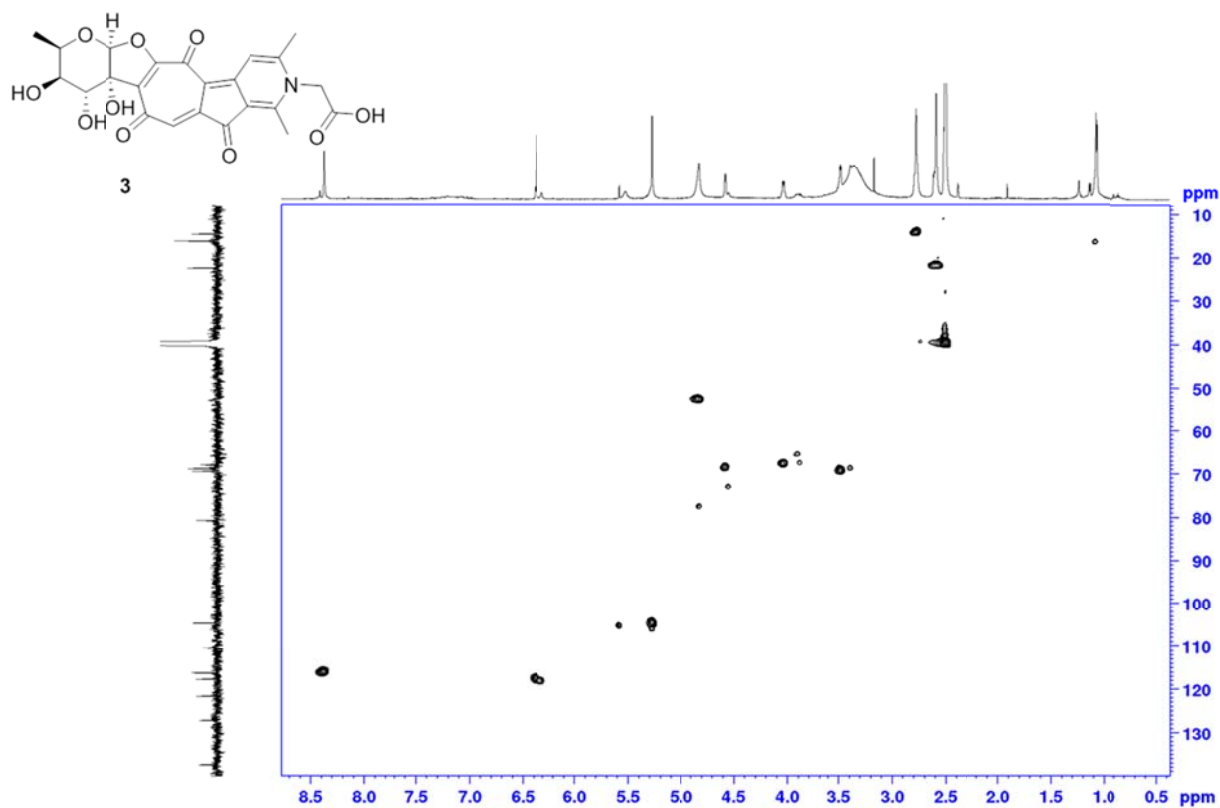
Figure S43. HSQC spectrum of rubterolone C (3) (DMSO-d$_6$, 303K, 600 MHz).

Figure S44. HMBC spectrum of rubterolone C (**3**) (DMSO-d_6, 303K, 600 MHz).

**Figure S45**. NOESY spectrum of rubterolone C (**3**) (DMSO-d_6, 303K, 600 MHz).
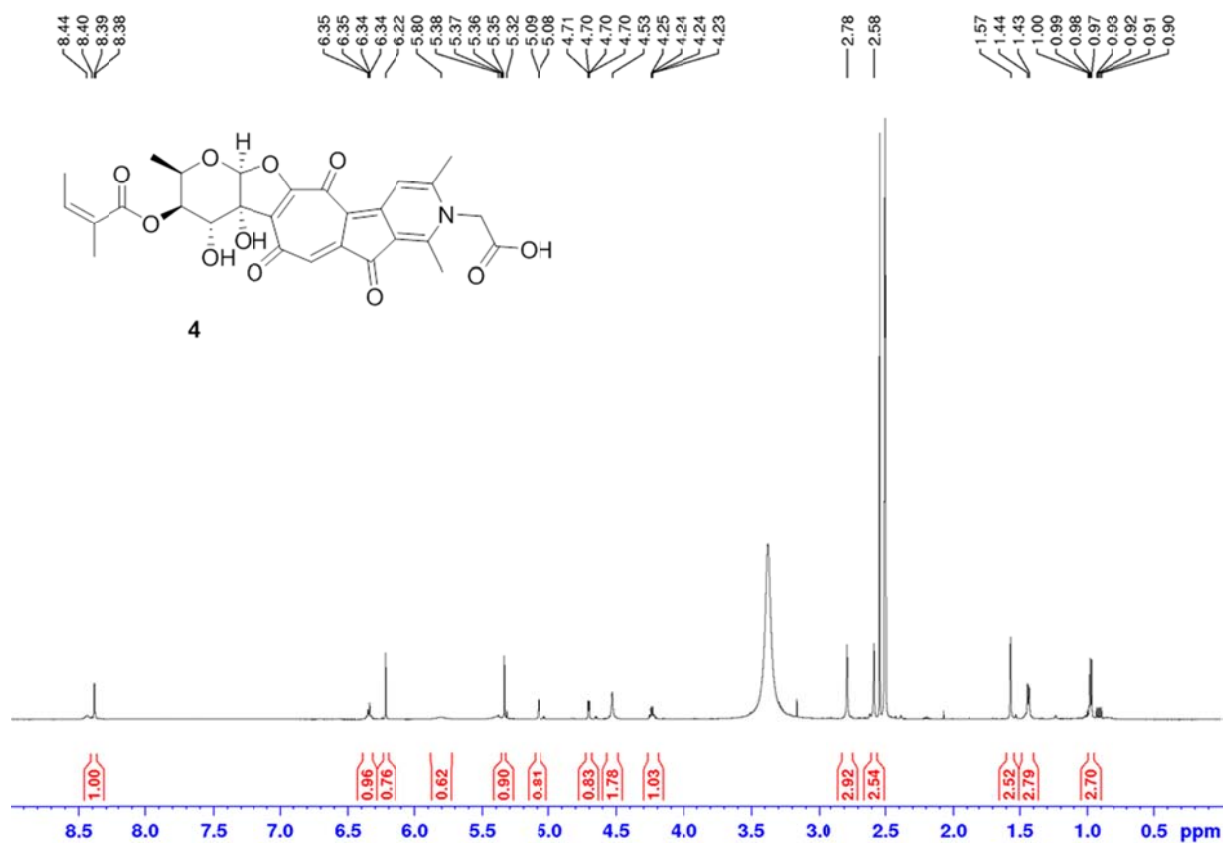
Figure S46. ^{1}H NMR spectrum of rubterolone D (**4**) (DMSO-d_6, 303K, 600 MHz).

Figure S47. ^{13}C NMR spectrum of rubterolone D (**4**) (DMSO-d_6, 303K, 150 MHz).

Figure S48. DEPT 135 spectrum of rubterolone D (**4**) (DMSO-d_6, 303K, 150 MHz).

Figure S49. ^{1}H-^{1}H COSY spectrum of rubterolone D (**4**) (DMSO-d_6, 303K, 600 MHz).
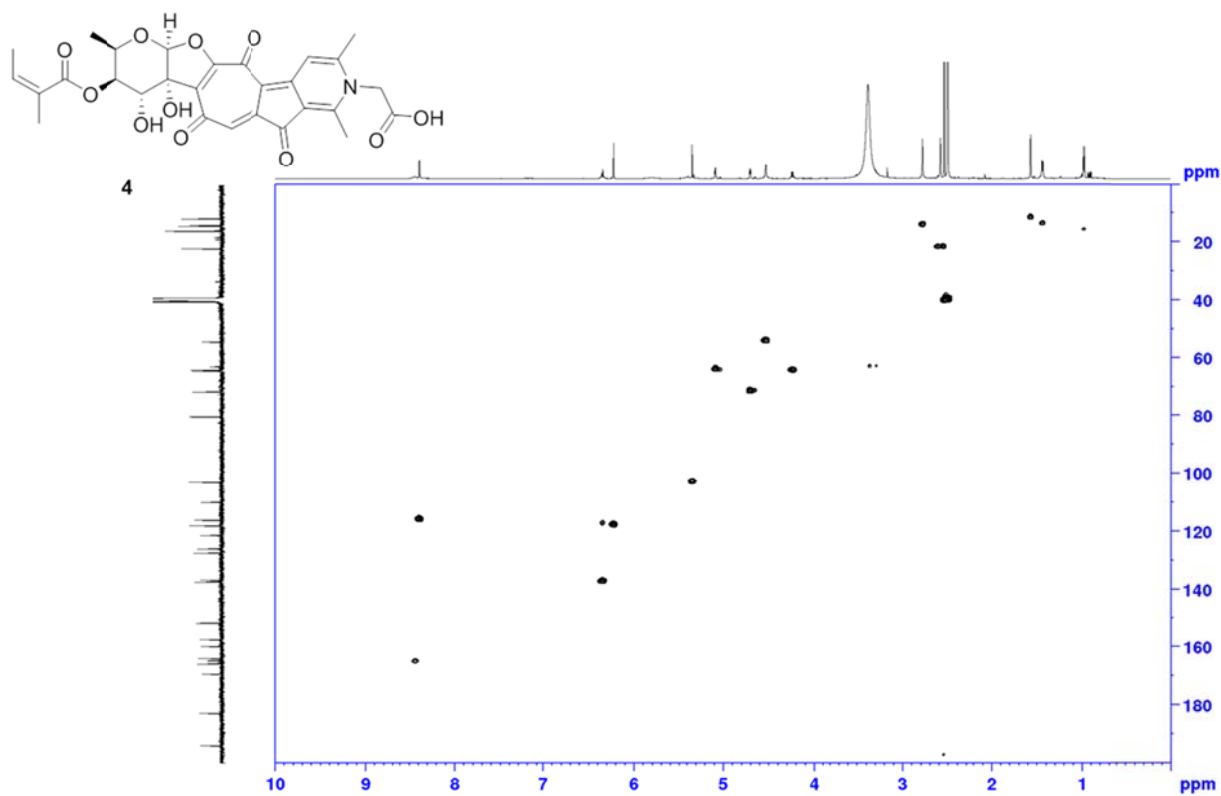
Figure S50. HSQC spectrum of rubterolone D (**4**) (DMSO-d_6, 303K, 600 MHz).

**Figure S51**. HMBC spectrum of rubterolone D (**4**) (DMSO-d_6, 303K, 600 MHz).

Figure S52. NOESY spectrum of rubterolone D (**4**) (DMSO-d_6, 303K, 600 MHz).
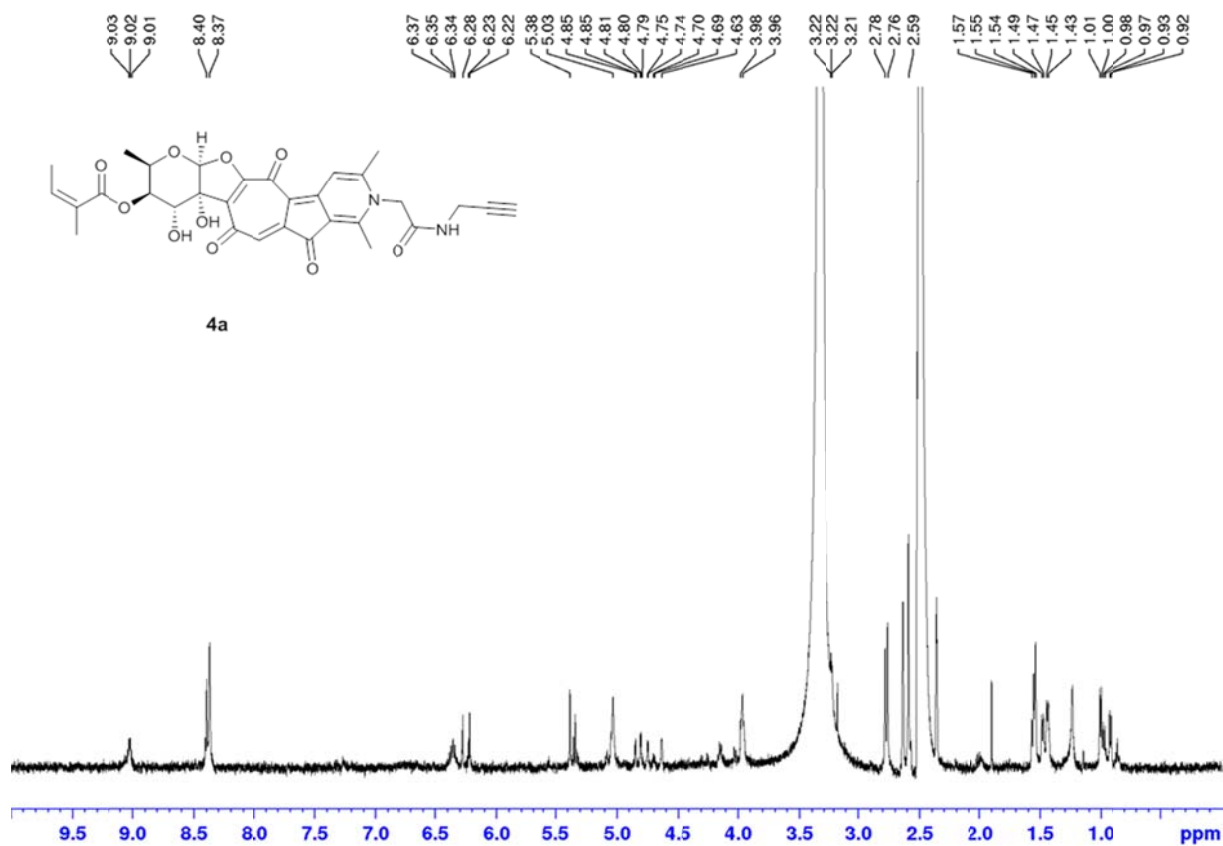
Figure S53. ^{1}H NMR spectrum of propargyl-rubterolone D (**4a**) (DMSO-d_6, 303K, 600 MHz).
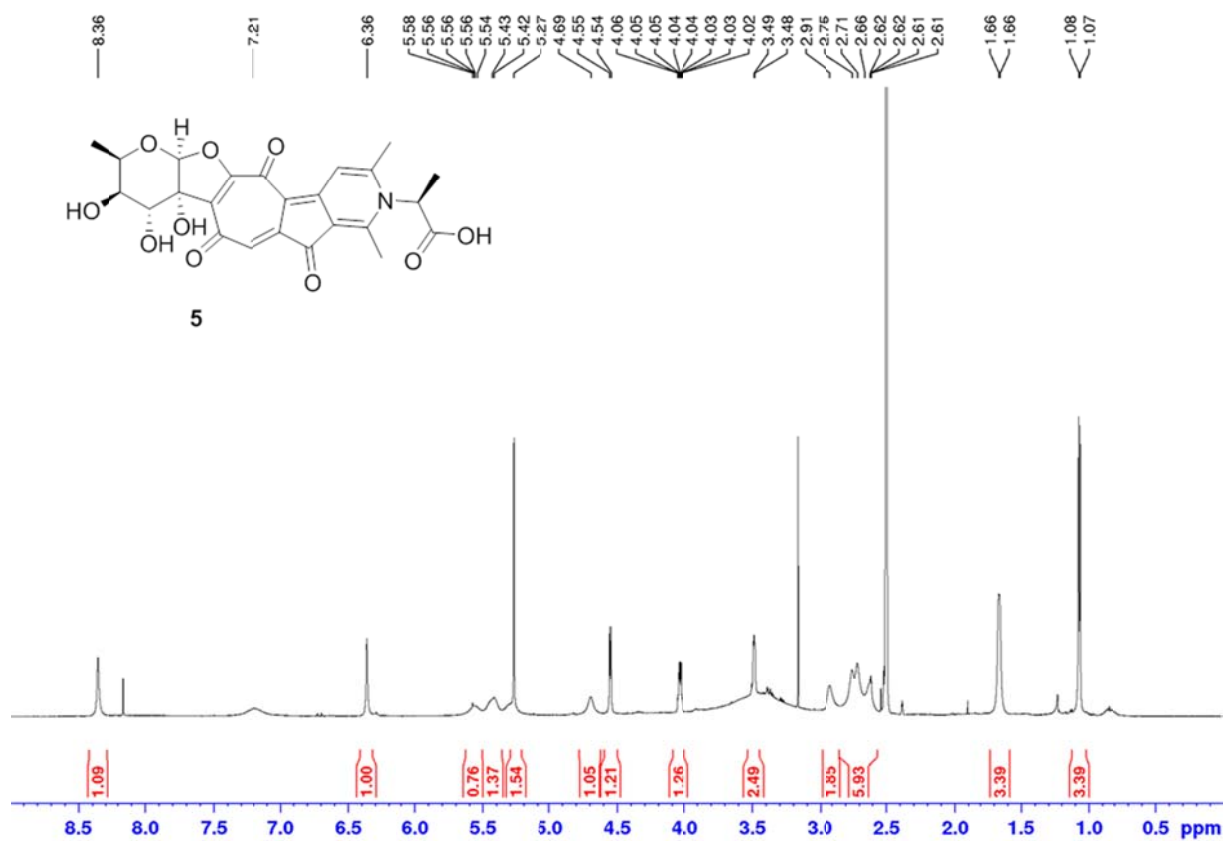
Figure S54. ^{1}H NMR spectrum of rubterolone E **(5)** (DMSO-d_6, 303K, 600 MHz).
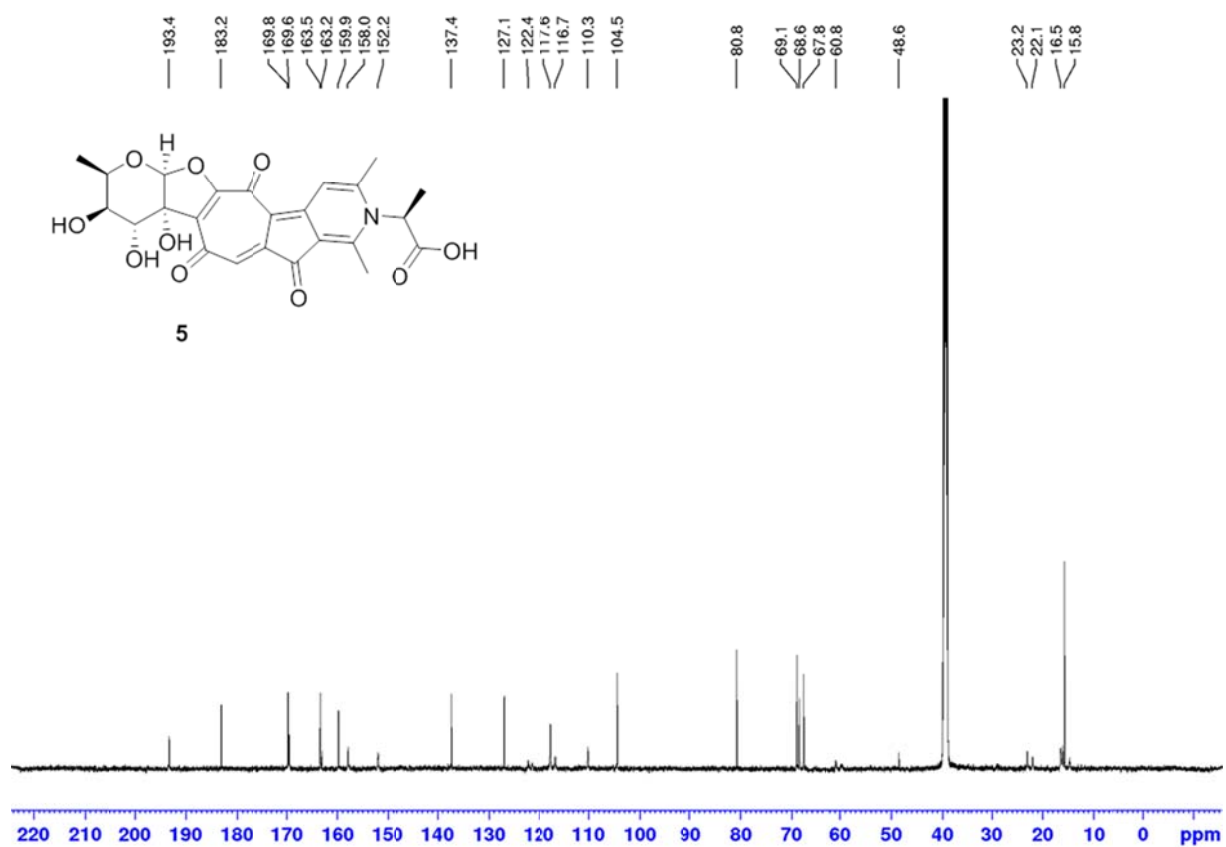
Figure S55. ^{13}C NMR spectrum of rubterolone E (**5**) (DMSO-d_6, 303K, 150 MHz).

Figure S56. DEPT 135 spectrum of rubterolone E (**5**) (DMSO-d_6, 303K, 150 MHz).

Figure S57. ^{1}H-^{1}H COSY spectrum of rubterolone E (**5**) (DMSO-d_6, 303K, 600 MHz).

Figure S58. HSQC spectrum of rubterolone E (**5**) (DMSO-d_6, 303K, 600 MHz).

Figure S59. HMBC spectrum of rubterolone E (**5**) (DMSO-d_6, 303K, 600 MHz).

Figure S60. NOESY spectrum of rubterolone E (**5**) (DMSO-d_6, 303K, 600 MHz).

Figure S61. ^{1}H NMR spectrum of rubterolone F (**6**) (DMSO-d_6, 303K, 600 MHz).
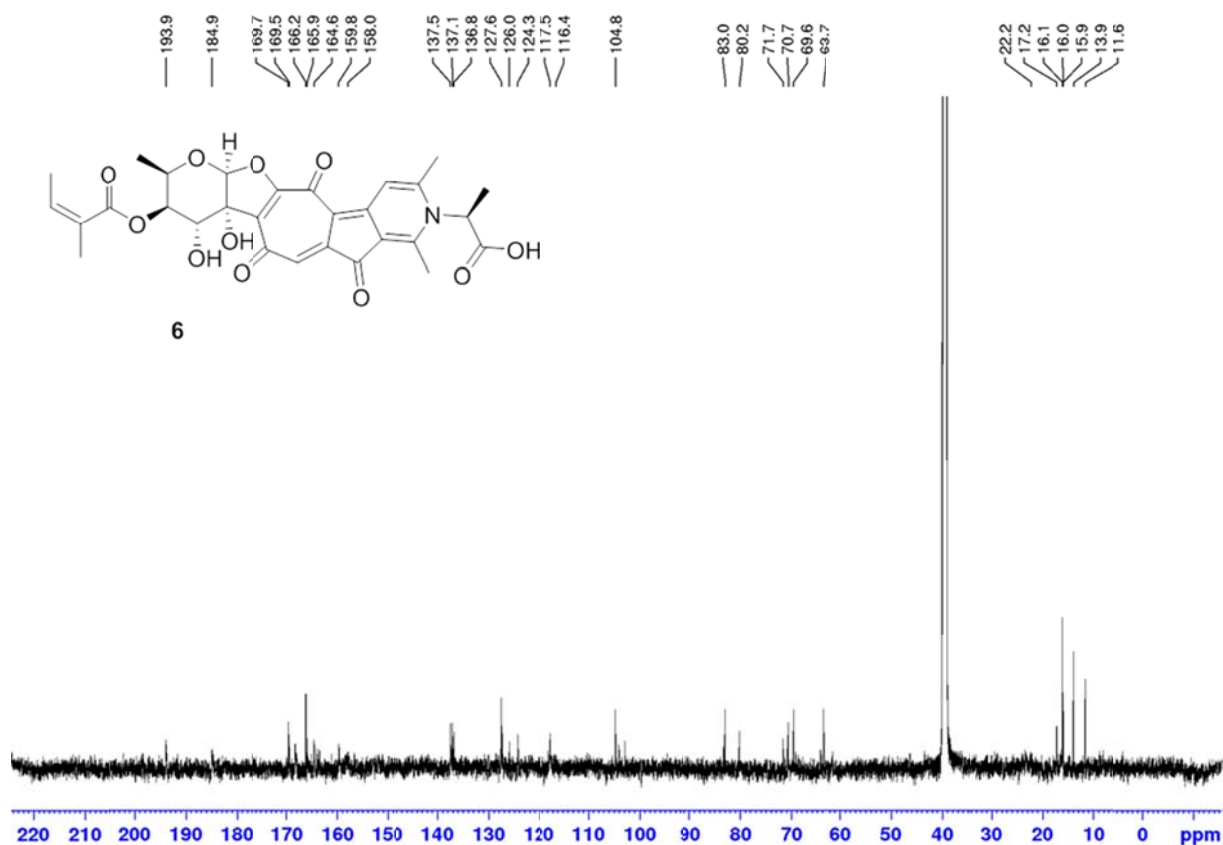
Figure S62. ^{13}C NMR spectrum of rubterolone F (**6**) (DMSO-d_6, 303K, 150 MHz).

Figure S63. DEPT 135 spectrum of rubterolone F (**6**) (DMSO-d_6, 303K, 150 MHz).
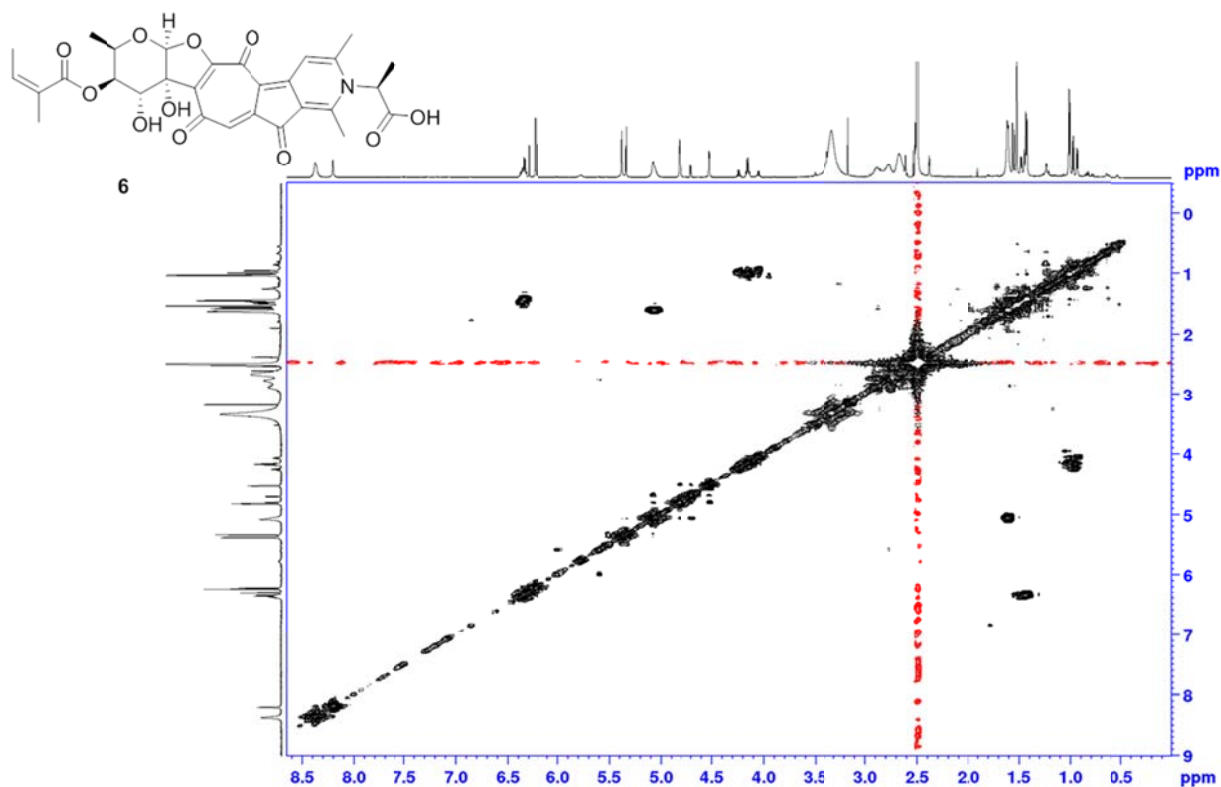
Figure S64. ^{1}H-^{1}H COSY spectrum of rubterolone F (**6**) (DMSO-d_6, 303K, 600 MHz).
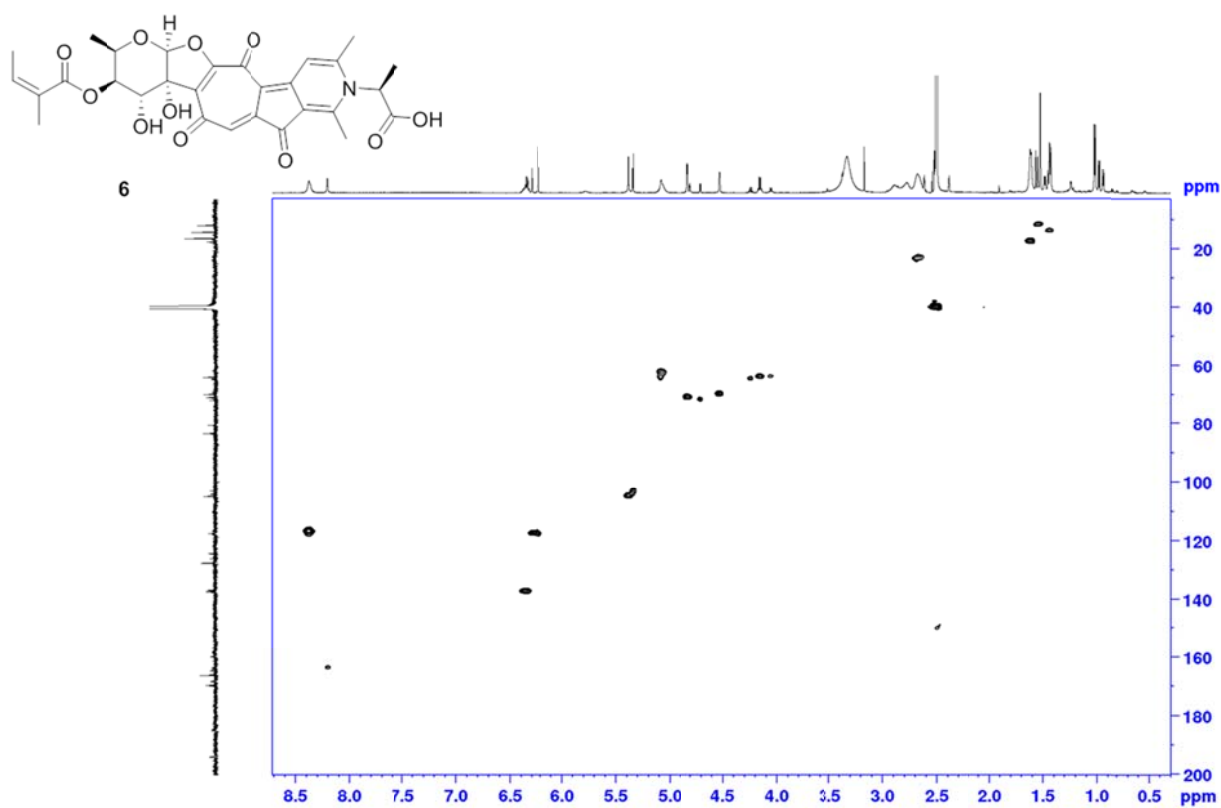
Figure S65. HSQC spectrum of rubterolone F (**6**) (DMSO-d_6, 303K, 600 MHz).
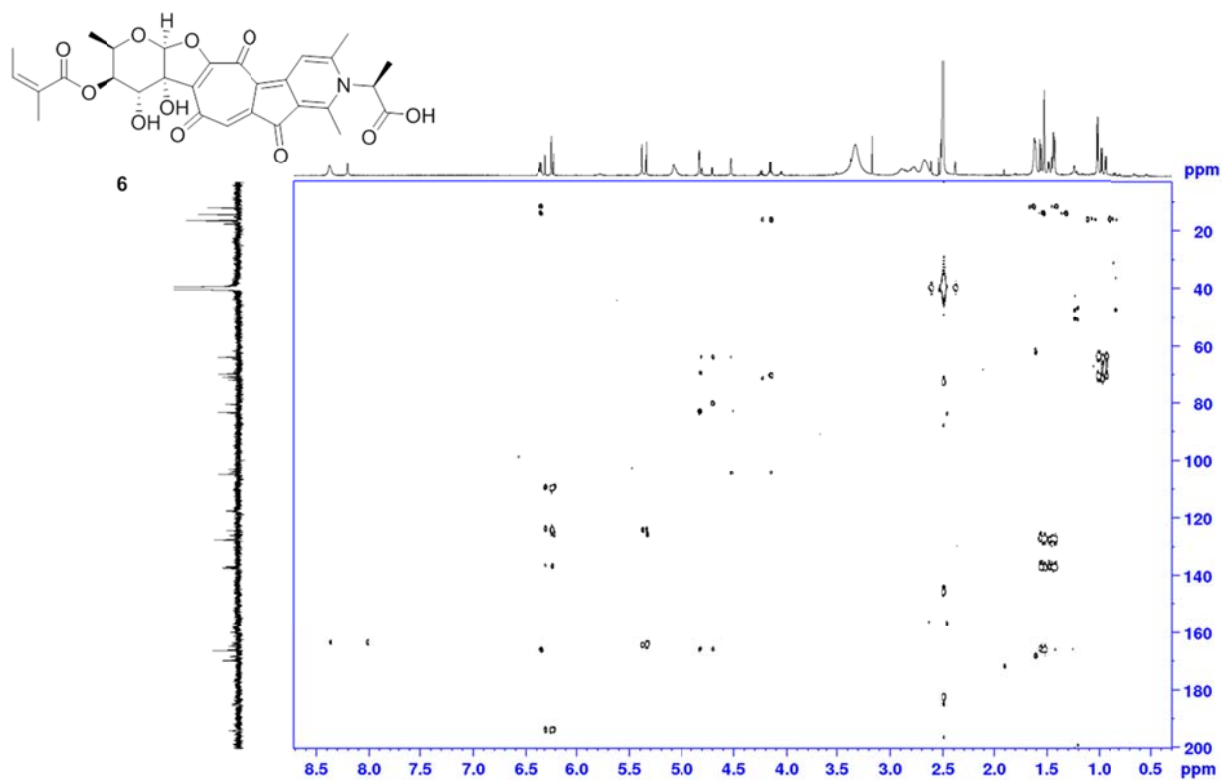
Figure S66. HMBC spectrum of rubterolone F (**6**) (DMSO-d_6, 303K, 600 MHz).
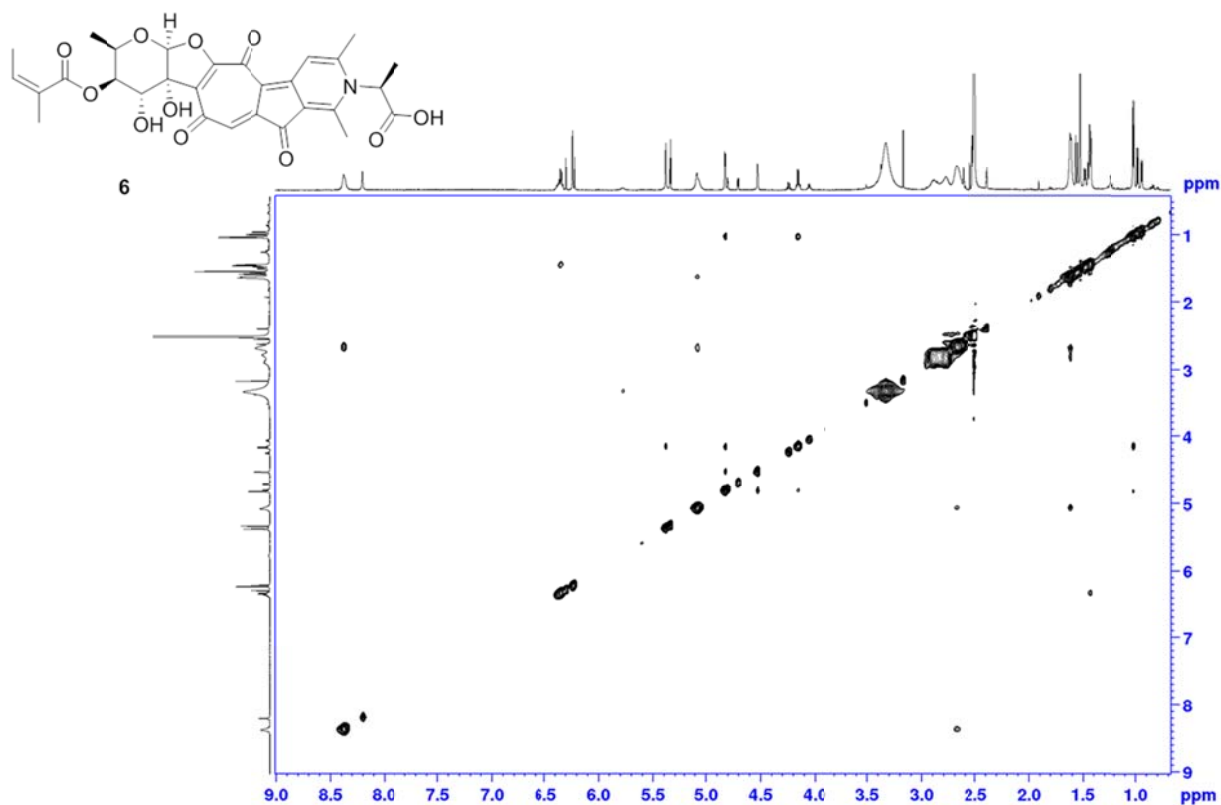
Figure S67. NOESY spectrum of rubterolone F (**6**) (DMSO-d_6, 303K, 600 MHz).
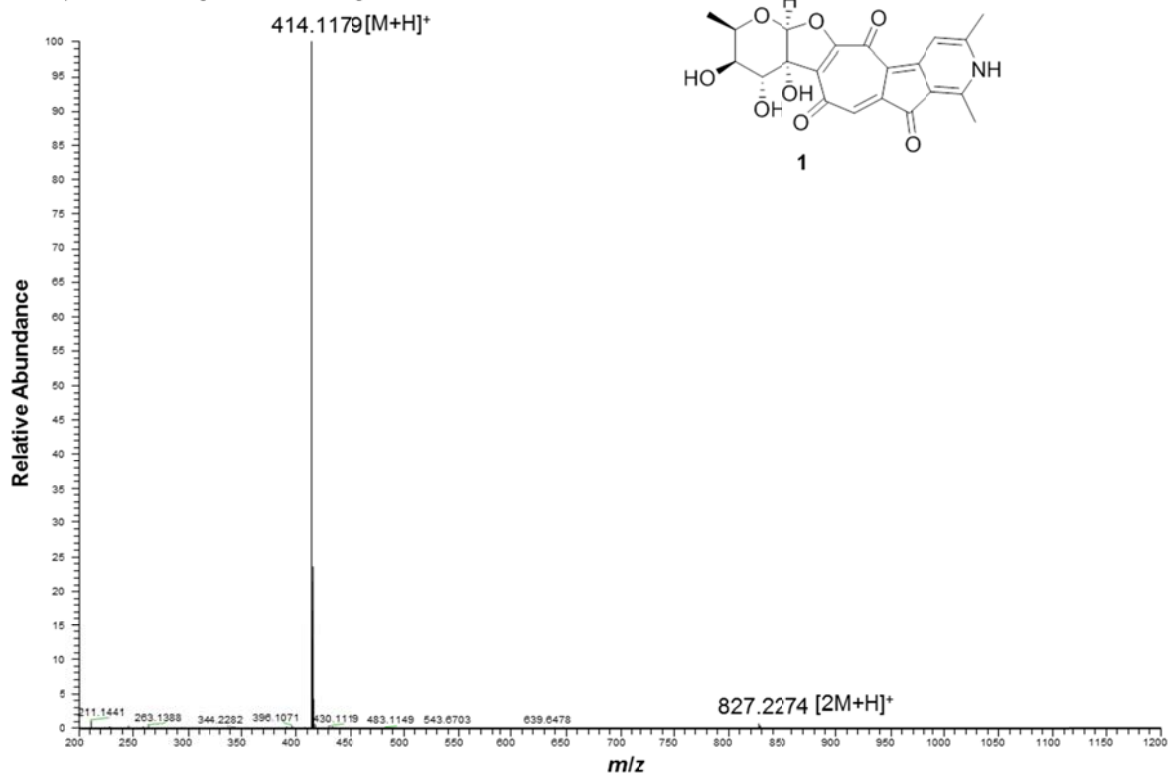
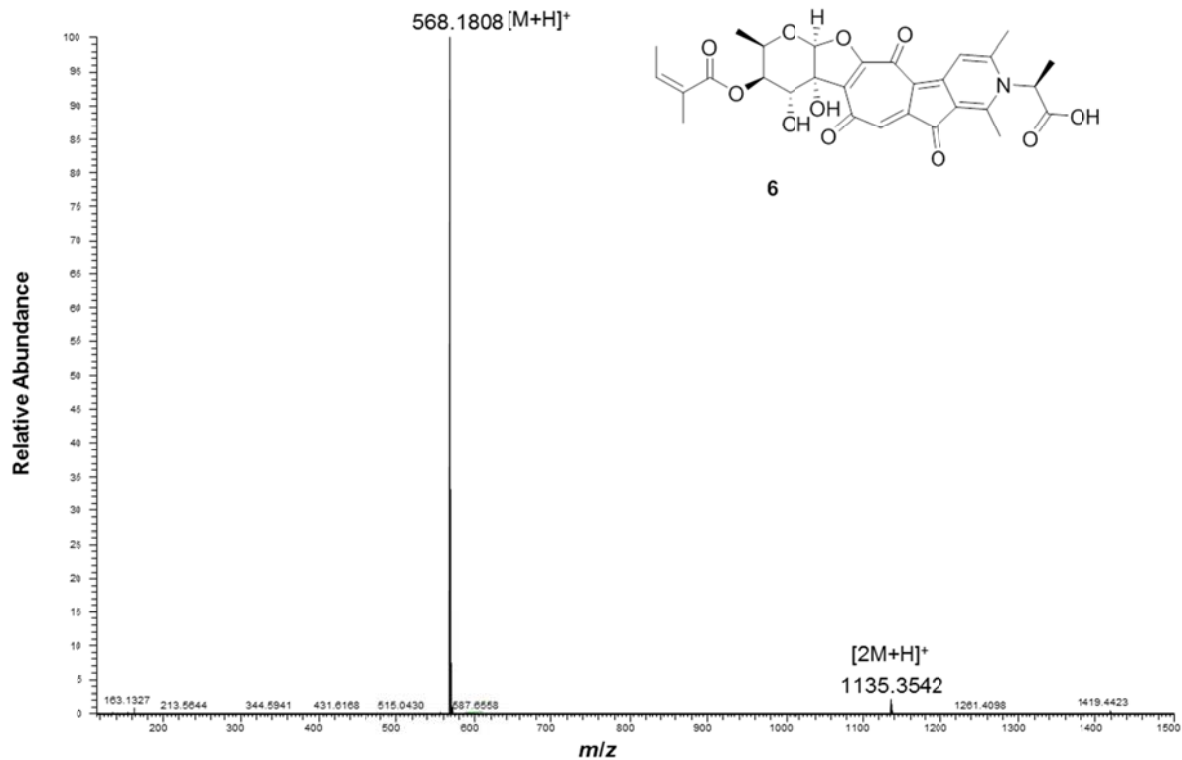**Figure S68**. ESI-HRMS (+) spectrum of rubterolone A (**1**).
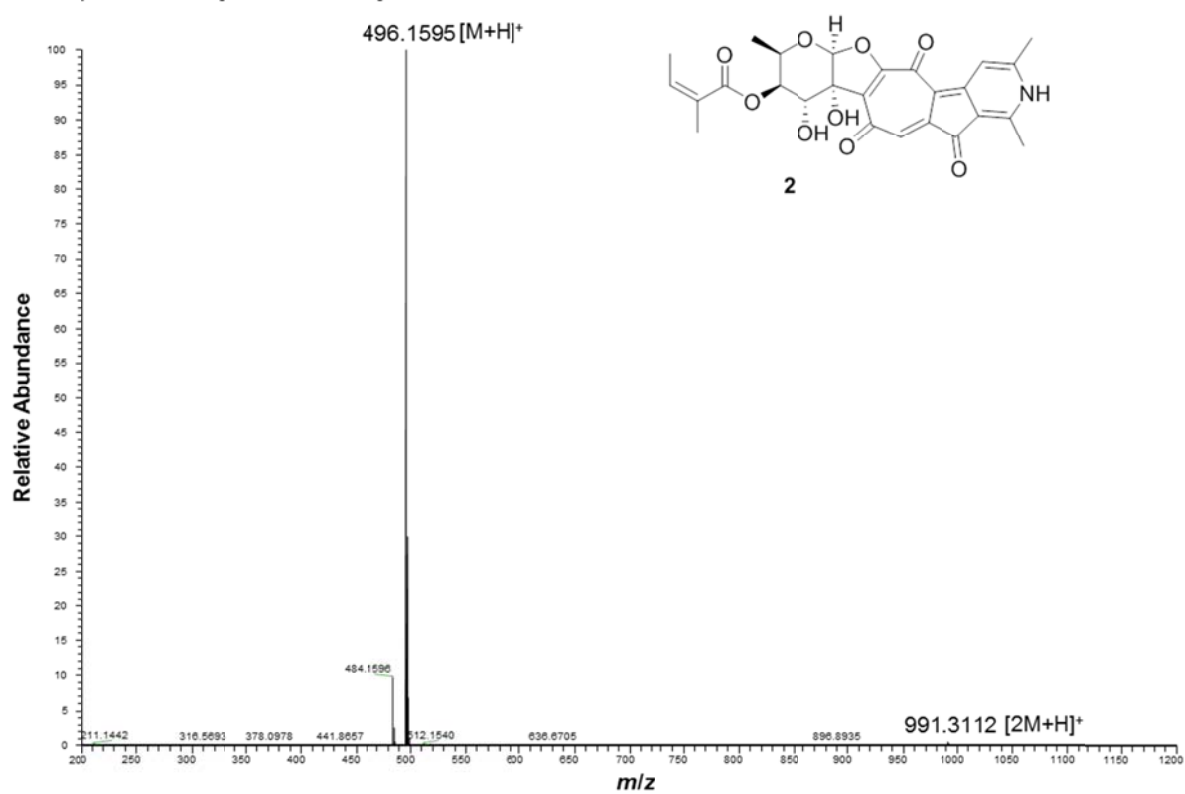
Figure S69. ESI-HRMS (+) spectrum of rubterolone B (**2**).

FTMS + p ESI Full ms [115.00-1500.00]
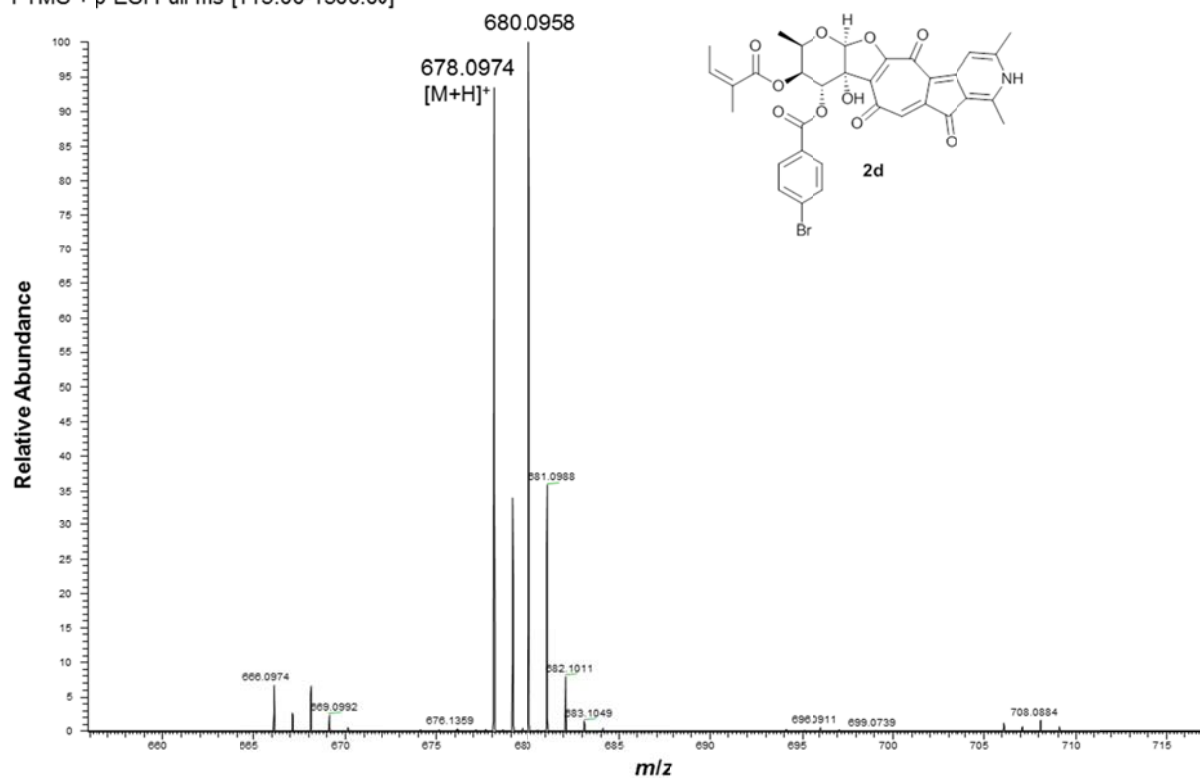
Figure S70. ESI-HRMS (+) spectrum of 4-bromobenzoyl rubterolone B (**2d**).

FTMS + p ESI Full ms [115.00-1500.00]
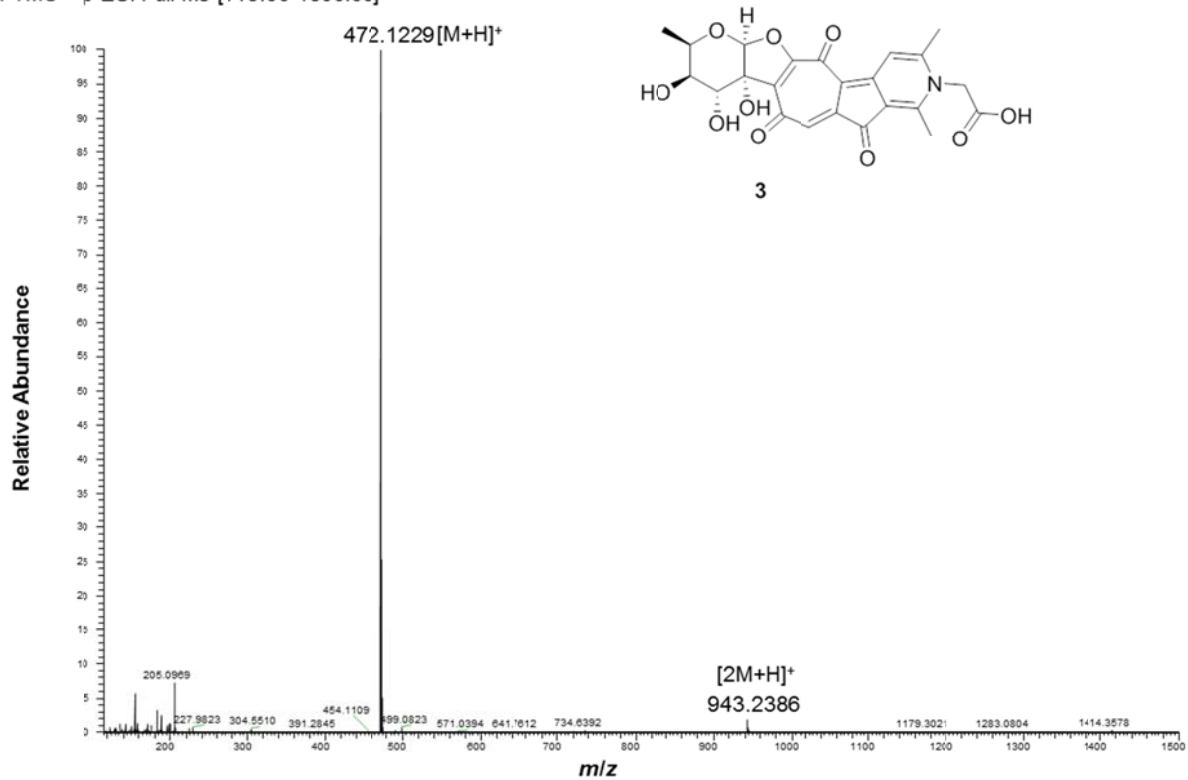
Figure S71. ESI-HRMS (+) spectrum of rubterolone C (**3**).
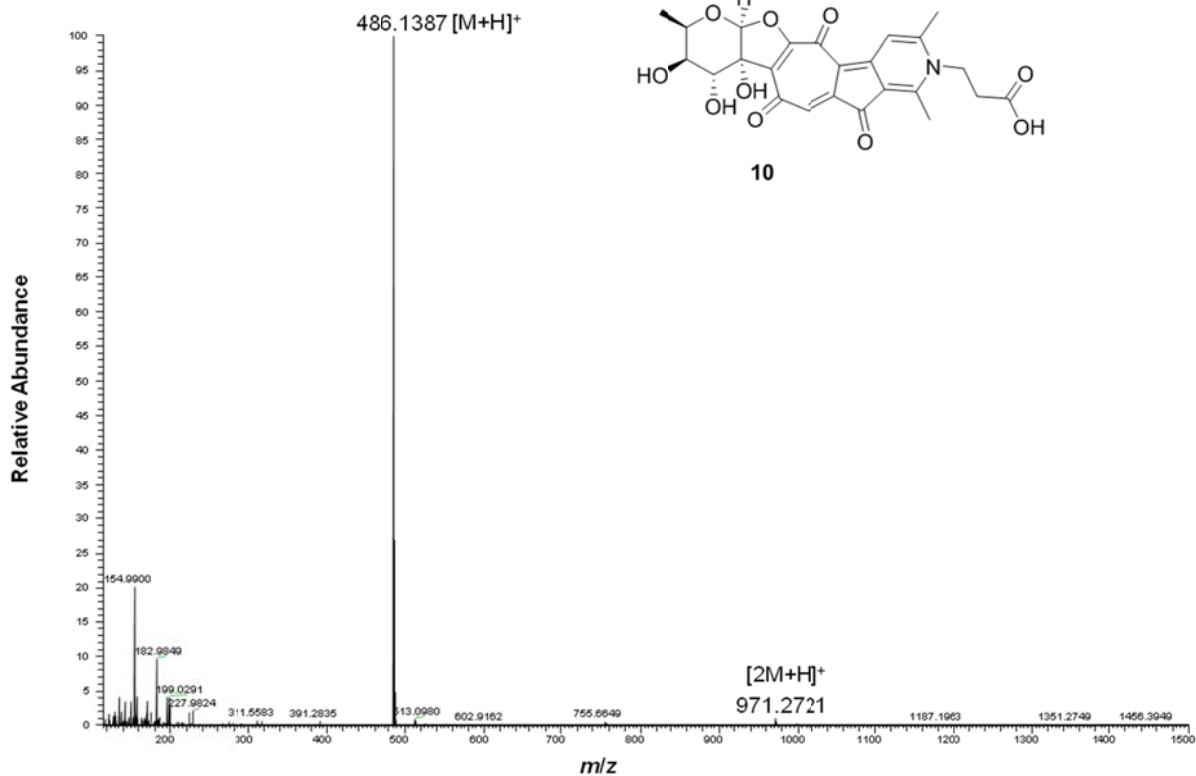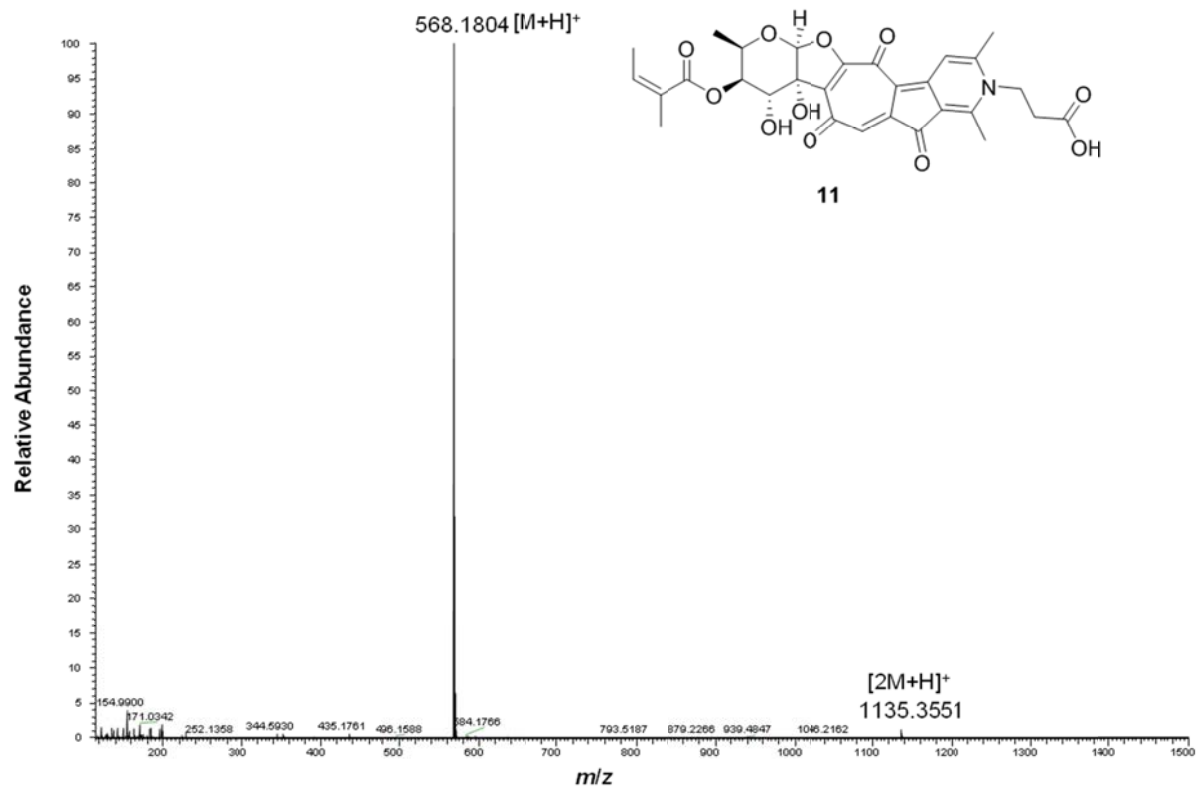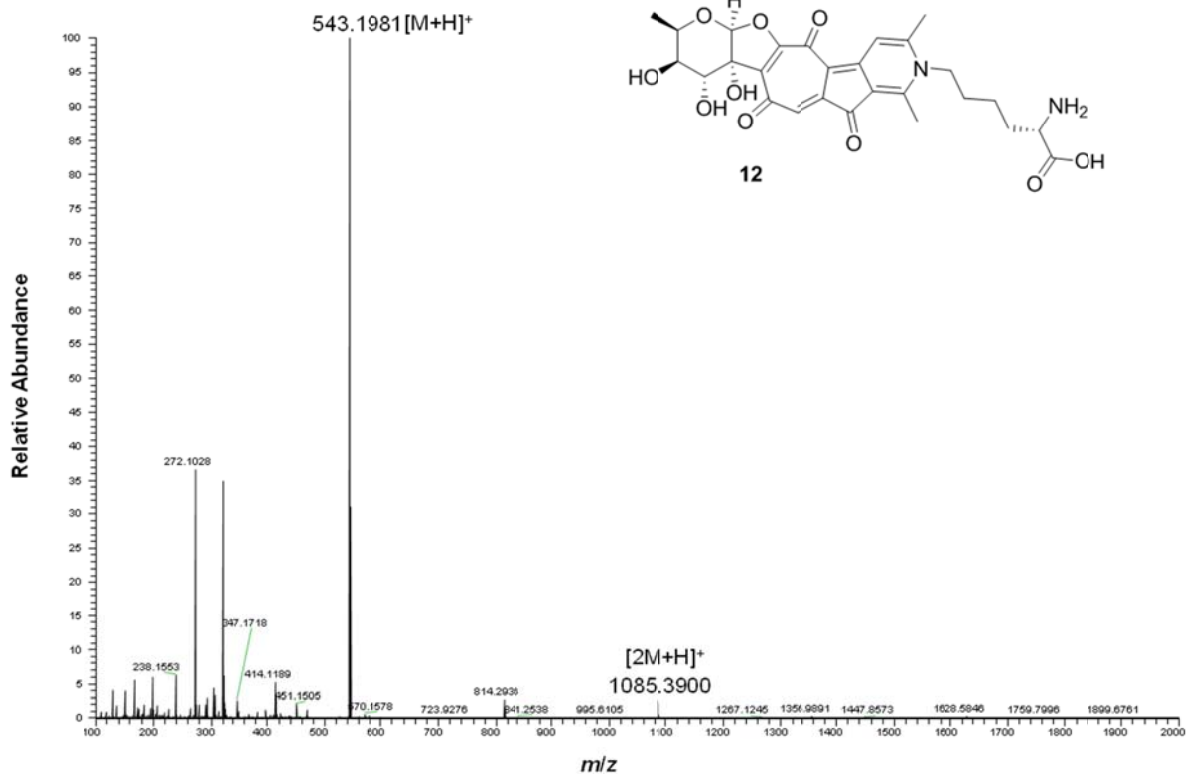
FTMS + p ESI Full ms [115.00-1500.00]
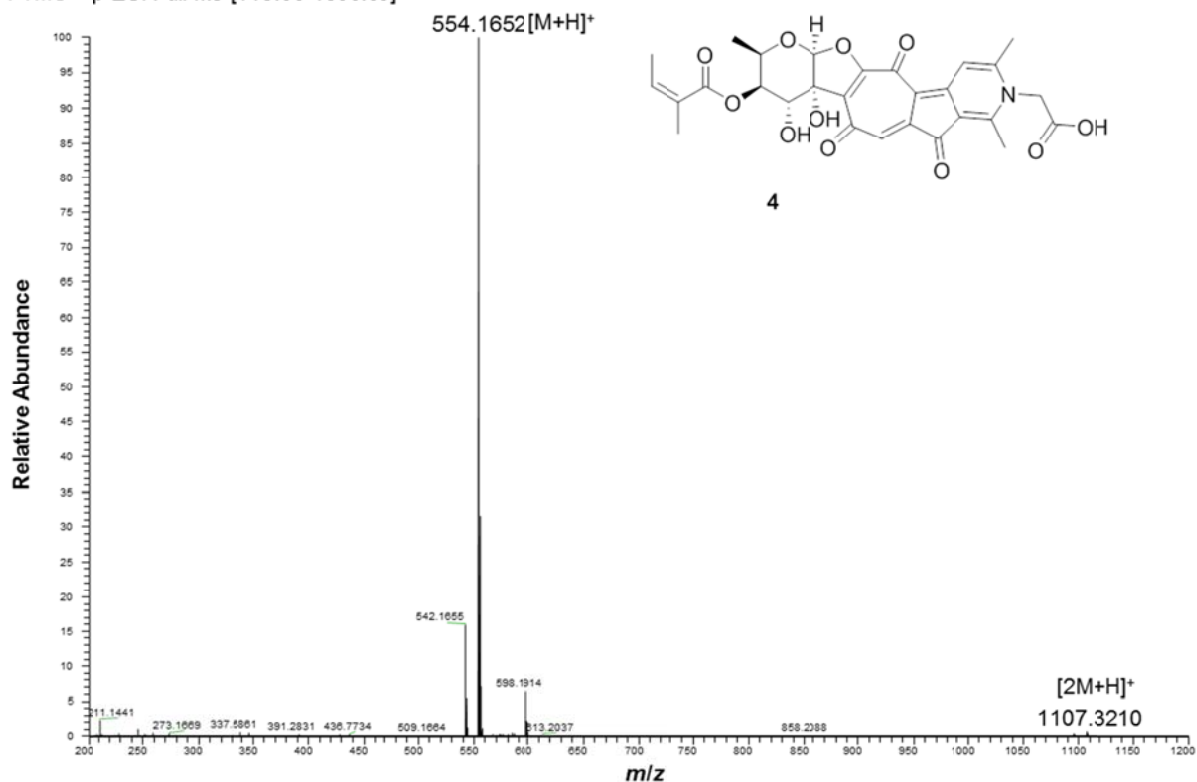
Figure S72. ESI-HRMS (+) spectrum of rubterolone D (**4**).

FTMS + p ESI Full ms [115.00-1500.00]
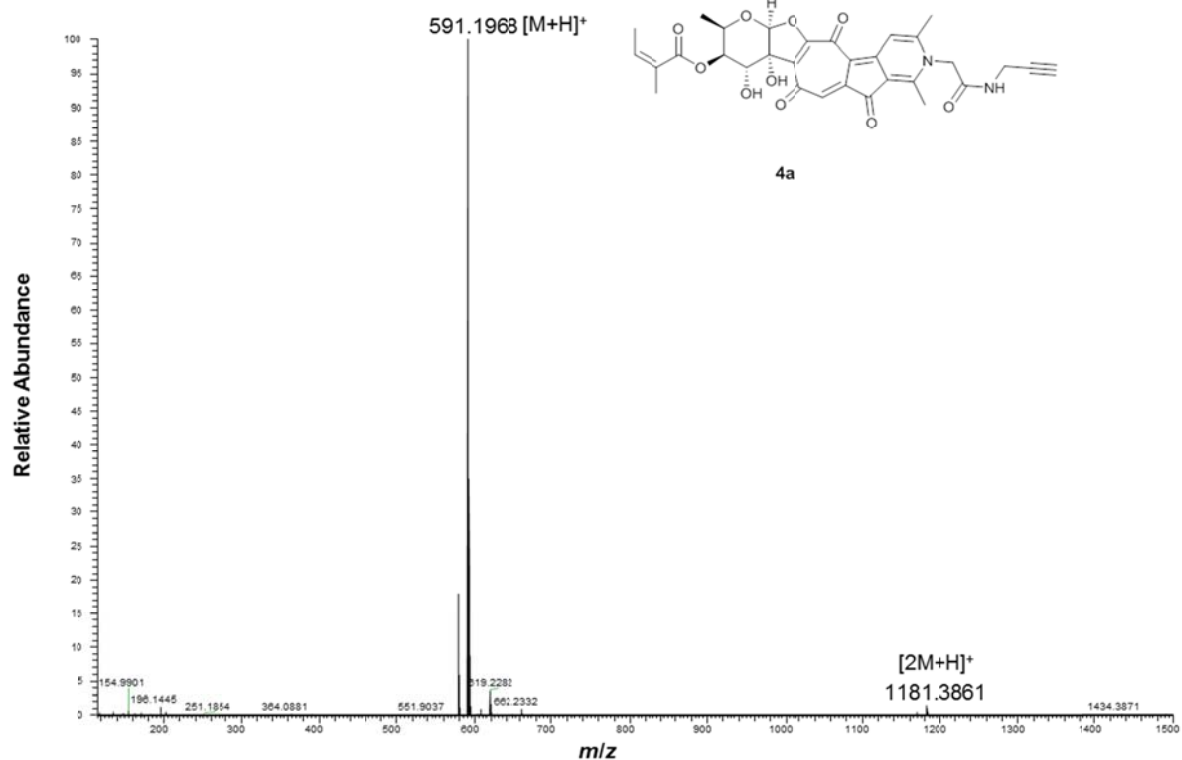
Figure S73. ESI-HRMS (+) spectrum of propargyl-rubterolone D (**4a**).
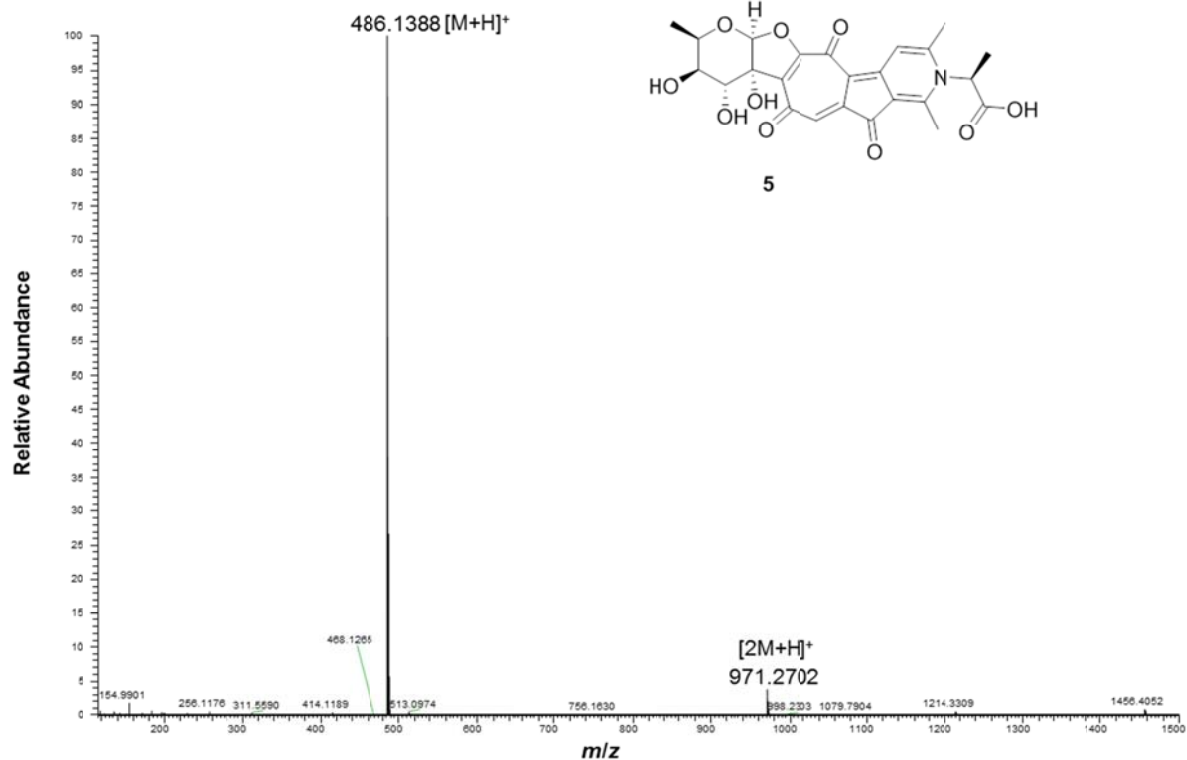
Figure S74. ESI-HRMS (+) spectrum of rubterolone E (**5**).

Figure S75. ESI-HRMS (+) spectrum of rubterolone F (**6**).

Figure S76. ESI-HRMS (+) spectrum of rubterolone G (**10**).

Figure S77. ESI-HRMS (+) spectrum of rubterolone H (**11**).

Figure S78. ESI-HRMS (+) spectrum of rubterolone I (**12**).
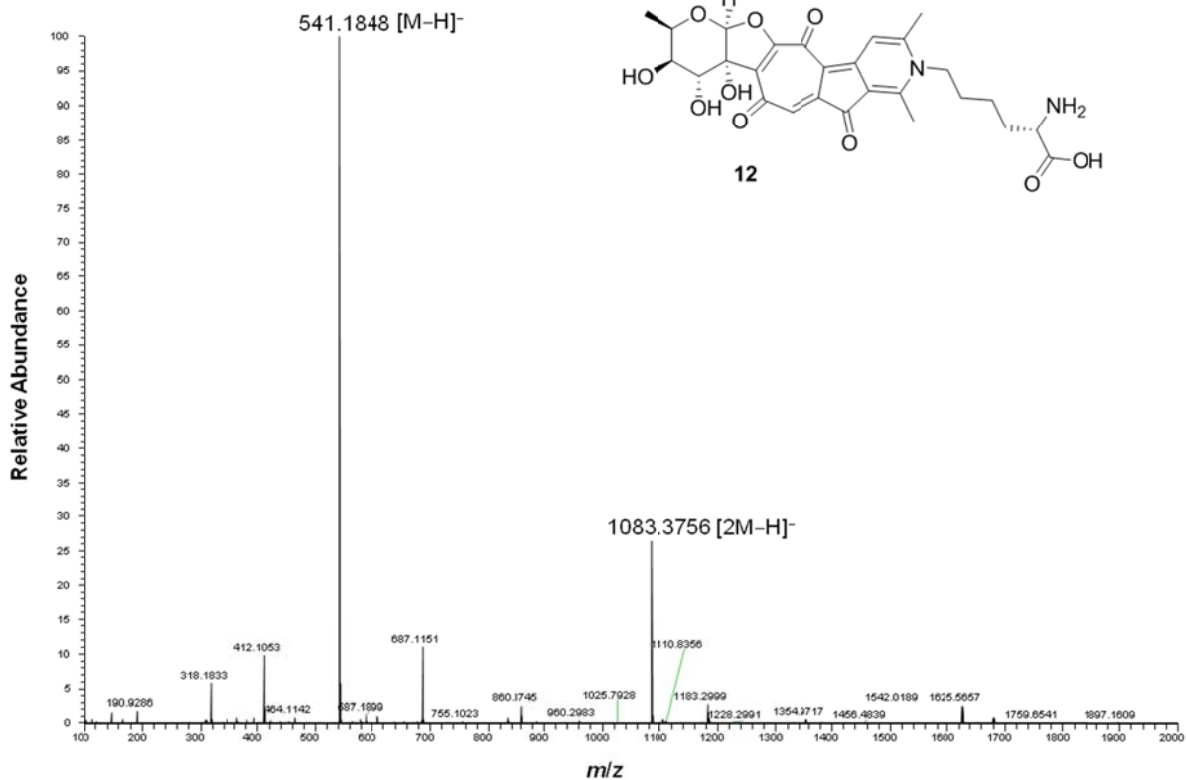
Figure S79. ESI-HRMS (−) spectrum of rubterolone I (**12**).
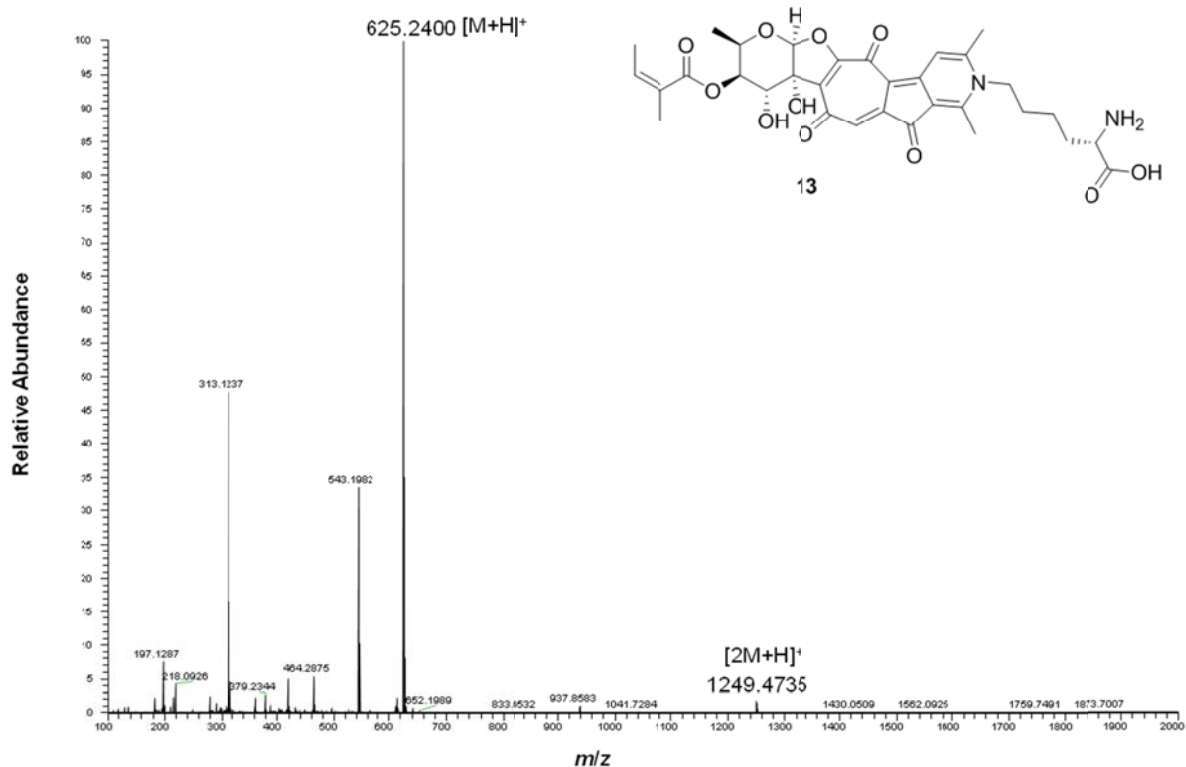
Figure S80. ESI-HRMS (+) spectrum of rubterolone J (**13**).
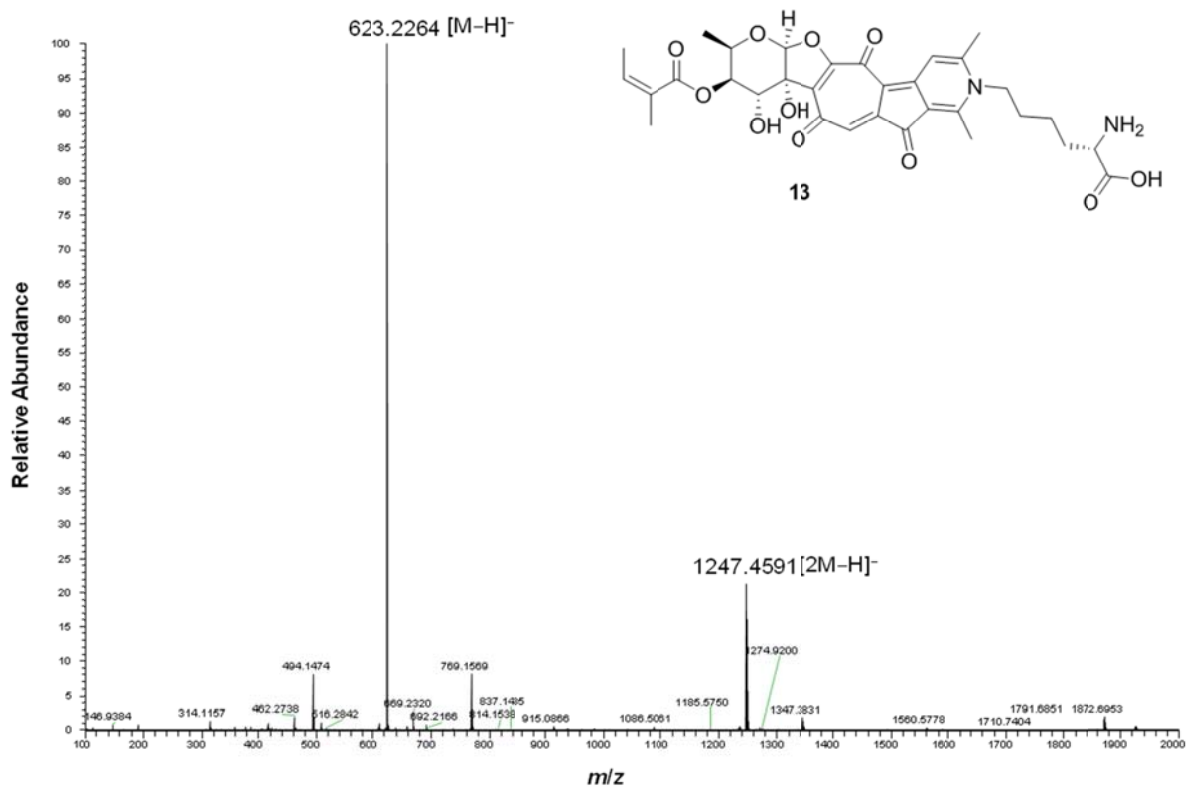
Figure S81. ESI-HRMS (−) spectrum of rubterolone J (**13**).
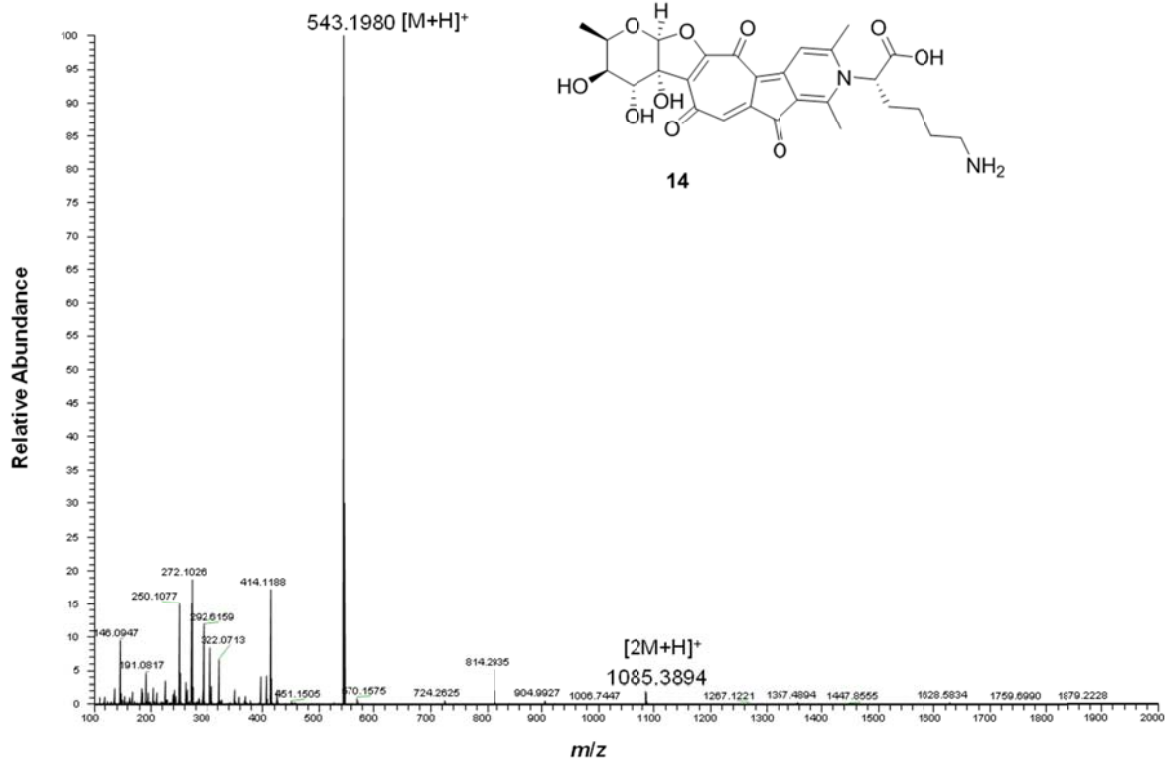
Figure S82. ESI-HRMS (+) spectrum of rubterolone K (**14**).
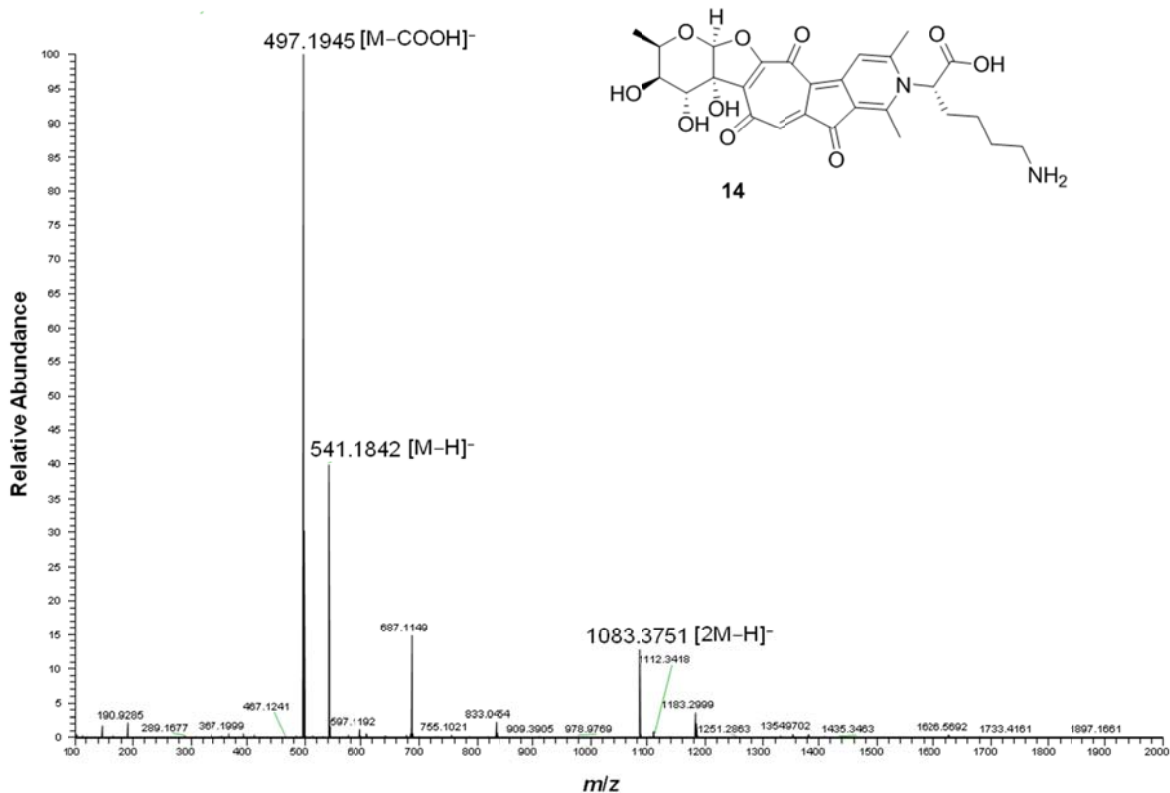
Figure S83. ESI-HRMS (–) spectrum of rubterolone K (**14**).
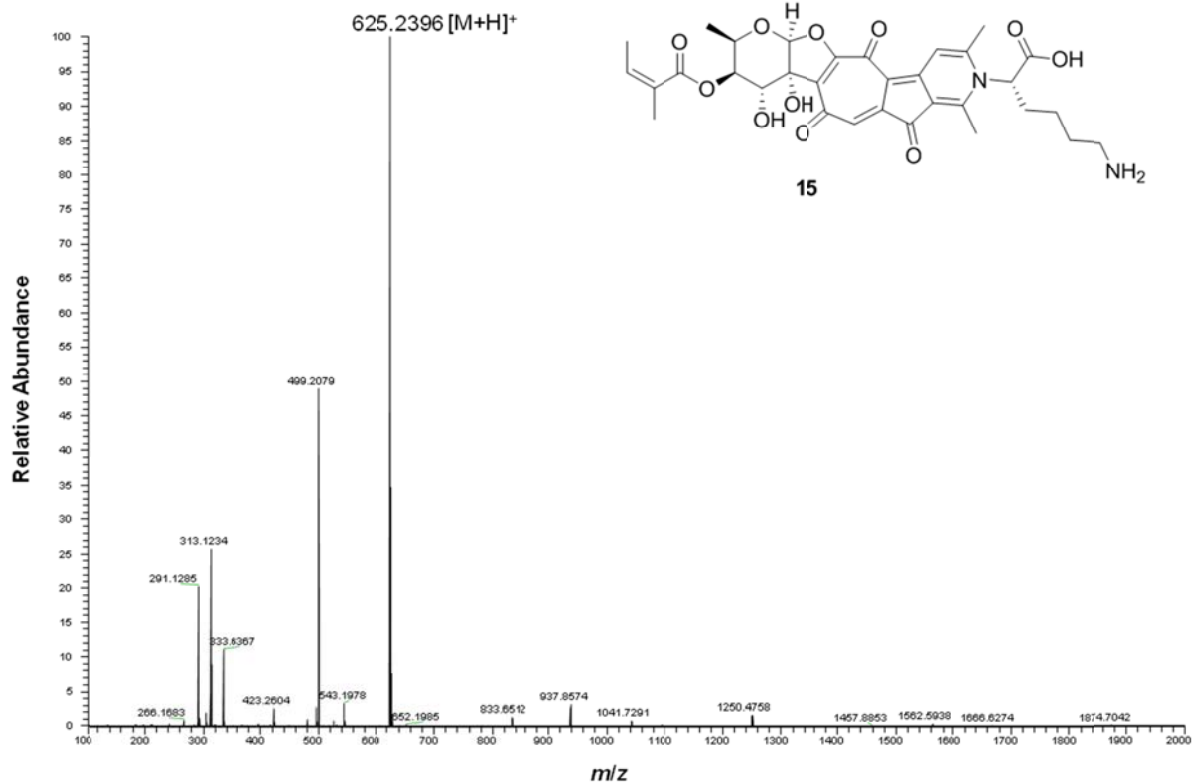
Figure S84. ESI-HRMS (+) spectrum of rubterolone L (**15**).
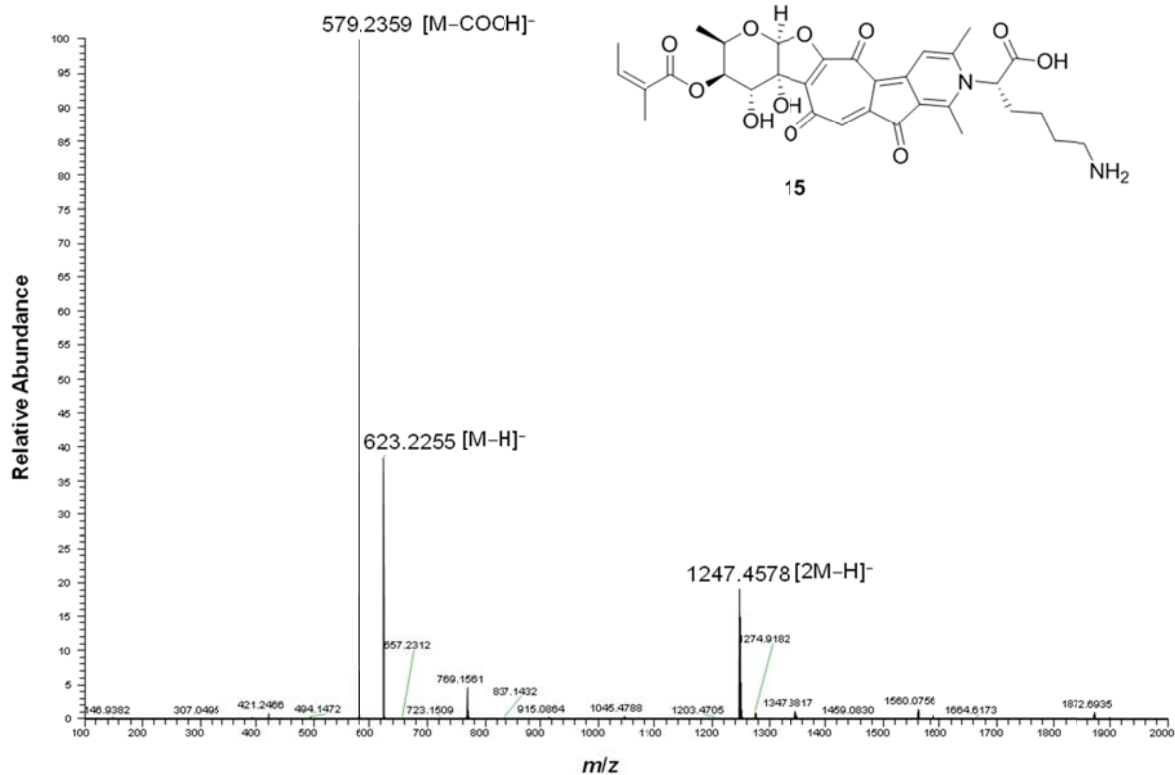
Figure S85. ESI-HRMS (−) spectrum of rubterolone L (**15**).

10.   References

[1]   S. C. Hsu, J. L. Lockwood, *Appl Microbiol.,* **1975**, *29*, 422–426.

[2]   a) A. A. Visser, T. Nobre, C. R. Currie, D. K. Aanen, M. Poulsen, *Microb. Ecol.* **2012**, *63*, 975–985; b) E. B. Shirling, D. Gottlieb, *Int. J. Syst. Bacteriol.* **1966**, *16*, 313–340.

[3]   P. J. Schumann, *J. Basic Microbiol.* **1991**, *31*, 479–555.

[4]   T. A. Hall, *Nucl. Acids Symp. Ser.* **1999**, *41*, 95–98.

[5]   http://decipher.cee.wisc.edu/FindChimerasOutputs.html

[6]   http://blast.ncbi.nlm.nih.gov/Blast.cgi

[7]   http://www.megasoftware.net/

[8]   A. M. Bolger, M. Lohse, B. Usadel, *Bioinformatics* **2014**, *30***,** 2114–2120.

[9]   A. Bankevich, S. Nurk, D. Antipov, A. A. Gurevich, M. Dvorkin, A. S. Kulikov, V. M. Lesin, S. I. Nikolenko, S. Pham, A. D. Prjibelski, A. V. Pyshkin, A. V. Sirotkin, N. Vyahhi, G. Tesler, M. A. Alekseyev, P. A. Pevzner, *J. Comput. Biol.* **2012**, *19*, 455–477.

[10]   D. H. Parks, M. Imelfort, C. T. Skennerton, P. Hugenholtz, G. W. Tyson, *Genome research* **2015**, *25*, 1043–1055.

[11]   T. Seemann, *Bioinformatics* **2014**, *30*, 2068–2069.

[12]   a) X. Cai, Y.-M. Shi, N. Pöhlmann, O. Revermann, I. Bahner, S. J. Pidot, F. Wesche, H. Lackner, C. Büchel, M. Kaiser, C. Richter, H. Schwalbe, T. P. Stinear, A. Zeeck, H. B. Bode, *Angew. Chem. Int. Ed.* **2017**, *56*, 4945; b) Y. Yan, J. Yang, Z. Yu, M. Yu, Y. Ma, L. Wang, C. Su, J. Luo, G. P. Horsman, S. Huang, *Nat. Commun.* **2016**, *7*, 13083; c) Y. Yan, Y. Ma, J. Yang, G. P. Horsman, D. Luo, X. Ji, S. Huang, *Org. Lett.* **2016**, *18*, 1254.

[13]   a) Y. Inhashi, T. Shiraishi, K. Palm, Y. Takahashi, S. Ōmura, T. Kuzuyama, T. Nakashima, *ChemBioChem* **2016**, *17*, 1442–1447; b) L. R. Pickens, W. Kim, P.Wang, H. Zhou, K. Watanabe, S. Gomi, Y. Tang, *J. Am. Chem. Soc.* **2009**, *131*, 17677.

[14]   a) M. Hatsu, T. Sasaki, S. Gomi, Y. Kodama, M. Sezaki, S. Inouye, S. Kondo, *J. Antibiot. (Tokyo)* **1991**, *45*, 325–330; b) B. Hartmann, A. M. Kanazawa, J.-P. Deprés, A. E. Greene, *Tetrahedron Lett.* **1991**, *32*, 5075–5077.

[15]   a) F. Gao, M. Leidig, T. J. Mabry, *Phytochemistry* **1986**, *25*, 1371–1376; b) I. S. Ismail, H. Ito, T. Hatano, S. Taniguchi, T. Yoshida, *Chem. Pharm. Bull.* **2004**, *52*, 1145–1147.

[16]   El-Faham, A.; Funosas, R. S.; Prohens, R.; Albericio, F. *Chem. Eur. J.* **2009**, *15*, 9404.

[17]   Methods for dilution antimicrobial susceptibility tests for bacteria that grow aerobically, Approved Standard, 4th ed.; Clinical and Laboratory Standards Institute: Wayne, PA, 2006; Vol. 26.

[18]   F. Krauth, H. M. Dahse, H. H. Ruttinger, P. Frohberg, *Bioorg. Med. Chem.* **2010**, *18*, 1816–1819.

[19]   COLLECT, Data Collection Software; Nonius B.V., Netherlands, 1998

[20]   Z. Otwinowski, W. Minor, Processing of X-Ray Diffraction Data Collected in Oscillation Mode", in Methods in Enzymology, Vol. 276, Macromolecular Crystallography, Part A, edited by C.W. Carter & R.M. Sweet, pp. 307–326, Academic Press, San Diego, USA, 1997

[21]   SADABS 2.10, Bruker-AXS inc., 2002, Madison, WI, U.S.A

[22]   G. M. Sheldrick, *Acta Cryst.* **2008**, *A46*, 112–122.

[23]   L. J. Farrugia, *J. Appl. Cryst.* **2012**, *45*, 849–854.